CATALYTIC ACTIVATION OF CARBON–HYDROGEN AND CARBON–OXYGEN BONDS

By

MICHAEL CLEMENT HAIBACH

A dissertation submitted to the

Graduate School-New Brunswick

Rutgers, The State University of New Jersey

in partial fulfillment of the requirements

for the degree of

Doctor of Philosophy

Graduate Program in Chemistry

Written under the direction of

Prof. Alan S. Goldman

and approved by

_____

_____

_____

_____

_____

New Brunswick, New Jersey

October, 2014

ABSTRACT OF THE DISSERTATION

Catalytic Activation of Carbon–Hydrogen and Carbon–Oxygen Bonds

By MICHAEL CLEMENT HAIBACH

Dissertation Director:

Prof. Alan S. Goldman

Efficient catalytic methods for the transformation of C–H, O–H, and C–O bonds are key to the efficient generation of both complex molecules and commodity chemicals, and for the processing of biomass. The work presented in this dissertation attempts to address these various goals using organocatalytic and organometallic approaches. Several new types of reactions have been developed: the hydride shift-triggered C–H functionalization using a bisnucleophile, the organometallic-catalyzed intermolecular olefin hydroaryloxylation, and the atom-economic C–O bond cleavage of aryl alkyl ethers. A new type of POP pincer ligand was developed and applied to investigate pincer rhodium hydride complexes, leading to the discovery of a robust olefin isomerization catalyst.

Dedication

To my family

Acknowledgement

The work that makes up this thesis was made possible with the help and guidance of many people. I benefitted from having excellent science teachers during my formative years, starting with my mother Patricia Boyd who homeschooled me until fourth grade. I was lucky to study under Mrs. Lisa Marchitello in junior high, because she strongly emphasized experimental design. In high school I learned chemistry from Bro. James Muffley, F.S.C. and remember being given what seemed like an amazing amount of serious chemicals at my disposal for laboratory work. Bro. Ernest Miller, F.S.C. was instrumental in training me to perform independent scholarship during that time.

During my undergraduate years, Profs. Kozmin, Rawal, and Yamamoto all had a major influence on my approach to studying and teaching organic chemistry. I also thank Prof. Yamamoto and his then-student (now also Prof.) Cheol-Hong Cheon for directing my initial foray into synthetic chemistry research. The late Prof. Hillhouse introduced me to organometallic chemistry and provided valuable advice on choosing a graduate program.

At Rutgers, I would like to thank all of the members of the Goldman and Seidel groups who have provided a fun, collegial, and collaborative atmosphere over the past five years. Dr. Jonwook Choi showed me the basics of Schlenk line manipulation, and Dr. David Wang got me started on DFT calculations. Special thanks is due to Dr. Thomas Emge for X-Ray crystallography expertise and crystal engineering advice, and to Dr. Linda Anthony for administering the NSF IGERT on Renewable and Sustainable Fuels where I was funded with a graduate trainee fellowship.

Most of all, I'd like to thank my PhD committee for their leadership and guidance both in generating new directions and in keeping me on track. Prof. Karsten Krogh-Jespersen oversaw the computational aspects of my projects on rhodium complexes and C–O bond formation and has been a consistent source of guidance for the mechanistic aspects of this thesis. Prof. Daniel

Seidel directed the organocatalytic portion of thesis and we have maintained a close interest in that growing area of organic chemistry that resulted in our review article in 2014. It was a pleasure to follow his group's incredible pace of progress over the past five years by attending group meetings and he has been a great role model and mentor. Finally, I could not ask for a better advisor than Prof. Alan Goldman, who directed the majority of this thesis. His standards for completeness, clarity, and innovation in publications are something that will always serve as a target for me in my future endeavors.

All of the work presented in this thesis has been published previously during my PhD career, and has been reproduced with permission from the respective copyright holders. Individual copyright acknowledgements are therefore provided at the beginning of the respective chapters. Chapter 2 was published under the direction of Prof. Seidel in 2011. Chapter 3 published in 2012 under the direction of Profs. Goldman and Krogh-Jespersen, and Dr. David Wang performed DFT calculations. Chapter 4 was published in 2013 under the direction of Profs. Goldman and Krogh-Jespersen, and Mr. Changjian Guan and Dr. David Wang performed DFT calculations. Chapter 5 was published in 2014 under the direction of Prof. Goldman.

Table of Contents

Chapter 1: Introduction

This thesis covers research in synthetic inorganic chemistry, organocatalysis, and organometallic catalysis. In the first two chapters of this thesis, I will discuss research dealing with the activation and functionalization of C–H bonds both from an organocatalytic and organometallic approach. In the second two chapters, I will focus on the catalytic breaking and forming of C–O bonds using organometallic catalysis.

The first half of this thesis concerns the broad field of C–H bond activation and functionalization. The ubiquity and inertness of most C–H bonds found in molecules has long been celebrated by researchers in this field, and Goldman and Goldberg have termed it "the unfunctional group" in their introduction to the landmark ACS Symposium Series on the topic.[1] Most of the previous work on C–H bond activation arose out of the field of transition metal or organometallic chemistry, and this topic has been reviewed very extensively.[2]

Alkane dehydrogenation catalysis is a subset of organometallic C–H activation, and one which has immense potential to offer more efficient processes for the use of limited fossil fuel resources.[3] In this area, I developed and characterized a series of rhodium "pincer" complexes as a starting point for new alkane dehydrogenation catalysts. This project lead to the discovery of unusual selectivity in olefin insertion into Rh–H bonds of these complexes, a robust olefin isomerization catalyst, and the first thermal alkane dehydrogenation complex based on a pincer rhodium framework. My results are recounted in Chapter 3.

Reactions where a relatively unreactive C–H bond is functionalized via hydride transfer are mechanistically different and not generally considered to be organometallic C–H functionalizations. These reactions were first discovered over 100 years ago, but they have experienced renewed interest over the past decade.[3] They have been previously classified under names such as the "*tert*-Amino Effect," "Meth-Cohn/Suschitzky/Reinhoudt Reactions," "HT-Cyclization," and "Internal Redox Cascade." An important subset of these reactions

involve the functionalization of the α C–H of an amine via a 1,5-hydride shift, resulting in the formation of a 6-membered ring. Chapter 2 discusses our contribution to this area in the form of an amine C–H functionalization involving the biologically relevant molecule indole. In this reaction, a 1,5-hydride shift results in the formation of a 7-membered ring for the first time.

In the second part of my thesis, I focus on the activation and formation of carbon–oxygen bonds. The carbon–oxygen bond is ubiquitous in renewable natural resources, such as biomass, and its efficient catalytic manipulation is key to the development of renewable fuels and commodity chemicals.[4] An account of our accomplishments, catalytic olefin hydroaryloxylation and catalytic ether cleavage, are given in Chapters 4 and 5. In chapter 4 I describe how prior research on stoichiometric C–H and C–O activation by the molecule (^{tBu}PCP)Ir lead to the discovery of transition-metal catalyzed olefin hydroaryloxylation. Chapter 4 also contains combined experimental and theoretic investigations into the mechanism of the olefin hydroaryloxylation, in which an acid-based mechanism common to previous systems is ruled out.

Chapter 5 focuses on the microsocopic reverse reaction, which represents a rare atom-economic cleavage of a strong C–O bond. Both linear and branched aryl alkyl ethers can be cleaved catalytically along the C_{sp3}–O bond to generate the corresponding phenol derivative and olefin resulting from the alkyl substituent. Very high conversions can be achieved in short reaction times, and a variety of substrates is tolerated in this novel catalytic process.

Chapter 1.1 References

(1) Goldman, A. S.; Goldberg, K. I. in *Activation and Functionalization of C-H Bonds*; Goldberg, K. I.; Goldman A. S., Eds. **2004**; ACS Symposium Series 885; 1-44.

(2) In addition to the reference above, see the following classic reviews of the subject: a) Shilov, A. E.; Shul'pin, G. B. *Chem. Rev.* **1997**, *97*, 2879-2932. b) Labinger, J. A.; Bercaw, J. E. *Nature*, **2002**, 507-514. For an account of our group's work in one such example, see: c) Haibach, M. C.; Kundu, S.; Brookhart, M.; Goldman, A. S. *Acc. Chem. Res.* **2012**, *45*, 947-958.

(3) See our review of the topic, and references therein: Haibach, M.C.; Seidel, D. *Angew. Chemie. Int. Ed.* **2014**, *53*, 5010-5036.

(4) a) Zakzeski, J; Bruijnincx, P. C. A.; Jongerius, A. L.; Weckhuysen, B. M. *Chem. Rev.* **2010**, *110*, 3552-3599. b) Ruppert, A. M.; Weinberg, K.; Palkovits, R. *Angew. Chem. Int. Ed.* **2012**, *51*, 2564-2601.

Chapter 2

Organocatalytic C–H Functionalization of Amines with Indoles

The direct functionalization of unactivated and relatively unreactive C–H bonds continues to be a major focus of inquiry.[1] Exciting progress in this intensely active research area has been achieved and many more advances can be anticipated. Much of the current research efforts are focused on the development of C–H bond functionalization processes by means of oxidative methods that require (super)stoichiometric amounts of oxidant. Fundamentally different from a mechanistic point of view and comparatively unexplored are reactions that lead to C–H bond functionalization through redox neutral processes (e.g. Figure 2.1).[2,3] In these reactions, the C–H bond to be functionalized serves as a hydride source for a pendant acceptor moiety. Subsequent to hydride transfer, the reduced and oxidized portions of the molecule recombine to form a new ring system.

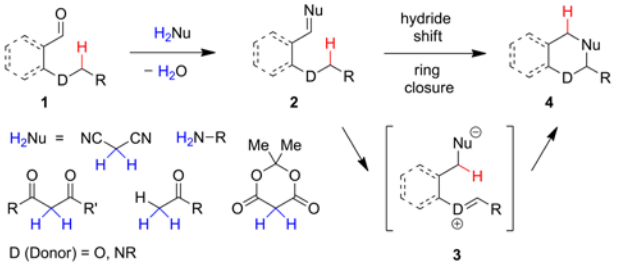

Figure 2.1. Redox neutral C–H bond functionalization.

Previously reported hydride shift initiated C–H bond functionalizations often follow the general reaction sequence shown in Figure 2.1.[4,5] In the first step, an aldehyde **1** is allowed to react with a nucleophile (H_2Nu) to form intermediate **2**. Thermal or catalyst promoted activation of compound **2** facilitates the hydride shift/ring closure event to form **4** via the intermediacy of the dipolar species **3**. In the majority of cases, this sequence is conducted in a stepwise manner that requires the isolation and purification of intermediates **2**. Many of these reactions involve 1,5-hydride shifts and result in the formation of products that contain six-membered rings.[6]

As part of a program aimed at developing redox neutral reaction cascades for the rapid buildup of molecular complexity,[7] we considered a new reaction cascade design in which an initial 1,5-

hydride shift would ultimately result in the formation of larger rings. As outlined in Figure 2.2, the acid catalyzed reaction of aldehyde **1** with a doubly nucleophilic compound is envisioned to initially result in the formation of the activated species **5**. Subsequent to intramolecular hydride transfer, the resulting intermediate **6** could react with the pendant nucleophile. Proton loss would then result in the formation of product **7**.

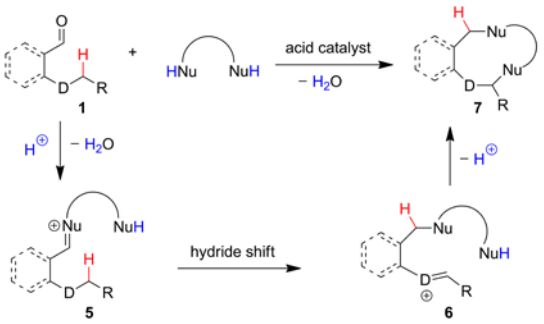

Figure 2.2. Design of a new redox neutral reaction cascade.

Due to its known nucleophilic properties, it occurred to us that indole should be able to serve as a double nucleophile in the proposed sequence.[8] Such a reaction would constitute a new one-step indole annulation. Whereas indole annulations to form carbazoles are numerous,[9] and indole annulations that lead to dearomatization of the indole nucleus have been reported,[10] direct annulation of (partially) saturated rings onto simple indoles is relatively rare in cases where indole retains its aromaticity. This is particularly true for annulations with larger than six-membered rings.[11]

Given the importance of indole in the context of medicinal chemistry,[12] the prospect of rapidly generating new indole containing molecular frameworks appeared particularly appealing. The reaction of an appropriate aminobenzaldehyde with indole should result in the one-step formation of azepinoindoles such as **8**. The azepinoindole substructure is found in a number of natural products (e.g., arboflorine and subincanadine F) and biologically active drug candidates.[13]

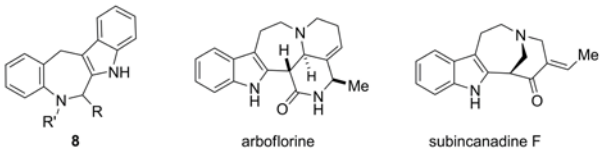

We initiated our studies by investigating the reaction of indole with aminobenzaldehyde **9a** under a variety of conditions. Not surprisingly, a reaction conducted in ethanol at room temperature led to the formation of the bis(indolyl)methane **10a** in 62% yield (eq. 1).[14] As outlined in eq. 2, using very similar conditions but higher reaction temperatures (reflux in n-butanol) resulted in the unexpected formation of the reduced product **11a** (vide infra). Gratifyingly, the desired product **12a** could be obtained in a reaction conducted in toluene under reflux and in the presence of catalytic amounts of p-toluenesulfonic acid (p-TSA). However, the azepinoindole **12a** was obtained in only 24% yield and its formation was accompanied by the generation of product **11a** in 29% yield (eq. 3). In addition, small amounts (7%) of the bis(indolyl)methane **10a** were isolated as well (not shown).

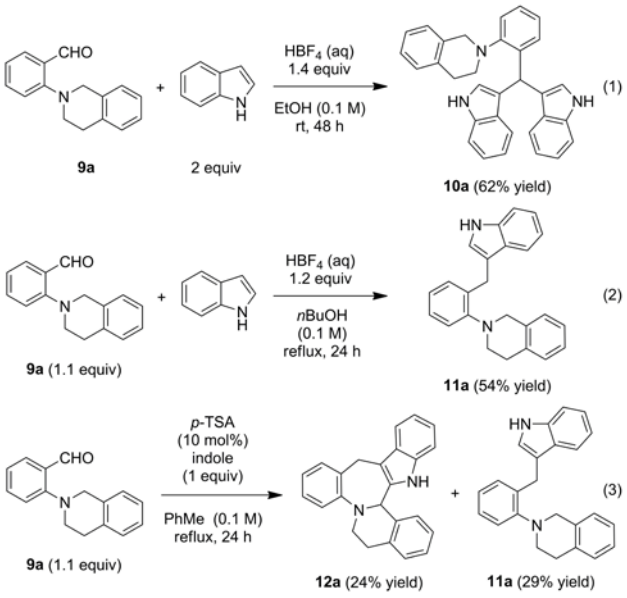

Various other reaction conditions were evaluated in order to improve the overall efficiency of this reaction and to maximize the yield of the desired product **12a**. As part of this study, we

found that reactions conducted under microwave irradiation produced particularly promising results and allowed for conveniently short reaction times.

Table 1.1. Evaluation of reaction parameters.[a]

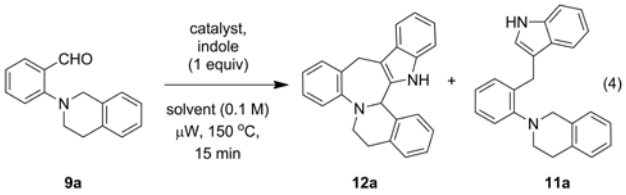

Entry	Catalyst (equiv.)	solvent	Yield of **12a** (%)	Yield of **11a** (%)
1	p-TSA (0.1)	PhMe	56	13
2	CF_3COOH (1.2)	PhMe	20	30
3	CH_3SO_3H (0.2)	PhMe	trace	trace
4	CSA (0.1)	PhMe	54	9
5	HBF_4•OEt_2 (0.1)	PhMe	trace	trace
6	4-Br-pyr•HCl (0.1)	PhMe	0	0
7	H_3PO_4(1.2)	PhMe	0	0
8	PhCOOH (0.2)	PhMe	0	0
9	DPP (0.1)	PhMe	81	4
10[b]	DPP (0.1)	Xylenes	69	4
11	DPP (0.1)	$C_2H_4Cl_2$	40	4
12[c]	DPP (0.1)	PhMe	79	6
13[d]	DPP (0.1)	PhMe	73	6
14	DPP (0.2)	PhMe	83	4

[a] Reactions were performed on a 0.25 mmol scale. [b] reaction run at 170 °C. [c],[d], Reactions were run with 1.1 and 1.3 equiv of indole, respectively. p-TSA = p-toluenesulfonic acid; CSA = camphorsulfonic acid; DPP = diphenyl phosphate.

A survey of different acid additives is summarized in Table 1.1. Optimal results were obtained with 20 mol% of diphenyl phosphate (DPP) in toluene (entry 14).[15] Under these conditions, the indole annulation product **12a** was obtained in 83% yield and the formation of the

undesired product **11a** was almost completely suppressed. A reaction conducted at reflux in toluene but otherwise identical conditions went to completion within three hours. In this instance, product **12a** was obtained in 57% yield in addition to **10a** (25%) and **11a** (10%). The corresponding reaction in refluxing xylenes gave **12a** (60%), **10a** (13%) and **11a** (11%) after two hours.

With the optimized reaction conditions at hand, a number of other readily available indoles were allowed to react with aminobenzaldehyde **9a**, including relatively electron-rich and electron-poor indoles. As summarized in Chart 1, the corresponding annulation products **12** were obtained in good yields. The structure of the N-methylindole derived product **12f** was confirmed further by X-ray crystallography.

Chart 1.1. Scope of the indole component.[a]

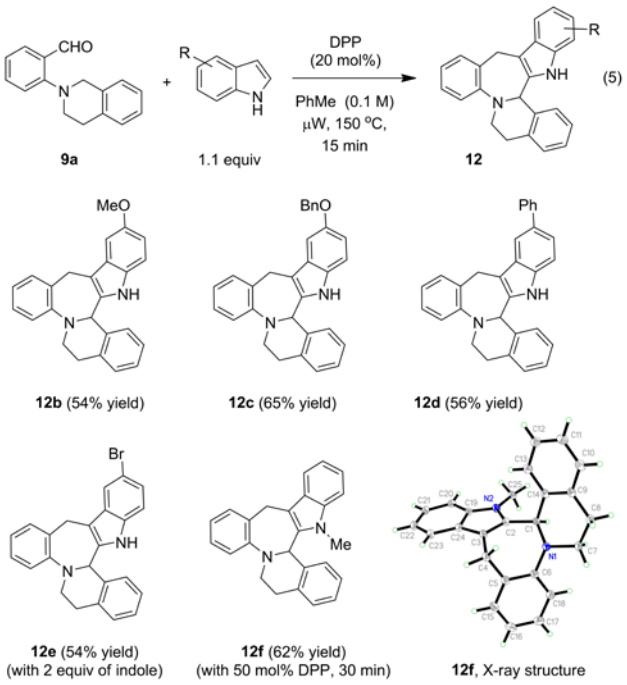

[a] Reactions were performed on a 0.25 mmol scale.

The scope of the indole annulation with regard to the aminobenzaldehyde is shown in Chart 2. A number of aminobenzaldehydes underwent reaction with indole to yield the expected products

14 in good to excellent yields. Minor amounts of the corresponding reduced products were isolated in some instances. In case of the 2-methylpyrrolidine derived aminobenzaldehyde **13e** (not shown), the resulting product **14e** was obtained as a single regioisomer. The fact that the more substituted of the two possible regioisomers was isolated is consistent with earlier observations[7b,c] and with the notion that a tertiary C–H bond is a better hydride donor than a secondary C–H bond. Interestingly, the corresponding 2-methylpiperidine derived product **14f** was obtained as a 4:1 mixture of regioisomers. However, the preference for the formation of the more substituted product was maintained (minor regioisomer not shown, dr = 3:2). The structure of compound **14h** was confirmed by X-ray crystallography.

Chart 2.2. Scope of the aminobenzaldehyde component.[a]

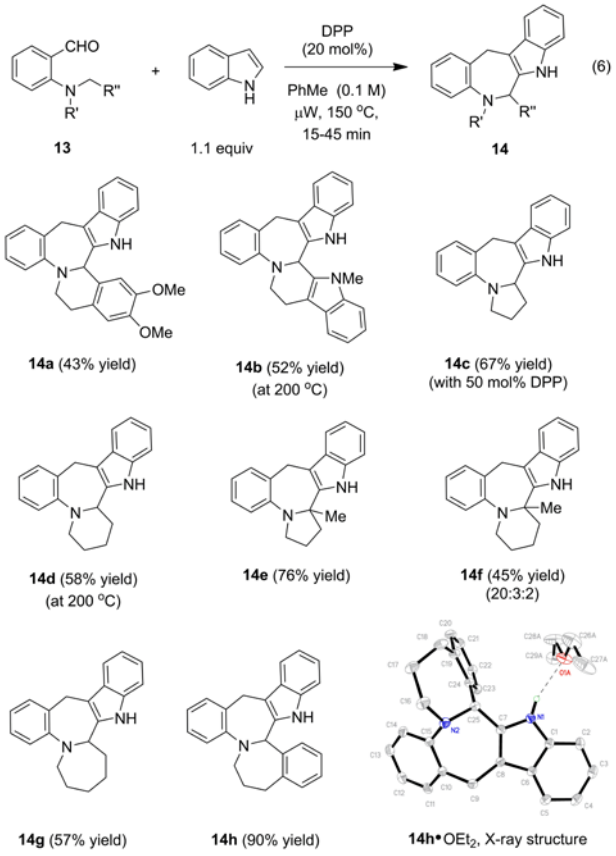

[a] Reactions were performed on a 0.25 mmol scale.

The new cascade reaction was successfully extended to double nucleophiles other than indole. As shown in eq. 7, the reaction of aminobenzaldehyde **9a** with 2,5-dimethylpyrrole resulted in the formation of the 3,4-pyrrole annulated benzazepine **15** in 59% yield.[16] In preliminary work, we have also considered entirely different double nucleophiles. For instance, substrate **9a** readily underwent reaction with N,N′-diphenylhydrazine to form the interesting triaza-heterocycle **16** in 72% yield. A reduced catalyst loading of 5 mol% proved beneficial in this case. The X-ray crystal structure of **16** was also obtained.

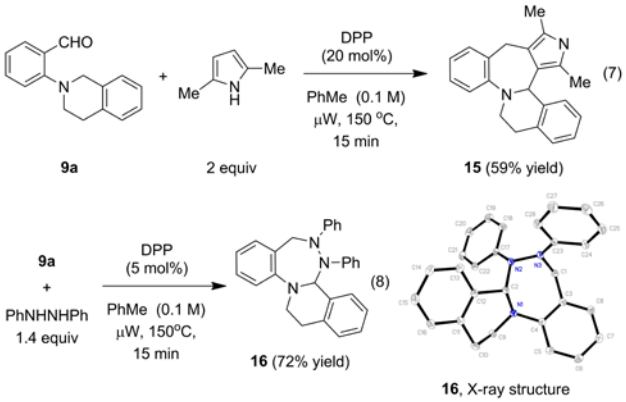

As outlined before, under certain reaction conditions, the formation of the desired annulation products was accompanied by varying amounts of apparently reduced product (i.e., **11a**) which in some cases was the only isolable material. Considering that products such as **12a** could potentially act as hydride donors, we proposed that **12a** might promote its own reduction in an interesting type of disproportionation reaction. In fact, we have observed that prolonged reaction times under microwave irradiation led to reduced yields of annulation products and the build-up of increased amounts of the reduced products. Furthermore, when compound **12a** was exposed to the reaction conditions outlined in eq 2, the reduced product **11a** was obtained in 33% yield as the only isolable product. As we have thus far been unable to isolate the corresponding oxidation product of **12a**, presumably due to its rapid decomposition, we devised an alternative experiment to establish the potential of **12a** to act as an intermolecular hydride delivery agent. Indeed, as shown in eq. 9, compound **12a** readily promoted the reduction of imine **17** to the corresponding

amine **18** in 70% yield (yield based on **12a**).[17] The product resulting from the oxidation of **12a** could not be isolated and the reduced compound **11a** was not formed in this process.

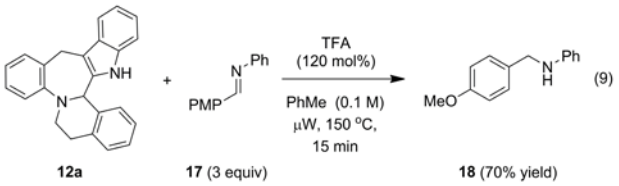

Lastly, we wanted to establish that formation of the well known and easily formed bis(indolyl)methanes[14] (e.g., **10a**) does not necessarily represent a dead end in this reaction. Rather, we speculated that under acid catalyzed conditions, compounds such as **10a** might be in equilibrium with the corresponding azafulvenium ions (e.g., **19**), presumed intermediates in the formation of the annulation products. Indeed, exposure of **10a** to the original reaction conditions gave rise to the formation of annulation product **12a** in 85% yield, accompanied by the expected recovery of indole in 84% yield (eq. 10). In addition, **11a** was formed in 5% yield (not shown).

Scheme 1.1. Transformation of a bis(indolyl)methane into an azepinoindole.

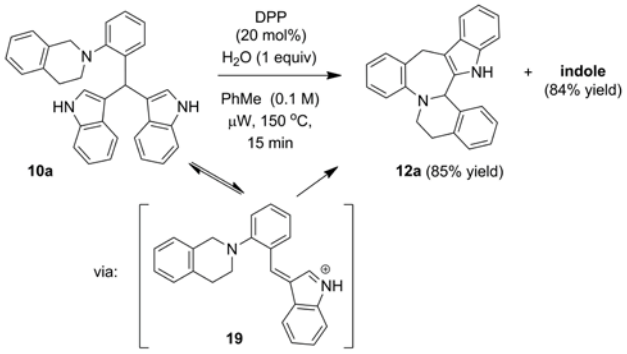

In conclusion, we have shown that reactions of doubly nucleophilic species such as indoles with aminobenzaldehydes lead to unprecedented reaction cascades. In this new redox neutral process, a 1,5-hydride shift results in the formation of seven-membered ring products. The resulting indole-fused benzazepines can be obtained in just two steps from commercially

available materials. Current studies are aimed at developing other redox-neutral reaction cascades for the rapid build-up of molecular complexity.

Acknowledgment. We are grateful to the National Science Foundation for support of this research (Grant CHE-0911192). MCH acknowledges Celgene for generous support through a Celgene Drug Discovery Fellowship. We thank Dr. Tom Emge for crystallographic analysis.

Chapter 2.1 References

(1) For selected reviews on C–H bond functionalization, see: a) Godula, K.; Sames, D. *Science* **2006**, *312*, 67; b) Dick, A. R.; Sanford, M. S. *Tetrahedron* **2006**, *62*, 2439; c) Davies, H. M. L. *Angew. Chem. Int. Ed.* **2006**, *45*, 6422; d) Alberico, D.; Scott, M. E.; Lautens, M. *Chem. Rev.* **2007**, *107*, 174; e) Bergman, R. G. *Nature* **2007**, *446*, 391; f) Campos, K. R. *Chem. Soc. Rev.* **2007**, *36*, 1069; g) Davies, H. M. L.; Manning, J. R. *Nature* **2008**, *451*, 417; h) Li, C.-J. *Acc. Chem. Res.* **2009**, *42*, 335; i) Thansandote, P.; Lautens, M. *Chem. Eur. J.* **2009**, *15*, 5874; j) Colby, D. A.; Bergman, R. G.; Ellman, J. A. *Chem. Rev.* **2010**, *110*, 624; k) Jazzar, R.; Hitce, J.; Renaudat, A.; Sofack-Kreutzer, J.; Baudoin, O. *Chem. Eur. J.* **2010**, *16*, 2654; l) Ishihara, Y.; Baran, P. S. *Synlett* **2010**, 1733.

(2) For reviews on C–H bond functionalization via hydride shifts, see: a) Meth-Cohn, O.; Suschitzky, H. *Adv. Heterocycl. Chem.* **1972**, *14*, 211; b) Verboom, W.; Reinhoudt, D. N. *Recl. Trav. Chim. Pays-Bas* **1990**, *109*, 311; c) Meth-Cohn, O. *Adv. Heterocycl. Chem.* **1996**, *65*, 1; d) Quintela, J. M. *Recent Res. Devel. Org. Chem.* **2003**, *7*, 259; e) Tobisu, M.; Chatani, N. *Angew. Chem. Int. Ed.* **2006**, *45*, 1683; f) Matyus, P.; Elias, O.; Tapolcsanyi, P.; Polonka-Balint, A.; Halasz-Dajka, B. *Synthesis* **2006**, 2625.

(3) For a discussion on redox-economy, see: Burns, N. Z.; Baran, P. S.; Hoffmann, R. W. *Angew. Chem. Int. Ed.* **2009**, *48*, 2854.

(4) For selected examples of redox neutral amine functionalizations, see: a) Ten Broeke, J.; Douglas, A. W.; Grabowski, E. J. J. *J. Org. Chem.* **1976**, *41*, 3159; b) Verboom, W.; Reinhoudt, D. N.; Visser, R.; Harkema, S. *J. Org. Chem.* **1984**, *49*, 269; c) De Boeck, B.; Jiang, S.; Janousek, Z.; Viehe, H. G. *Tetrahedron* **1994**, *50*, 7075; d) Pastine, S. J.; McQuaid, K. M.; Sames, D. *J. Am. Chem. Soc.* **2005**, *127*, 12180; e) Ryabukhin, S. V.; Plaskon, A. S.; Volochnyuk, D. M.; Shivanyuk, A. N.; Tolmachev, A. A. *Synthesis* **2007**, 2872; f) Ryabukhin, S. V.; Plaskon, A. S.; Volochnyuk, D. M.; Shivanyuk, A. N.; Tolmachev, A. A. *J. Org. Chem.* **2007**, *72*, 7417; g) Polonka-Balint, A.; Saraceno, C.; Ludányi, K.; Bényei, A.; Matyus, P. *Synlett* **2008**, 2846; h) Barluenga, J.; Fananas-Mastral, M.; Aznar, F.; Valdes, C. *Angew. Chem. Int. Ed.* **2008**, *47*, 6594; i) Mori, K.; Ohshima, Y.; Ehara, K.; Akiyama, T. *Chem. Lett.* **2009**, *38*, 524; j) Ruble, J. C.; Hurd, A. R.; Johnson, T. A.; Sherry, D. A.; Barbachyn, M. R.; Toogood, P. L.; Bundy, G. L.; Graber, D. R.; Kamilar, G. M. *J. Am. Chem. Soc.* **2009**, *131*, 3991; k) Cui, L.; Peng, Y.; Zhang, L. *J. Am. Chem. Soc.* **2009**, *131*, 8394; l) Vadola, P. A.; Sames, D. *J. Am. Chem. Soc.* **2009**, *131*, 16525; m) Pahadi, N. K.; Paley, M.; Jana, R.; Waetzig, S. R.; Tunge, J. A. *J. Am. Chem. Soc.* **2009**, *131*, 16626; n) Lo, V. K.-Y.; Zhou, C.-Y.; Wong, M.-K.; Che, C.-M. *Chem. Commun.* **2010**, *46*, 213; o) Kuang, J.; Ma, S. *J. Am. Chem. Soc.* **2010**, *132*, 1786; p) Cui, L.; Ye, L.; Zhang, L. *Chem. Commun.* **2010**, *46*, 3351; q) Kang, Y. K.; Kim, S. M.; Kim, D. Y. *J. Am. Chem. Soc.* **2010**, *132*, 11847; r) Dunkel, P.; Turos, G.; Benyei, A.; Ludanyi, K.; Matyus, P. *Tetrahedron* **2010**, *66*, 2331.

(5) For other examples of C–H bond functionalizations via hydride shift processes, see: a) Atkinson, R. S. *Chem. Commun.* **1969**, 735; b) Atkinson, R. S.; Green, R. H. *J. Chem. Soc., Perkin Trans. 1* **1974**, 394; c) Schulz, J. G. D.; Onopchenko, A. *J. Org. Chem.* **1978**, *43*, 339; d) Kanishchev, M. I.; Shegolev, A. A.; Smit, W. A.; Caple, R.; Kelner, M. J. *J. Am. Chem. Soc.* **1979**, *101*, 5660; e) Wolfling, J.; Frank, E.; Schneider, G.; Tietze, L. F. *Angew. Chem., Int. Ed.* **1999**, *38*, 200; f) Woelfling, J.; Frank, E.; Schneider, G.; Tietze, L. F. *Eur. J. Org. Chem.* **2004**, 90; g) Pastine, S. J.; Sames, D. *Org. Lett.* **2005**, *7*, 5429; h) Odedra, A.; Datta, S.; Liu, R.-S. *J. Org. Chem.* **2007**, *72*, 3289; i) Donohoe, T.

J.; Williams, O.; Churchill, G. H. *Angew. Chem. Int. Ed.* **2008**, *47*, 2869; j) Harmata, M.; Huang, C.; Rooshenas, P.; Schreiner, P. R. *Angew. Chem. Int. Ed.* **2008**, *47*, 8696; k) McQuaid, K. M.; Sames, D. *J. Am. Chem. Soc.* **2009**, *131*, 402; l) Alajarin, M.; Bonillo, B.; Sanchez-Andrada, P.; Vidal, A.; Bautista, D. *Org. Lett.* **2009**, *11*, 1365; m) McQuaid, K. M.; Long, J. Z.; Sames, D. *Org. Lett.* **2009**, *11*, 2972; n) Shikanai, D.; Murase, H.; Hata, T.; Urabe, H. *J. Am. Chem. Soc.* **2009**, *131*, 3166; o) Frank, E.; Schneider, G.; Kadar, Z.; Woelfling, J. *Eur. J. Org. Chem.* **2009**, 3544; p) Maemoto, M.; Kimishima, A.; Nakata, T. *Org. Lett.* **2009**, *11*, 4814; q) Tobisu, M.; Nakai, H.; Chatani, N. *J. Org. Chem.* **2009**, *74*, 5471; r) Mahoney, S. J.; Moon, D. T.; Hollinger, J.; Fillion, E. *Tetrahedron Lett.* **2009**, *50*, 4706; s) Barluenga, J.; Fernandez, A.; Rodriguez, F.; Fananas, F. J. *Chem. Eur. J.* **2009**, *15*, 8121; t) Mori, K.; Kawasaki, T.; Sueoka, S.; Akiyama, T. *Org. Lett.* **2010**, *12*, 1732; u) Jurberg, I. D.; Odabachian, Y.; Gagosz, F. *J. Am. Chem. Soc.* **2010**, *132*, 3543; v) Alajarin, M.; Bonillo, B.; Ortin, M. M.; Sanchez-Andrada, P.; Vidal, A.; Orenes, R. A. *Org. Biomol. Chem.* **2010**, *8*, 4690; w) Jin, T. N.; Himuro, M.; Yamamoto, Y. *J. Am. Chem. Soc.* **2010**, *132*, 5590; x) Richter, H.; Mancheno, O. G. *Eur. J. Org. Chem.* **2010**, 4460.

(6) For the formation of eight-membered rings via Vilsmeier intermediates, see: a) Meth-Cohn, O.; Taylor, D. L. *J. Chem. Soc., Chem. Commun.* **1995**, 1463; b) Cheng, Y.; Wang, B.; Meth-Cohn, O. *Synthesis* **2003**, 2839.

(7) a) Zhang, C.; De, C. K.; Mal, R.; Seidel, D. *J. Am. Chem. Soc.* **2008**, *130*, 416; b) Murarka, S.; Zhang, C.; Konieczynska, M. D.; Seidel, D. *Org. Lett.* **2009**, *11*, 129; c) Zhang, C.; Murarka, S.; Seidel, D. *J. Org. Chem.* **2009**, *74*, 419; d) Murarka, S.; Deb, I.; Zhang, C.; Seidel, D. *J. Am. Chem. Soc.* **2009**, *131*, 13226; e) Zhang, C.; Seidel, D. *J. Am. Chem. Soc.* **2010**, *132*, 1798; f) Deb, I.; Seidel, D. *Tetrahedron Lett.* **2010**, *51*, 2945; g) Zhang, C.; Das, D.; Seidel, D. *Chem. Sci.* **2011**, *2*, Advance Article DOI: 10.1039/C0SC00432D.

(8) For selected reviews on indole chemistry, see: a) Gribble, G. W. *J. Chem. Soc., Perkin Trans. 1* **2000**, 1045; b) Cacchi, S.; Fabrizi, G. *Chem. Rev.* **2005**, *105*, 2873; c) Humphrey, G. R.; Kuethe, J. T. *Chem. Rev.* **2006**, *106*, 2875; d) Bandini, M.; Eichholzer, A. *Angew. Chem., Int. Ed.* **2009**, *48*, 9608; e) Palmieri, A.; Petrini, M.; Shaikh, R. R. *Org. Biomol. Chem.* **2010**, *8*, 1259.

(9) a) Lee, L.; Snyder, J. K. In *Advances in Cycloaddition*; Harmata, M., Ed.; JAI: Stamford, CT, 1999; Vol. 6, p 119; b) Knolker, H. J.; Reddy, K. R. *Chem. Rev.* **2002**, *102*, 4303.

(10) For recent examples, see: a) Bajtos, B.; Yu, M.; Zhao, H. D.; Pagenkopf, B. L. *J. Am. Chem. Soc.* **2007**, *129*, 9631; b) Barluenga, J.; Tudela, E.; Ballesteros, A.; Tomas, M. *J. Am. Chem. Soc.* **2009**, *131*, 2096; c) Lian, Y. J.; Davies, H. M. L. *J. Am. Chem. Soc.* **2010**, *132*, 440; d) Repka, L. M.; Ni, J.; Reisman, S. E. *J. Am. Chem. Soc.* **2010**, *132*, 14418.

(11) For examples, see: a) Arcadi, A.; Bianchi, G.; Chiarini, M.; D'Anniballe, G.; Marinelli, F. *Synlett* **2004**, 944; b) Ferrer, C.; Amijs, C. H. M.; Echavarren, A. M. *Chem. Eur. J.* **2007**, *13*, 1358; c) Amijs, C. H. M.; Lopez-Carrillo, V.; Raducan, M.; Perez-Galan, P.; Ferrer, C.; Echavarren, A. M. *J. Org. Chem.* **2008**, *73*, 7721; d) Silvanus, A. C.; Heffernan, S. J.; Liptrot, D. J.; Kociok-Kohn, G.; Andrews, B. I.; Carbery, D. R. *Org. Lett.* **2009**, *11*, 1175; e) Lu, Y. H.; Du, X. W.; Jia, X. H.; Liu, Y. H. *Adv. Synth. Catal.* **2009**, *351*, 1517.

(12) a) Alves, F. R. D.; Barreiro, E. J.; Fraga, C. A. M. *Mini-Rev. Med. Chem.* **2009**, *9*, 782; b) Welsch, M. E.; Snyder, S. A.; Stockwell, B. R. *Curr. Opin. Chem. Biol.* **2010**, *14*, 347; c) Kochanowska-Karamyan, A. J.; Hamann, M. T. *Chem. Rev.* **2010**, *110*, 4489.

(13) a) Kobayashi, J.; Sekiguchi, M.; Shimamoto, S.; Shigemori, H.; Ishiyama, H.; Ohsaki, A. *J. Org. Chem.* **2002**, *67*, 6449; b) Enzensperger, C.; Lehmann, J. *J. Med. Chem.* **2006**, *49*, 6408; c) Lim, K. H.; Kam, T. S. *Org. Lett.* **2006**, *8*, 1733; d) Sharma, S. K.; Sharma, S.;

Agarwal, P. K.; Kundu, B. *Eur. J. Org. Chem.* **2009**, 1309; e) Lundquist, J. T. el al.: *J. Med. Chem.* **2010**, *53*, 1774; f) Stewart, S. G.; Ghisalberti, E. L.; Skelton, B. W.; Heath, C. H. *Org. Biomol. Chem.* **2010**, *8*, 3563; g) Chen, P.; Cao, L.; Tian, W.; Wang, X.; Li, C. *Chem. Commun.* **2010**, *46*, 8436.

(14) Shiri, M.; Zolfigol, M. A.; Kruger, H. G.; Tanbakouchian, Z. *Chem. Rev.* **2010**, *110*, 2250.

(15) While the results in Table 1 indicate that catalyst pKa is certainly important, there appears to be no direct correlation between catalyst activity and acidity. Acids with similar pKa's (e.g., DPP and phosphoric acid) gave vastly different results. We thus speculate that catalyst reactivity might be partially dependent on catalyst solubility in the non-polar reaction medium (or on the corresponding solubility of protonated starting material/product).

(16) Related furan containing compounds have been prepared from relatively complex starting materials via an intriguing gold catalyzed cascade reaction that involves a 1,5-hydride shift: Zhou, G.; Zhang, J. *Chem. Commun.* **2010**, *46*, 6593.

(17) No reduction of **17** was observed in the absence of **12a**.

Chapter 2.2 Experimental Section

General Information: Reagents and solvents were purchased from commercial sources and were used as received. Microwave reactions were carried out in a CEM Discover reactor. Silicon carbide (SiC) passive heating elements were purchased from Anton Paar. Purification of reaction products was carried out by flash chromatography using Sorbent Technologies Standard Grade silica gel (60 Å, 230–400 mesh). Analytical thin layer chromatography was performed on EM Reagent 0.25 mm silica gel 60 F_{254} plates. Visualization was accomplished with UV light and PMA stain, followed by heating. Melting points were recorded on a Thomas Hoover capillary melting point apparatus and are uncorrected. Infrared spectra were recorded on an ATI Mattson Genesis Series FT-Infrared spectrophotometer. Proton nuclear magnetic resonance spectra (^{1}H-NMR) were recorded on a Varian VNMRS-500 MHz and Varian VNMRS-400 MHz instrument and are reported in ppm using the solvent as an internal standard ($CDCl_3$ at 7.26 ppm, $(CD_3)_2SO$ at 2.50 ppm, $(CD_3)_2CO$ at 2.05 ppm). Data are reported as app = apparent, s = singlet, d = doublet, t = triplet, q = quartet, m = multiplet, comp = complex, br = broad; coupling constant(s) in Hz. Proton-decoupled carbon nuclear magnetic resonance spectra (^{13}C-NMR) spectra were recorded on a Varian VNMRS-500 MHz and Varian VNMRS-400 MHz instrument and are reported in ppm using the solvent as an internal standard ($CDCl_3$ at 77.0 ppm, $(CD_3)_2SO$ at 39.5 ppm, $(CD_3)_2CO$ at 29.8 ppm). Mass spectra were recorded on a Finnigan LCQ-DUO mass spectrometer. The starting materials 2-(3,4-dihydroisoquinolin-2(1H)-yl)benzaldehyde[1] (**9a**), 2-(pyrrolidin-1-yl)benzaldehyde[2], 2-(piperidin-1-yl)benzaldehyde[2], 2-(azepan-1-yl)benzaldehyde[3], 2-(2-methylpiperidin-1-yl) benzaldehyde[2], 2-(2-methylpyrrolidin-1-yl) benzaldehyde[2], 2-(6,7-dimethoxy-3,4-

dihydroisoquinolin-2(1H)-yl)benzaldehyde[1], 2-(9-methyl-3,4-dihydro-1H-pyrido[3,4-b]indol-2(9H)-yl)benzaldehyde[4], and 2,3,4,5-tetrahydro-1H-benzo[c]azepine[5] were prepared according to literature procedures.

2-(4,5-dihydro-1*H*-benzo[c]azepin-2(3*H*)-yl)benzaldehyde (13h):

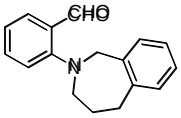

Starting from 2-fluorobenzaldehyde and 2,3,4,5-tetrahydro-1H-benzo[c]azepine, the title compound was prepared according to a literature procedure[1] and isolated as a yellow solid in 70 % yield, mp 80–83 ºC (R_f = 0.3 Hexanes/EtOAc 9:1 v/v); IR (KBr) 3061, 2926, 2741, 1677, 1590, 1481, 1444, 1385, 1349, 1269, 1191, 1086, 931, 888, 755 cm^{-1}; ^1H NMR (500 MHz, $CDCl_3$) δ 10.17 (s, 1H), 7.8 (app dd, *J* = 7.5, 1.5 Hz, 1H), 7.44 (ddd, *J* = 9.0, 7.2, 1.7 Hz, 1H), 7.15–7.23 (comp, 4H), 7.12 (app d, *J* = 6.2 Hz, 1H), 7.03 (app t. *J* = 7.4 Hz, 1H), 4.38 (s, 2H), 3.59 (t, *J* = 5.5 Hz, 2H), 3.01 (t, *J* = 5.5 Hz, 2H), 2.00 (quintet, *J* = 5.0 Hz, 2H); ^{13}C NMR (125 MHz, $CDCl_3$) δ 192.1, 156.9, 142.1, 138.8, 134.5, 129.6, 129.4, 128.9, 128.3, 127.5, 126.4, 121.4, 119.6, 62.7, 59.1, 34.7, 28.7; *m/z* (ESI-MS) 252.3 $[M+H]^+$.

General Procedure A:

A 10 mL microwave reaction tube was charged with indole (0.275 mmol, 1.1 equiv.), aminobenzaldehyde (0.25 mmol, 1.0 equiv.), toluene (2.5 mL), diphenyl phosphate (0.05 mmol, 0.2 equiv.) and a Teflon stir bar. The reaction tube was sealed with a Teflon-lined snap cap, and heated in the microwave reactor at 150 ºC (250 W, 25–50 psi) for the appropriate time under efficient stirring (setting = "HIGH"). After cooling with compressed air flow, the crude reaction mixture was diluted with EtOAc (5 mL) and washed with saturated aqueous $NaHCO_3$ (3 x 5 mL). The aqueous layers were extracted with EtOAc (3 x 5 mL) and the combined organic layers dried over anhydrous Na_2SO_4. The resulting solution was adsorbed on Celite, the solvent was removed in vacuo, and the Celite was loaded onto a column for purification.

General Procedure B:

A 10 mL microwave reaction tube was charged with indole (0.275 mmol, 1.1 equiv.), aminobenzaldehyde (0.25 mmol, 1.0 equiv.), toluene (2.5 mL), diphenyl phosphate (0.05 mmol, 0.2 equiv.) and a Teflon stir bar. The reaction mixture was stirred for 1 min at room temperature, and the stir bar was removed. A 10 x 8 mm SiC passive heating element was carefully added to the reaction tube. The reaction tube was sealed with a Teflon-lined snap cap, and heated in the microwave reactor at 200 ºC, (250 W, 50–100 psi) for the appropriate time. (***Note: SiC passive heating elements must not be used in conjunction with stir bars; they may score glass and cause vessel failure***). The reaction was worked up as in general procedure A.

Characterization data:

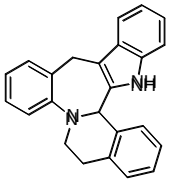

6,12,17,17b-tetrahydro-5H-benzo[6,7]indolo[2',3':3,4]azepino[2,1-a]isoquinoline (12a):

Following general procedure A, compound **12a** was obtained as an orange solid in 83% yield. mp 164–167 ºC; R_f = 0.25 (Hexanes/EtOAc 95:5 v/v); IR (KBr) 3401, 3056, 2921, 1607, 1486, 1454, 1332, 1148, 1043, 942, 746 cm^{-1}; ^1H NMR (500 MHz, $CDCl_3$) δ 7.63–7.61 (m, 1H), 7.56 (br s, 1H), 7.33–7.27 (comp, 6H), 7.23–7.19 (comp, 2H), 7.13–7.08 (comp, 3H), 5.49 (s, 1H), 4.39 (d, *J* = 16.8 Hz, 1H), 4.12 (d, *J* = 16.8 Hz, 1H), 3.65 (ddd, *J* = 11.4, 7.4, 4.6 Hz, 1H), 3.42 (app dt, *J* = 11.4, 5.5 Hz, 1H), 3.10 (app dt, *J* = 15.9, 6.1 Hz, 1H), 2.97 (app dt, *J* = 15.9, 5.5 Hz, 1H); ^{13}C NMR (125 MHz, $CDCl_3$) δ 151.6, 138.3, 136.6, 136.1, 135.3, 130.2, 129.8, 129.8, 128.5, 127.6, 127.5, 126.7, 126.4, 126.1, 125.2, 121.7, 119.6, 118.2, 110.9, 109.3, 60.3, 47.0, 30.9, 30.3; *m/z* (ESI-MS) 335.3 $[M-H]^+$.

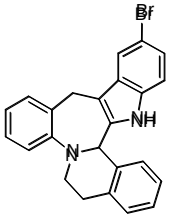

14-bromo-6,12,17,17b-tetrahydro-5H-benzo[6,7]indolo[2',3':3,4]azepino[2,1-a]isoquinoline (12e): Following general procedure A using 2.0 equiv. of indole, compound **12e** was obtained as an orange solid in 54% yield. mp 207–210 ºC; R_f = 0.54 (Hexanes/EtOAc 9:1 v/v); IR (KBr) 3443, 3021, 2914, 2826, 1586, 1456, 1372, 1290, 1224, 1145, 1045, 943, 861, 796, 752, 579, 431 cm^{-1}; ^1H NMR (500 MHz, $CDCl_3$) δ 7.74 (app d, *J* = 1.5 Hz, 1H), 7.68 (br s, 1H), 7.34–7.28 (comp, 7H), 7.23 (app td, *J* = 7.5, 1.1 Hz, 1H), 7.16 (app dd, *J* = 8.5, 1.5 Hz, 1H), 7.11 (app dt, *J* = 7.5, 1.1 Hz, 1H), 7.07 (app d, *J* = 8.5 Hz, 1H), 5.45 (s, 1H), 4.34 (d, *J* = 16.7 Hz, 1H), 4.02 (d, *J* = 16.7 Hz, 1H), 3.61 (ddd, *J* = 11.2, 6.9, 4.6 Hz, 1H), 3.42 (app dt, *J* = 11.2, 6.0 Hz, 1 H), 3.08 (ddd, *J* =

16.0, 6.9, 5.4 Hz, 1H), 2.99 (app dt, *J* = 16.0, 5.4 Hz, 1H); ^{13}C NMR (125 MHz, $CDCl_3$) δ 151.5, 140.0, 136.8, 136.7, 135.7, 133.8, 130.3, 130.3, 129.7, 127.7, 127.7, 126.7, 126.5, 125.9, 125.3, 124.4, 120.9, 112.9, 112.4, 109.1, 60.3, 40.1, 30.9, 30.2; *m/z* (ESI-MS) 413.4 $[M-H]^+$.

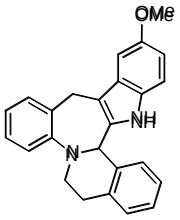

14-methoxy-6,12,17,17b-tetrahydro-5H-benzo[6,7]indolo[2',3':3,4]azepino[2,1-a]isoquinoline (12b): Following general procedure A, compound **12b** was obtained as a light yellow solid in 54% yield. mp = 160–162 ºC; R_f = 0.30 (Hexanes/EtOAc 9:1 v/v); IR (KBr) 3449, 33.95, 2924, 2824, 1590, 1482, 1449, 1285, 1212, 103, 1031, 906, 824 cm^{-1}; ^{1}H NMR (500 MHz, $CDCl_3$) δ 7.62 (s, 1H), 7.50 (app d, *J* = 7.5 Hz, 1H), 7.46 (app dd, *J* = 5.5, 3.4 Hz, 2H), 7.41–7.45 (comp, 3H), 7.39 (app dt, *J* = 7.1, 1.5 Hz, 1H), 7.28 (app dd, *J* = 7.4, 1.4 Hz, 1H), 7.24 (app d, *J* = 7.1 Hz, 2H), 6.95 (app dd, *J* = 8.6, 2.5 Hz, 1H), 5.61 (s, 1H), 4.53 (d, *J* = 16.6 Hz, 1H), 4.24 (d, *J* = 16.6 Hz, 1H), 4.06 (s, 3H), 3.79 (ddd, *J* = 11.3, 7.2, 4.6 Hz, 1H), 3.56 (app dt *J* = 11.3, 5.4 Hz, 1H), 3.24 (ddd, *J* = 15.7, 7.2, 5.5 Hz, 1H), 3.12 (app dt, *J* = 15.7, 5.5 Hz, 1H); ^{13}C NMR (125 MHz, $CDCl_3$) δ 154.0, 151.3, 137.8, 136.2, 135.9, 135.7, 130.1, 129.9, 129.5, 128.6, 127.2, 127.1, 126.4, 126.0, 125.6, 124.7, 111.4, 111.3, 108.9, 100.1, 60.0, 55.9, 46.9, 30.5, 30.1; *m/z* (ESI-MS) 365.2 $[M-H]^+$.

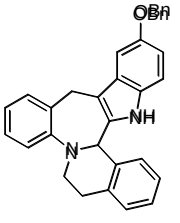

14-benzyloxy-6,12,17,17b-tetrahydro-5H-benzo[6,7]indolo[2',3':3,4]azepino[2,1-a]isoquinoline (12c): Following general procedure A, compound **12c** was obtained as a yellow solid in

65% yield. mp = 101–103 ºC; Rf = 0.40 (Hexanes/EtOAc 7:3 v/v); IR (KBr)) 3446, 2919, 1626, 1482, 1454, 1376, 1285, 1195 cm^{-1}; ^{1}H NMR (500 MHz, $(CD_3)_2SO$) δ 10.67 (s, 1H), 7.48 (app d, *J* = 7.2 Hz, 2H), 7.39 (app t, *J* = 6.7 Hz, 2H), 7.32 (app dt, *J* = 7.4, 1.3 Hz, 1H), 7.26–7.08 (comp, 9 H), 6.88 (app dt, *J* = 6.9, 1.9 Hz, 1H), 6.75 (app dd, *J* = 8.0, 2.0 Hz, 1H), 5.37 (s, 1H), 5.12 (dd, *J* = 16.4, 11.9 Hz, 2H), 4.09 (d, *J* = 14.2 Hz, 1H), 3.77 (d, *J* = 14.1 Hz, 1H), 3.60 (ddd, *J* = 12.0, 6.2, 3.7 Hz, 1H), 3.50 (ddd, *J* = 14.1, 5.4, 8.9 Hz, 1H), 3.11 (app dt, *J* = 16.2, 7.4 Hz, 1H), 2.96 (app dt, *J* = 16.2, 3.7 Hz, 1H); ^{13}C NMR (125 MHz, $(CD_3)_2SO$) δ 152.2, 149.9, 140.8, 137.8, 137.1, 134.9, 134.5, 130.3, 128.9, 128.3, 127.6, 127.5, 127.1, 126.8, 126.7, 126.6, 126.4, 125.6, 123.0, 122.7, 111.7, 111.2, 110.7, 101.4, 69.5, 61.4, 49.2, 29.6, 27.9; *m/z* (ESI-MS) 441.2 $[M-H]^+$.

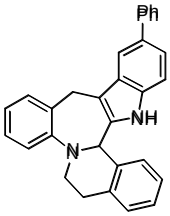

14-phenyl-6,12,17,17b-tetrahydro-5H-benzo[6,7]indolo[2',3':3,4]azepino[2,1-a]isoquinoline (12d): Following general procedure A, compound **12d** was obtained as a white solid in 54% yield. mp = 135–138 ºC; Rf = 0.25 (Hexanes/EtOAc 9:1 v/v); IR (KBr) 3449, 2919, 1597, 1488, 1469, 1453, 761, 750, 698 cm^{-1}; ^{1}H NMR (500 MHz, $CDCl_3$) δ 7.83 (app d, *J* = 1.5 Hz, 1H), 7.68 (app dt, *J* = 8.1, 1.5 Hz, 2H), 7.60 (br s, 1H), 7.45 (app t, *J* = 7.5 Hz, 2H), 7.40–7.27 (comp, 9H), 7.23 (app dt, *J* = 7.4, 1.4 Hz, 1H), 7.11 (app dt, J = 7.4, 1.4 Hz, 1H), 5.51 (s, 1H), 4.43 (d, *J* = 16.8 Hz, 1H), 4.22 (d, *J* = 16.8 Hz, 1H), 3.67 (ddd, *J* = 11.4, 7.3, 5.2 Hz, 1H), 3.44 (app dt, *J* = 11.4, 5.2 Hz, 1H), 3.11 (ddd, *J* = 15.9, 7.3, 5.2 Hz, 1H), 2.98 (app dt, *J* = 15.9, 5.2 Hz, 1H); ^{13}C NMR (125 MHz, $CDCl_3$) δ 151.3, 142.7, 137.9, 136.3, 135.8, 135.7, 134.4, 133.0, 130.0, 129.6, 128.8, 128.6,

127.4, 127.4, 127.3, 126.5, 126.2, 126.2, 125.9, 125.0, 121.3, 116.5, 110.9, 109.4, 60.06, 46.8, 30.6, 30.1; *m/z* (ESI-MS) 411.3 $[M-H]^+$.

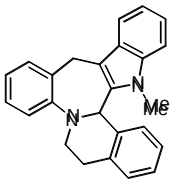

17-methyl-6,12,17,17b-tetrahydro-5H-benzo[6,7]indolo[2',3':3,4]azepino[2,1-a]isoquinoline (12f): Following general procedure A using 0.5 equiv. diphenyl phosphate, compound **12f** was obtained as a yellow solid in 62% yield. mp = 164–167 ºC; Rf = 0.71 (Hexanes/EtOAc 9:1 v/v); IR (KBr) 3416, 3055, 2922, 2807, 1600, 1478, 1369, 1257, 1130, 1049, 933, 744, 653, 554 cm^{-1}; ^1H NMR (400 MHz, $CDCl_3$) δ 7.71 (app dt, *J* = 9.8, 1.1 Hz, 1H), 7.32 (app d, *J*=10.0 Hz, 1H), 7.27–7.19 (comp, 3H) 7.16 (app tt, *J* = 10.0, 1.2 Hz, 2H), 7.05 (app td, *J* = 9.8, 2.0 Hz, 1H), 7.0 (app t, *J* = 7.3 Hz, 1H), 6.91 (app dd, *J* = 9.1, 0.9 Hz, 1 H), 6.57 (d, *J* = 9.7 Hz, 1H), 5.42 (s, 1H), 4.20 (d, 17.8 Hz, 1H) 3.93–3.85 (comp, 3H), 3.64 (s, 3H), 3.37 (app dt, *J* = 17.1, 8.4 Hz, 1H), 3.17 (ddd, *J* = 8.6, 5.5, 3.5 Hz, 1H); ^{13}C NMR (100 MHz, $CDCl_3$) δ 149.2, 141.1, 138.2, 135.2, 128.9, 127.5, 127.2, 126.7, 126.25, 125.7, 122.5, 121.6, 121.5, 119.4, 118.3, 113.4, 109.2, 61.64, 51.1, 30.4, 29.1, 28.7 ; *m/z* (ESI-MS) 349.5 $[M-H]^+$.

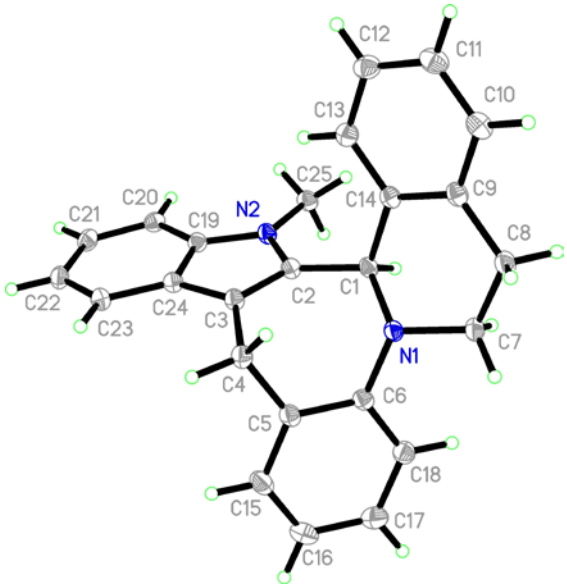

Compound **12f** was further characterized by X-ray crystallography. Suitable orange

crystals were grown from the vapor phase of a DCM/ether solution of the compound over several days at room temperature. The requisite CIF file has been deposited with the CCDC (deposition # 795970).

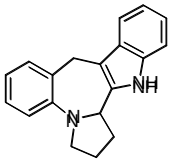

1,2,3,9,14,14b-hexahydrobenzo[6,7]pyrrolo[1',2':1,2]azepino[3,4-b]indole (14c): Following general procedure A using 0.5 equiv. diphenyl phosphate, compound **14c** was obtained as a white solid in 67% yield. mp = 121–124 ºC; R_f = 0.20 (Hexanes/EtOAc 9:1 v/v); IR (KBr) 3407, 2954, 1491, 1465, 1453, 1331, 1263, 1156, 741 cm^{-1}; ^1H NMR (500 MHz, $CDCl_3$) δ 7.69-7.63 (m, 1H), 7.61 (s, 1H), 7.31–7.19 (comp, 3H), 7.19–7.10 (comp, 3H), 6.98 (app t, *J* = 7.3 Hz, 1H), 4.31 (d, *J* = 15.0 Hz, 1H), 3.98 (app t, *J* = 8.2 Hz, 1H), 3.82 (d, *J* = 15.0 Hz, 1H), 3.42 (app dd, *J* = 17.4, 8.8 Hz, 1H), 3.32 (app dt, *J* = 6.5, 2.3 Hz, 1H), 2.53–2.39 (m, 1H), 2.18–2.00 (comp, 3H); ^{13}C NMR (125 MHz, $CDCl_3$) δ 148.0, 137.4, 135.8, 135.5, 128.6, 127.3, 126.9, 122.9, 121.3, 119.3, 118.3, 117.9, 110.3, 108.7, 61.6, 50.9, 32.4, 28.9, 21.8; *m/z* (ESI-MS) 275.5 $[M+H]^+$.

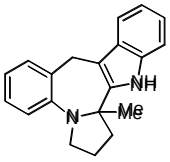

14b-methyl-1,2,3,9,14,14b-hexahydrobenzo[6,7]pyrrolo[1',2':1,2]azepino[3,4-b]indole (14e): Following general procedure A, compound **14e** was obtained as a white solid in 76% yield. mp = 87–92 ºC; R_f = 0.23 (Hexanes/EtOAc 9:1 v/v); IR (KBr) 3452, 3399, 2927, 2826, 1590,1484, 1451, 1215, 1095, 1031, 760, 731 cm^{-1}; ^1H NMR (500 MHz, $CDCl_3$) δ 7.71–7.63 (m, 1H), 7.57 (br s, 1H), 7.34–7.27 (comp, 2H), 7.24–7.19 (comp, 2H), 7.18–7.14 (comp, 2H), 7.00 (app td, *J* = 7.0, 1.8 Hz, 1H), 4.30 (d, *J* = 16.0 Hz, 1H), 3.83 (d, *J* = 16.0 Hz, 1H), 3.73 (app dd, *J* = 17.0, 9.0 Hz, 1H), 3.25 (ddd, *J* =10.0, 7.0, 3.0 Hz, 1H), 2.42 (ddd, *J* = 12.0 10.0, 6.0 Hz , 1H), 2.28–2.16 (m, 1H), 2.13–1.94 (comp, 2H), 1.19 (s, 3H); ^{13}C NMR (125 MHz, $CDCl_3$) δ 146.3, 140.8, 137.9, 135.3, 128.8, 127.4, 126.4, 123.0, 121.5, 121.2, 119.2, 118.0, 110.3, 107.1, 62.9, 48.2, 40.0, 29.3, 23.1, 21.4; *m/z* (ESI-MS) 289.4 $[M+H]^+$.

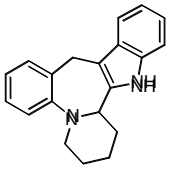

2,3,4,10,15,15b-hexahydro-1H-benzo[6,7]pyrido[1',2':1,2]azepino[3,4-b]indole (14d): Following general procedure B, compound **14d** was obtained as a light green solid in 58% yield. mp = 100–105 ºC; R_f = 0.52 (Hexanes/EtOAc 9:1 v/v); IR (KBr) 3405, 3055, 2931, 2853, 2356, 1608, 1454, 1339, 1242, 1111, 1054, 941, 835, 746, 613, 478 cm^{-1}. ^1H NMR (500 MHz) δ 7.61–7.60 (m, 1H), 7.56 (br s, 1H), 7.21–7.08 (comp, 6H), 6.88 (app td, *J* = 1.0, 7.1 Hz, 1H), 4.44 (d, *J* = 14.0 Hz, 1H), 3.91 (app d, *J* = 10.0 Hz, 1H), 3.60 (d, *J* = 14.0 Hz, 1H), 3.37 (app d, *J* = 11.4 Hz, 1H), 3.19 (app td, *J* = 1.5, 11.4 Hz, 1H), 2.08 (app d, *J* = 13.1 Hz 1H), 1.96–1.85 (comp, 3H), 1.82–1.74 (m, 1H), 1.62–1.58 (m, 1H); ^{13}C NMR (125 MHz, $CDCl_3$) δ 150.8, 142.7, 136.1, 135.0, 127.4, 127.0, 126.7, 122.9, 121.4, 121.0, 119.5, 117.9, 111.7, 110.6, 62.6, 53.5, 36.4, 27.9, 26.8, 25.0; *m/z* (ESI-MS) 287.2 $[M-H]^+$

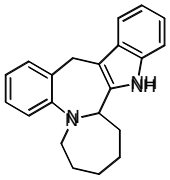

1,2,3,4,5,11,16,16b-octahydroazepino[1',2':1,2]benzo[6,7]azepino[3,4-b]indole (14g): Following general procedure A, compound **14g** was obtained as an orange solid in 57% yield. mp = 143–147 ºC; R_f = 0.70 (Hexanes/EtOAc 9:1 v/v); IR (KBr) 3394, 3059, 2926, 2864, 1611, 1455, 1330, 1250, 748; ^1H NMR ($CDCl_3$, 500 MHz) δ 7.62–7.61 (comp, 2H), 7.27–7.17 (comp, 4H), 7.12–7.10 (comp, 2H), 6.98 (app t, *J* = 6.9 Hz, 1H), 4.43 (app t, *J* = 4.7 Hz, 1H), 4.34 (d, *J* = 14.9 Hz, 1H), 3.81 (d, *J* = 14.9 Hz, 1H), 3.46 (app t, *J* = 5.2 Hz, 1H), 2.31–2.27 (m, 1H) 2.09–2.05 (m, 1H), 1.86–1.62 (comp, 7H); ^{13}C (125 MHz, $CDCl_3$) δ 152.8, 141.9, 137.3, 136.4, 135.4, 132.5, 128.0, 125.7, 124.2, 121.4, 119.4, 117.9, 111.6, 110.5, 61.0, 52.5, 34.8, 33.0, 29.2, 29.0, 24.4; *m/z* (ESI-MS) 301.3 $[M-H]^+$.

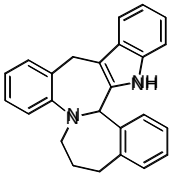

5,6,7,13,18,18b-hexahydrobenzo[6,7]benzo[3',4']azepino[1',2':1,2]azepino[3,4-b]indole (14h): Following general procedure A, compound **14h** was obtained as a light yellow solid in 90% yield. mp = 115–121 ºC; R_f = 0.30 (Hexanes/EtOAc 9:1 v/v); IR (KBr) 3403, 3055, 3017, 2929, 1849, 1489, 1455, 1363, 1322, 1236, 1157, 1146, 1133, 741, 483 cm^{-1}; ^1H NMR (500 MHz, $(CD_3)_2SO$) δ 10.54 (s, 1H), 7.72–7.56 (m, 1H), 7.31–7.15 (comp, 3H), 7.12–6.97 (comp, 3H), 6.93–6.84 (m, 1H), 6.80 (app td, *J* = 7.2, 2.5 Hz, 1H) 6.73 (app t, *J* = 7.5 Hz, 1H), 6.26 (s, 1H), 5.98 (app d, *J* = 7.5 Hz, 1H), 4.08 (d, *J* = 4.5 Hz, 1H), 4.02–3.80 (comp, 2H), 3.75– 3.48 (app dd, *J* = ? Hz, 2H), 2.96 (app dd, *J* = 12.8, 4.5 Hz, 1H), 2.25-2.12 (m, 1H), 1.86 (app d, *J* = 12.8 Hz, 1H); ^{13}C NMR (125 MHz, $(CD_3)_2SO$) δ 149.0, 141.5, 141.3, 137.9, 135.5, 134.1, 128.3, 128.3, 126.9, 126.7, 126.6, 126.5, 125.4, 122.8, 122.0, 120.6, 118.1, 117.5, 110.7, 109.5, 61.0, 57.0, 40.0, 39.9, 39.8, 39.7, 39.5, 39.4, 39.2, 39.0, 33.3, 29.2, 28.6; *m/z* (ESI-MS) 351.2 $[M+H]^+$.

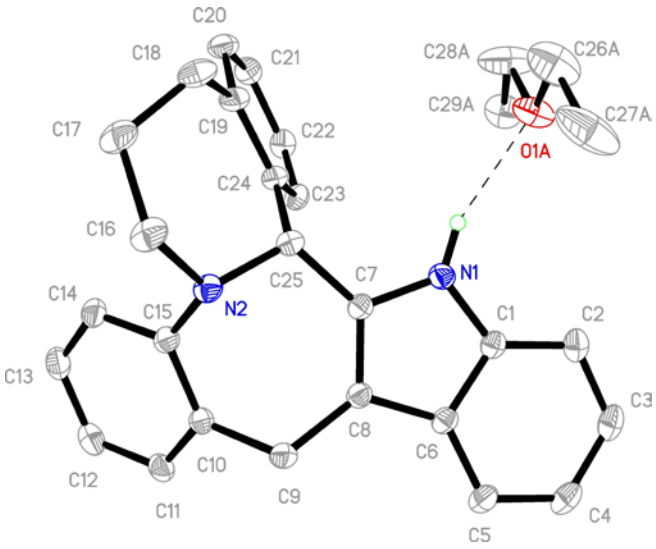

Compound **14h** was further characterized by X-ray crystallography. Suitable white crystals were grown from the vapor phase of an ether solution of the compound over one day at room temperature. The requisite CIF file has been deposited with the CCDC (deposition # 795971).

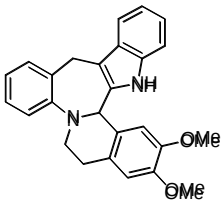

2,3-dimethoxy-6,12,17,17b-tetrahydro-5H-benzo[6,7]indolo[2',3':3,4]azepino[2,1-a]isoquinoline (14a): Following general procedure A, compound **14a** was obtained as a yellow solid in 43% yield. mp = 118–119 ºC; R_f = 0.40 (Hexanes/EtOAc 7:3 v/v); IR (KBr) 3371, 2921, 1605, 1514, 1454, 1365, 1338, 1256, 1113, 853, 743 cm^{-1}; ^1H NMR (500 MHz, $CDCl_3$) δ 7.63–7.61 (m, 1H), 7.56 (s, 1H), 7.31 (app d, *J* = 7.4 Hz, 1H), 7.25 (app d, *J* = 5.7 Hz, 1H), 7.23–7.19 (comp, 2H), 7.12 (app t, *J* =3.7 Hz, 2H), 7.08 (app t, *J* = 7.4 Hz, 1H), 6.80 (app s, 1H), 6.77 (app s, 1H), 5.49 (s, 1H), 4.36 (d, *J* = 17.1 Hz, 1H), 4.21 (d, *J* = 17.1 Hz, 1H), 3.91 (s, 3H), 3.90 (s, 3H), 3.56 (ddd *J* = 11.5, 8.3, 4.5 Hz, 1H), 3.39 (app dt, *J* = 11.1, 3.3, Hz 1H), 3.05 (ddd, *J* = 15.7, 8.0, 5.6 Hz, 1H), 2.85 (app dt, *J* = 15.7, 4.9 Hz, 1H); ^{13}C NMR (125 MHz, $CDCl_3$) δ 151.3, 148.4, 147.4, 136.5, 135.8, 134.8, 129.9, 128.5, 128.2, 127.2, 127.1, 126.2, 124.5, 121.4, 119.4, 117.9, 112.6, 110.7, 110.0, 108.9, 59.0, 56.4, 55.9, 47.1, 30.2, 30.1; *m/z* (ESI-MS) 395.3$[M-H]^+$.

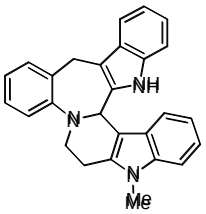

1-methyl-1,5c,6,9,15,16-hexahydrobenzo[6',7']indolo[2'',3'':3',4']azepino[1',2':1,2]pyrido[4,3-b] indole (14b): Following general procedure B, compound **14b** was obtained as a yellow solid in 52% yield. mp = 126–128 ºC; R_f = 0.40 (Hexanes/EtOAc 7:3 v/v); IR (KBr) 3436, 3051, 1606, 1460, 1368, 1339, 1273, 1230 cm^{-1}; ^1H NMR (500 MHz, $CDCl_3$) δ 7.62–7.66 (comp, 2H), 7.56 (s, 1H), 7.43 (app d, *J* = 8.2 Hz, 1H), 7.34–7.30 (comp, 2H), 7.23–7.20 (comp, 4H), 7.14 (ddd, *J* = 7.4, 3.8, 1.5 Hz, 2H), 7.05 (ddd, *J* = 8.0, 6.6, 2.0 Hz, 1H), 5.96 (s, 1H), 4.55 (d, *J* = 18.0 Hz, 1H), 4.34 (d, *J* = 18.0 Hz, 1H), 3.70 (s, 3H), 3.50 (app dd, *J* = 12.2, 5.6 Hz, 1H), 3.42 (app dt, *J* = 11.0, 3.8 Hz, 1H), 3.18 (ddd, *J* = 15.1, 3.8, 1.6 Hz, 1H), 2.83 (ddd, *J* = 12.1, 6.1, 1.6 Hz, 1H); ^{13}C NMR (125 MHz, $CDCl_3$) δ 151.1, 137.7, 135.0, 134.8, 133.4, 132.1, 131.3, 128.1, 128.0, 127.2 (x 2), 123.7, 121.8, 121.5, 119.7, 119.6, 118.6, 118.0, 111.0, 110.1, 109.3, 109.2, 52.4, 48.7, 30.3, 30.0, 23.2; *m/z* (ESI-MS) 388.3 $[M-H]^+$.

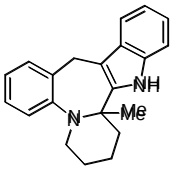

15b-methyl-2,3,4,10,15,15b-hexahydro-1H-benzo[6,7]pyrido[1',2':1,2]azepino[3,4-b]indole (14f): Following general procedure A, compound **14f** was obtained as a yellow liquid in 45% yield, as an inseparable mixture of regioisomers. ^1H NMR indicated a 20:3:2 ratio of the major regioisomer to the two diatereomers of the minor regioisomer. Data for the major regioisomer (pictured): R_f = 0.30 (Hexanes/EtOAc 9.5:0.5 v/v); IR (KBr) 3467, 3055, 2980, 2936, 1451, 1265, 1154, 1117, 896 cm^{-1}; ^1H NMR (500 MHz, $CDCl_3$) δ 7.61 (app dd, *J* = 5.9, 3.0 Hz, 1H), 7.58 (s, 1H), 7.26–7.24 (m, 1H), 7.20–7.18 (comp, 2H), 7.16–7.13 (comp, 2H), 7.11 (app dd, *J* = 5.9, 3.0 Hz, 1H), 7.00 (app dt, *J* = 7.6, 1.5 Hz, 1H), 4.43 (d, *J* = 15.5 Hz, 1H), 3.78 (d, *J* = 15.5 Hz, 1H), 3.30 (ddd, *J* = 11.4, 8.1, 3.5 Hz,

1H), 3.20 (ddd, *J* = 11.5, 6.5, 3.5 Hz, 1H), 2.12–2.06 (m, 1H), 1.94–1.89 (m, 1H), 1.81–1.75 (comp, 2H), 1.72–1.65 (comp 2H), 1.31 (s, 3H); ^{13}C NMR (125 MHz, $CDCl_3$) δ 149.4, 141.9, 140.3, 134.8, 128.1, 127.7, 127.3, 126.4, 124.3, 121.2, 119.2, 117.8, 110.3, 108.9, 58.1, 47.8, 40.3, 29.1, 26.9, 22.7, 21.5; *m/z* (ESI-MS) 303.2 $[M+H]^+$.

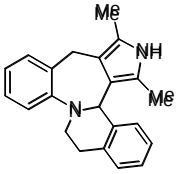

5,7-dimethyl-6,8,14,15-tetrahydro-4bH-benzo[6,7]pyrrolo[3',4':3,4]azepino[2,1-a]isoquinoline (15): Following general procedure A using 2.0 equiv. of 2,5-dimethylpyrrole, compound **15** was obtained as an orange solid in 59% yield. mp = 172–178 ºC; R_f = 0.23 (Hexanes/EtOAc 9:1 v/v); IR (KBr) 3427, 3410, 2909, 2852, 1487, 1448, 1257, 1220, 1219, 1134, 758, 740, 512 cm^{-1}; ^{1}H NMR (500 MHz, $CDCl_3$) δ 7.25–7.15 (comp, 3H), 7.15–7.10 (comp, 2H), 7.07 (app dd, *J* = 7.4, 1.6 Hz, 1H), 7.03 (app dd, *J* = 8.0, 1.0 Hz, 1H), 6.97 (app d, *J* = 7.6 Hz, 1H), 6.81 (app td, *J* = 7.4, 1.0 Hz, 1H), 5.44 (s, 1H), 3.80 (d, *J* = 14.6 Hz, 1H), 3.76 (app dt, *J* = 11.6, 5.5 Hz, 1H), 3.68 (d, *J* = 14.6 Hz, 1H), 3.62 (ddd, *J* = 13.1, 7.6, 5.9 Hz, 1H), 3.20–3.04 (comp, 2H), 2.22 (s, 3H), 1.85 (s, 3H); ^{13}C NMR (125 MHz, $CDCl_3$) δ 149.8, 139.1, 136.5, 135.3, 135.2, 128.7, 128.3, 126.6, 126.6, 126.2, 125.7, 122.9, 122.2, 121.0, 119.4, 117.4, 117.1, 59.5, 50.5, 30.6, 30.3, 11.4, 10.7; *m/z* (ESI-MS) 315.1 $[M+H]^+$.

1,2-diphenyl-1,2,3,9,10,14b-hexahydrobenzo[5,6][1,2,4]triazepino[3,4-a]isoquinoline (16) :

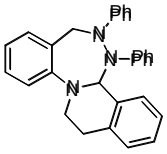

Following the general procedure A using 1.4 equiv. of 1,2-diphenylhydrazine and 0.05 equiv. of diphenyl phosphate, compound **16**

was obtained as an off-white solid in 72% yield. mp = 205–206 ºC; R_f = 0.86 (Hexanes/EtOAc 9:1 v/v); IR (KBr) 3444, 3025, 2930, 2893, 1590, 1489, 1358, 1281, 1228, 1147, 1097, 1033, 999, 957, 922, 870, 819, 753, 681, 553, 510, 422 cm^{-1}; ^1H NMR (500 MHz, $CDCl_3$) δ 7.70–7.68 (m, 1H), 7.40 (app dd, *J* = 2.3, 1.4 Hz, 1H), 7.29–7.15 (comp, 7H), 7.12–7.05 (comp, 4H), 6.96, (app dd, *J* = 3.5, 0.9 Hz, 2H), 6.91 (app td, J = 7.4, 0.8 Hz 1H) 6.82–6.76 (comp, 2H), 5.46 (s, 1H), 4.70 (dd, *J* = 14.6, 3.6 Hz, 2H), 4.04 (app dt, *J* = 14.0, 3.9 Hz, 1H), 3.69 (ddd, *J* =14.0, 11.5, 2.8 Hz, 1H), 3.14 (ddd, *J* = 15.3, 11.5, 4.2 Hz, 1H), 2.99 (app dt, *J* = 15.3, 2.8 Hz); ^{13}C NMR (100 MHz, $CDCl_3$) δ 153.1, 148.8, 146.3, 136.1, 135.0, 131.7, 129.50 129.3, 128.9, 128.5, 127.5, 127.4, 127.3, 121.3, 120.3, 119.3, 117.7, 117.8, 114.5, 77.4, 52.9, 47.1, 30.6; *m/z* (ESI-MS) 402.4 $[M-H]^+$.

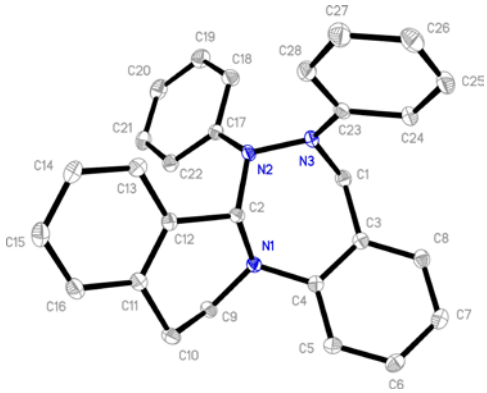

Compound **16** was further characterized by X-ray crystallography. Suitable white crystals were grown in solution by allowing ether to slowly evaporate from a 10% ether/hexanes solution of the compound over 5 hours at room temperature. The requisite CIF file has been deposited with the CCDC (deposition # 795972).

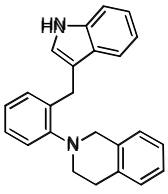

2-(2-((1H-indol-3-yl)methyl)phenyl)-1,2,3,4-tetrahydroisoquinoline (11a): A round bottom flask was charged with indole (0.250 mmol, 1.00 equiv), **9a** (0.275 mmol, 1.1 equiv), *n*BuOH (2.50 mL), 48% aqueous HBF_4 (0.300 mmol, 1.2 equiv), and a Teflon stir bar. The reaction mixture was refluxed for 24 h under efficient stirring, and worked up following the general procedures. Compound **11a** was obtained as a yellow oil in 61% yield. R_f = 0.3

(Hexanes/EtOAc 9:1 v/v); IR (KBr) 3417, 3054, 2919, 1591, 1489, 1453, 1376, 1218 cm^{-1}; ^1H NMR (500 MHz, $CDCl_3$) δ 7.91 (s, 1H), 7.52 (app d, *J* = 8.0 Hz, 1H), 7.35 (app d, *J* = 8.0 Hz, 1H), 7.24 (app d, *J* = 7.5 Hz, 1H), 7.22–7.21 (comp, 2H), 7.20–7.15 (comp, 4H), 7.06 (app dt, *J* = 7.9, 1.0 Hz, 2H), 7.03–6.99 (m, 1H), 6.91 (app t, *J* = 1.0 Hz, 1H), 4.24 (s, 2H), 4.19 (s, 2H), 3.27 (t, *J* = 5.6 Hz, 2H), 3.016 (t, *J* = 5.6 Hz, 2H); ^{13}C NMR (125 MHz, $CDCl_3$) δ 151.2, 136.4, 136.2, 135.5, 134.6, 130.5, 128.9, 127.7, 126.7, 126.4, 126.1, 125.6, 123.7, 122.3, 121.9, 119.9, 119.3, 119.2, 116.2, 110.9, 54.9, 51.1, 29.7, 26.2; *m/z* (ESI-MS) 337.3 $[M-H]^+$.

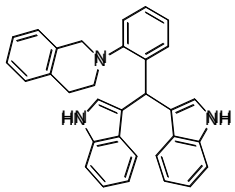

2-(2-(di(1H-indol-3-yl)methyl)phenyl)-1,2,3,4-tetrahydroisoquinoline (10a): A round bottom flask was charged with indole (1.00 mmol, 2.0 equiv), **9a** (0.500 mmol, 1.0 equiv), 5.00 mL of absolute EtOH, 48% aqueous HBF_4 (0.600 mmol, 1.2 equiv), and a Teflon stir bar. The reaction mixture was stirred at room temperature. After 48 hours, a brilliant orange precipitate formed. EtOH was removed in vacuo, and the reaction was worked up following the general procedures. Compound **10a** was obtained in 62% yield as an off-white solid. R_f = 0.18 (Hexanes/CH_2Cl_2 1:1 v/v); mp 154–158 ºC; IR (KBr) 3405, 3052, 2892, 2804, 1604, 1487, 1454, 1417, 1373, 1340, 1281, 1214, 1148, 1089, 1048, 1009, 936, 862, 744, 595, 465, 428 cm^{-1}; ^1H NMR (500 MHz, $(CD_3)_2CO$) δ 9.97 (br s, 2H), 7.41 (app dd, *J* = 7.8, 0.8 Hz, 1H), 7.37 (app d, *J* = 8.1 Hz, 2H), 7.33 (app dd, *J* = 8.1, 0.8 Hz, 1H), 7.30 (app d, *J* = 7.6 Hz, 2H), 7.21 (app td, *J* = 7.6, 1.6 Hz, 1H), 7.12–6.99 (comp, 6H), 6.89 (app d, *J* = 7.8 Hz, 1H), 6.85–6.82 (comp, 4H), 6.60 (s, 1H) 4.20 (s, 2H), 3.19 (t, *J* = 5.7 Hz, 2H), 2.90 (t, *J* = 5.7 Hz, 2H). ^{13}C NMR (500 MHz, $(CD_3)_2CO$) δ 150.9, 140.3, 137.5, 135.9, 134.6, 130.6, 128.9, 127.6, 126.8,

126.6, 126.2, 125.7, 123.7, 123.6, 121.4, 120.3, 120.0, 119.6, 118.6, 111.4, 55.2, 51.7, 33.2, 30.0; *m/z* (ESI-MS) 454.1 $[M+H]^+$.

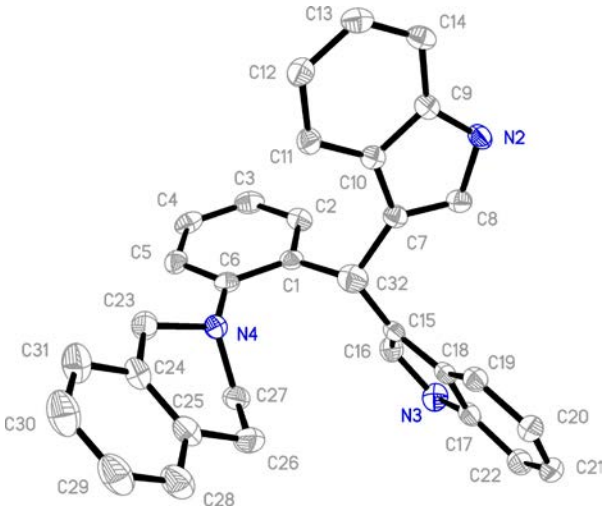

Compound **10a** was further characterized by X-Ray crystallography. Suitable colorless crystals were grown from the vapor phase of a DCM/ether solution of the compound at room temperature over one day. The requisite CIF file has been deposited with the CCDC (deposition # 796538).

Chapter 2.3 Experimental Section References

(1) W. H. N. Nijhuis, G. R. B. Leus, R. J. M. Egberink, W. Verboom, D. N. Reinhoudt, *Recl. Trav. Chim. Pays–Bas.* **1989**, *108*, 172–178.

(2) W. H. N. Nijhuis, W. Verboom, A. Abuelfadl, S. Harkema, D. N. Reinhoudt, *J. Org. Chem.* **1989**, *54*, 199–209.

(3) E. V. D'yachenko, T. V. Glukhareva, E. F. Nikolaenko, A. V. Tkachev, Yu. Yu. Morzherin, *Russ. Chem. Bull.* **2004**, *53*, 1240–1247.

(4) S. Murarka, I. Deb, C. Zhang, D. Seidel, *J. Am. Chem. Soc.* **2009**, *131*, 13226–13227.

(5) G. L. Grunewald, V. H. Dahunkar, P. Ching, K. R. Criscione, *J. Med. Chem.* **1996**, *39*, 3539–3546.

Chapter 3

C–H Activation and Olefin Isomerization by New Pincer Rhodium Complexes

Originally published as:

(POP)Rh pincer hydride complexes: unusual reactivity and selectivity in oxidative addition and olefin insertion reactions.

Michael C. Haibach, David Y. Wang, Thomas J. Emge, Karsten Krogh-Jespersen, Alan S. Goldman

Chemical Science **2013**, *4*, 3683-3692.

Introduction

Since their introduction by Shaw in 1976[1], complexes featuring pincer ligands have received much attention for their applications in fundamental organometallic chemistry, catalysis, and materials chemistry.[2] One particularly attractive application is in catalytic dehydrogenation, where pincer-Ir and Ru complexes occupy "privileged" status. For the most part, pincer-Ru chemistry has found applicability in the dehydrogenation of functionalized substrates[3] and pincer-Ir chemistry in alkane dehydrogenation.[4] (For a notable exception, see the recent work by Roddick on alkane dehydrogenation by (^{CF3}PCP)Ru(H).[5]) We have reported a tandem catalytic system for alkane metathesis that uses PCP- and POCOP-ligated Ir catalysts (Figure 3.3.1) for dehydrogenation and Schrock-type W and Mo olefin metathesis catalysts.[6] Currently, one bottleneck to improving catalytic activity in this system is catalyst interoperability; the pincer-Ir catalysts operate best at temperatures above 150 °C, at which temperature the preferred olefin metathesis catalysts have limited lifetimes. Partly for this reason, we are interested in the development of catalysts for alkane transfer dehydrogenation that operate at lower temperatures.

Figure 3.3.1 (PCP)M and (POCOP)M fragments

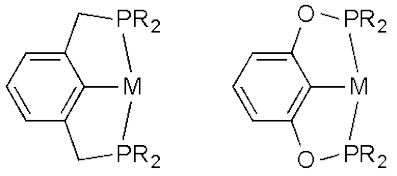

(^{R}PCP)M (^{R}POCOP)M

Since alkane transfer dehydrogenation is approximately thermoneutral there is no intrinsic barrier to development of a low-temperature alkane dehydrogenation catalyst. Earlier work in our group led to the development of efficient Rh-based precatalysts for thermochemical alkane dehydrogenation, $(PMe_3)_2RhClL$ and $[(PMe_3)_2Rh(\mu\text{-}Cl)]_2$, which operated at relatively low

temperature (ca. 50 °C)[7]. This class of complexes requires H_2 atmosphere to continuously regenerate a catalytically active species, $(PMe_3)_2RhCl(H)_2$, by cleavage of either the Rh-L bond or the di(μ-chloride) bridge. The presence of H_2 results in loss of multiple moles of acceptor (through simple hydrogenation) per mol of substrate dehydrogenated, thereby limiting practical applications. However, the fast kinetics of these systems are remarkable, particularly in view of the fact that most of the rhodium is in an inactive out-of-cycle state at any time; this suggested that we might attempt to emulate the stereoelectronic features of the $(PMe_3)_2RhCl$ fragment in a pincer-Rh complex, with the hope of creating an analogue which does not suffer from dimer formation.

Initial efforts towards this goal focused on the (PCP)Rh framework;[8] however these complexes showed very low activity for alkane dehydrogenation.[9] We soon realized that oxidative addition to (PCP)Rh was much less favorable than addition to the catalytically active $(PMe_3)_2RhCl$ fragment.[8-9] In order to understand the factors that govern the thermodynamics of H-H and C-H addition to these and related 3-coordinate complexes more generally, we have undertaken a combined theoretical and experimental study.[10] We found that in (PXP)Rh and Ir pincer complexes, the *trans* influence of the X-bound coordinating group exerts a very strong influence on oxidative addition thermodynamics. Strongly sigma-donating ligands were found to strongly *disfavor* oxidative addition, in contrast with the conventional view that electron-rich metal centers *favor* oxidative addition. The magnitude of this effect is easily large enough that a PXP ligand with decreased *trans* influence relative to the aryl group of PCP could be expected to afford a (PXP)Rh complex that could undergo addition of alkane C-H bonds and possibly act as a catalyst for alkane dehydrogenation.[10]

Figure 3.3.2 Selected PNP pincer complexes of rhodium

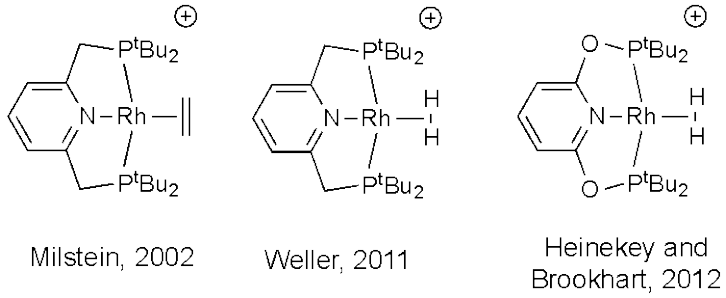

PNP complexes of rhodium have been investigated by several groups, particularly in the last few years (Figure 3.3.2). Milstein reported the synthesis of the cationic $(PN^{py}P)Rh(C_2H_4)^+$ complex and derivatives in his seminal report on the pyridine-based PNP ligand.[11] Rhodium complexes of the anionic $PN^{amido}P$ ligand,[12] have been synthesized and investigated in depth by Ozerov. Weller recently reported a variety of $(PN^{py}P)Rh(L)^+$ complexes;[13] notably, the $(PN^{py}P)Rh$ fragment was found not to oxidatively add H_2, instead forming the dihydrogen complex. Similar oxidative addition thermodynamics were detailed recently by Heinekey and Brookhart for the related $(PONOP)Rh(H_2)^+$ complex.[14] Most recently, Brookhart has prepared rhodium complexes of anionic PNP ligands derived from pyrrole and carbazole.[15]

Considering the lesser *trans*-influence of ethers versus N-ligating groups, we decided to investigate the relatively unexplored (POP)Rh class of complexes. In 1980, Timmer *et al.* investigated the reaction of $O(CH_2CH_2P^tBu_2)_2$ ($PO^{ether}P$) with a variety of rhodium precursors.[16] While these workers were unable to form complexes such as $(PO^{ether}P)RhCl$ or $(PO^{ether}P)Rh(olefin)^+$, the pincer complex $[(PO^{ether}P)Rh(CO)]OTf$ (Figure 3.3) was isolated and characterized by NMR and IR. This was the sole report of a pincer (POP)Rh complex until recently, when several groups reported pincer rhodium complexes of Xantphos. Weller reported Xantphos (^{Ph}xanPOP) rhodium complexes (Figure 3.3.3) bearing a $P(cyclo\text{-}C_5H_9)_3$ ligand and found the Xantphos ligand equilibrating between *fac* and *mer* coordination modes.[17] Haynes reported that (^{Ph}xanPOP)Rh iodide complexes catalyzed methanol carbonylation[18] while Hartwig

reported that the pincer complex (^{Me2N}xanPOP)Rh(NCMe)$^{+}$ catalyzes the intramolecular hydroamination of simple aminoalkenes.[19] In this article we report the synthesis and novel reactivity of several neutral and cationic (POP)Rh complexes, particularly hydride complexes, using a range of bulky, neutral POP ligands, and their relevance to rhodium catalyzed C-H activation.

Figure 3.3 Some previously reported (POP)Rh complexes

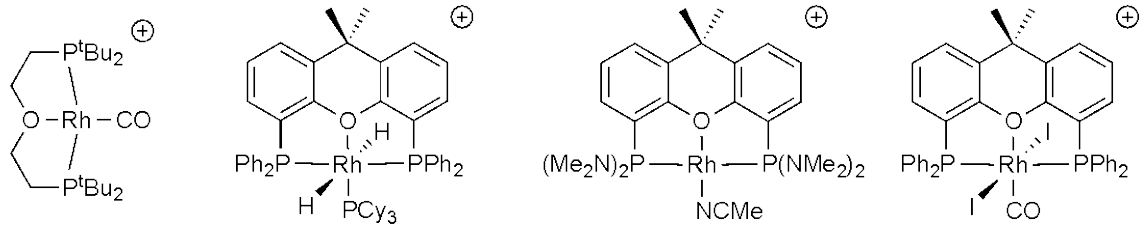

Timmer, 1988 Weller, 2012 Hartwig, 2010 Haynes, 2011

Results and Discussion

In light of the recent work reported with Xantphos derivatives, we decided to select ^{tBu}xanPOP as a starting point for this study (Figure 3.4). ^{tBu}xanPOP features the bulky (dimerization-inhibiting) and cyclometalation-resistant P^{t}Bu$_2$ groups that lend stability to the (PCP)Ir catalysts[4]. While it is commercially available, ^{tBu}xanPOP has seen limited application since its synthesis in 2005 by Perrio[20]. For reasons discussed below, we also studied the analogous ^{iPr}xanPOP (Figure 3.4) recently prepared by Asensio and Esteruelas in their study of (POP)Os and (POP)Ru complexes.[21]

Figure 3.4 Bulky, neutral POP ligands studied in this work

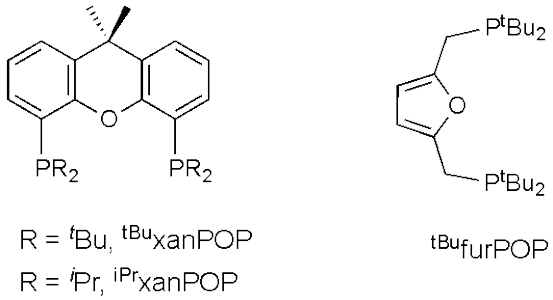

Given the high degree of crowding engendered by the xanthene ligand backbone, we also designed a furan-based ligand ^{tBu}furPOP.[22] Surprisingly, no phosphine pincer ligands using a furan backbone have been reported previously in the literature although 4,6-bis(phosphino)dibenzofurans[23] have been investigated, including 4,6-bis(diisopropylphosphino)dibenzofuran, reported by Asensio and Esteruelas.[21, 24] (^{Ph}furPOP is claimed in two 1980s patents dealing explicitly with *bidentate* ligands although no synthetic procedure is given.[25]) After some fruitless experimentation with attempted lithiation or free-radical bromination of 2,5-dimethylfuran, we arrived at a viable synthetic route to ^{tBu}furPOP, shown in eq 1. Commercially available 2,5-bis(hydroxymethyl)furan is converted to 2,5-bis(chloromethyl)furan according to Cook's protocol.[26] Phosphination occurs under mild

conditions (owing to the high reactivity of the bis(chloromethyl)furan), and after deprotonation of the bis(hydrochloride) salt, ^{tBu}furPOP is obtained as an air-sensitive solid in acceptable yield and high purity.

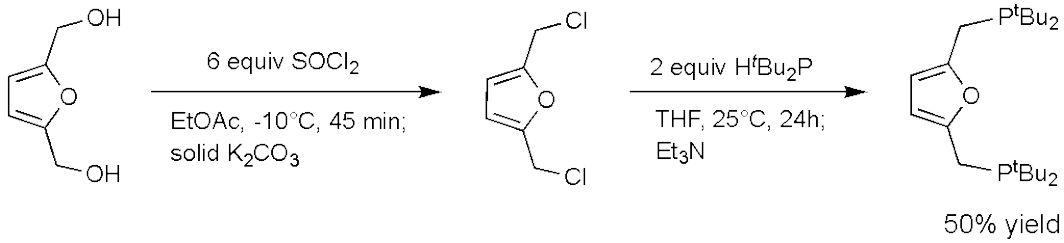

(1)

With the *t*-Bu_2P-substituted POP ligands in hand, we investigated their reactivity with Rh(I) precursors. Initial attempts at metalation of ^{tBu}xanPOP with $[Rh(NBD)Cl]_2$ (NBD = norbornadiene) resulted in no complexation, even at elevated temperatures. ^{tBu}furPOP reacted with $[Rh(NBD)Cl]_2$ at 25 °C to yield the undesired bimetallic complex (κ^2-^{tBu}furPOP)$[Rh(NBD)Cl]_2$ which was crystallographically characterized (Figure 3.5). Timmer obtained a similar complex in the reaction of PO^{ether}P with $[Rh(COD)Cl]_2$.[16]

Figure 3.5 X-ray structure of (κ^2-^{tBu}furPOP)$[Rh(NBD)Cl]_2$

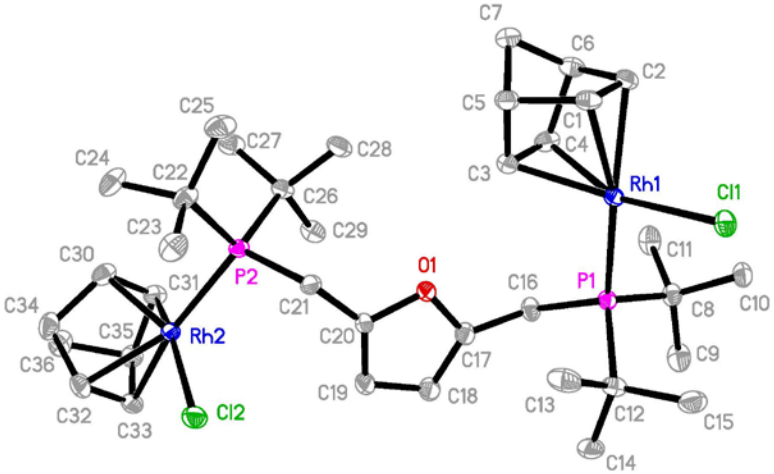

As in our group's modification of the synthesis of (^{tBu}PCP)Ir(H)Cl [27] we attempted to use H_2 to drive the reaction by hydrogenating the NBD ligands (Figure 3.6). Unfortunately, heating a solution of ^{tBu}xanPOP and $[Rh(NBD)Cl]_2$ under H_2 above 40 °C resulted in the formation of rhodium black within minutes; no metalated product was observed by ^{31}P NMR spectroscopy.

Figure 3.6 Initial metalation attempts and unexpected formation of (^{tBu}furPOP)Rh(H)$_2$Cl

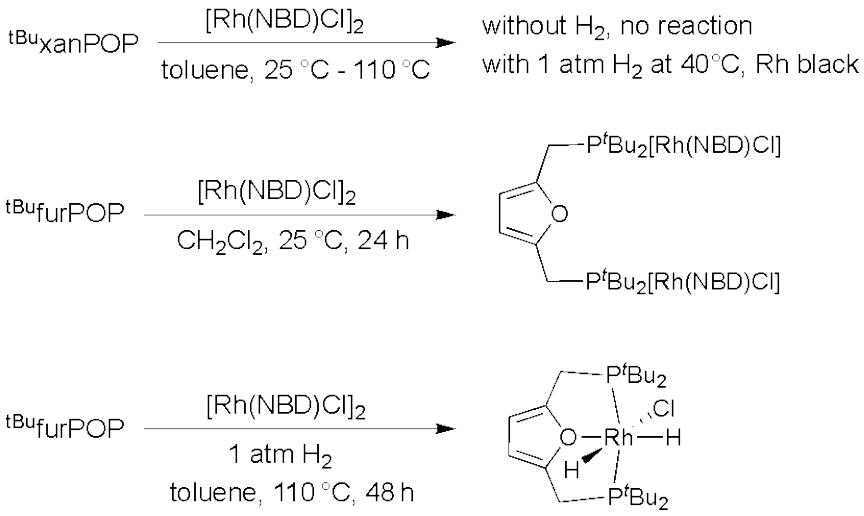

The same problem was not encountered with ^{tBu}furPOP, however, probably due to faster initial coordination with this more flexible ligand. Thus, refluxing ^{tBu}furPOP and $[Rh(NBD)Cl]_2$ in toluene for 48 hours under H_2 led to the formation of a metalated product in 54% yield. Surprisingly, the product was not the expected (^{tBu}furPOP)RhCl species but rather *cis*-(^{tBu}furPOP)Rh(H)$_2$Cl, as indicated by ^{1}H and ^{31}P NMR spectroscopy.

When the analogous reaction was carried out with the PN^{py}P ligand, (PN^{py}P)RhCl[11] was obtained in quantitative yield, suggesting that the stability of the ^{tBu}furPOP-ligated H_2 addition product derives from the reduced *trans* influence of furPOP relative to PN^{py}P. Nozaki has shown that *cis*-(PN^{py}P)Ir(H)$_2$Cl forms from PN^{py}P and $[Ir(COE)_2Cl]_2$ under similar conditions.[28] Hence, the (^{tBu}furPOP)Rh system seems closer in character to the PN^{py}P iridium complex in this respect than to the previously reported PN^{py}P rhodium systems.

Figure 3.7 Synthesis of monomeric (POP)RhCl complexes

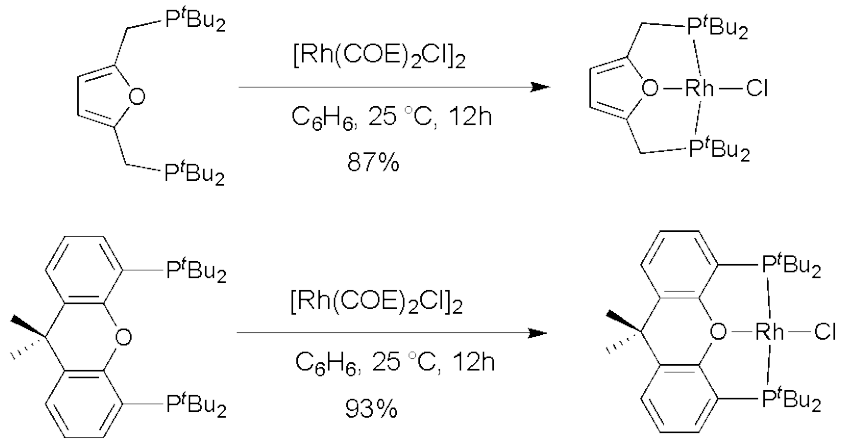

Using the more labile $[Rh(COE)_2Cl]_2$ precursor in lieu of $[Rh(NBD)Cl]_2$, we could obtain both (^{tBu}xanPOP)RhCl and (^{tBu}furPOP)RhCl in high yield (Figure 3.7). Both are monomeric pincer complexes as revealed by their X-ray structures (Figure 3.8). The slightly more acute O-Rh-P angles in (^{tBu}furPOP)RhCl relative to (^{tBu}xanPOP)RhCl (average of 82.2 ° vs. 83.6 °) reflect the difference between the five- and six-member oxygen-containing rings. In both cases the coordination environment is almost perfectly planar (the total of the four *cis*-L-Rh-L angles is 361° for both complexes).

Figure 3.8 X-ray structures of (^{tBu}xanPOP)RhCl and (^{tBu}furPOP)RhCl

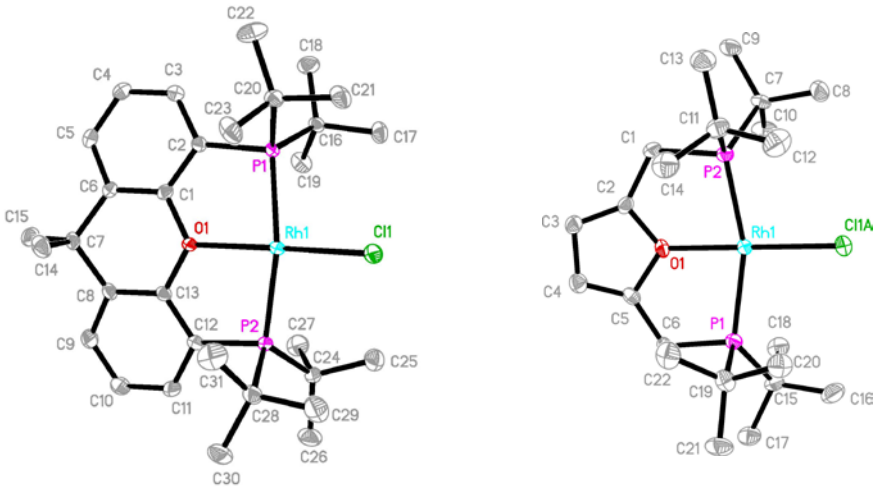

Figure 3.9 Oxidative addition of H_2 by (POP)RhCl complexes

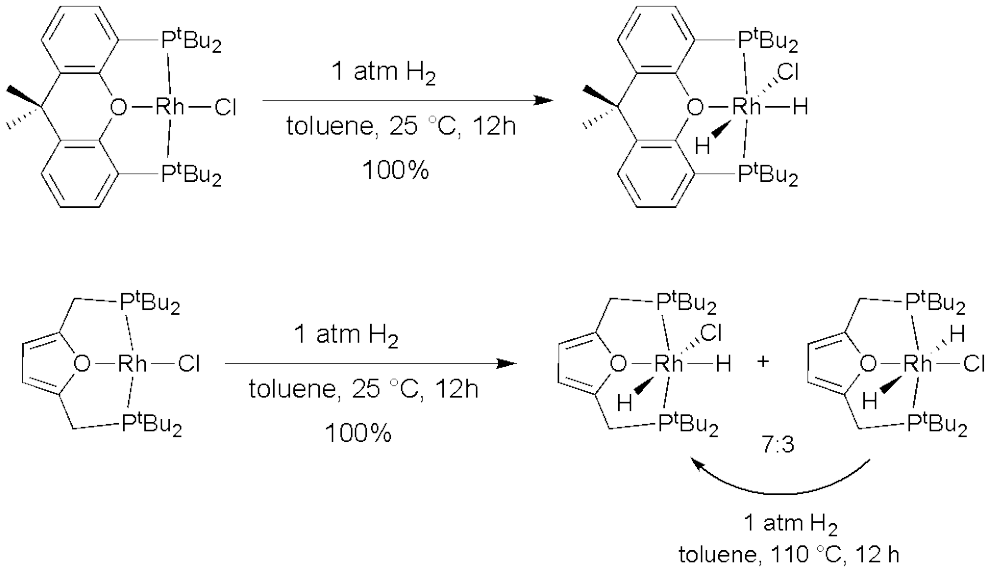

Both (^{tBu}xanPOP)RhCl and (^{tBu}furPOP)RhCl add H_2 at room temperature to afford the corresponding (POP)Rh(H)$_2$Cl complexes in high yield (Figure 3.9). (^{tBu}xanPOP)Rh(H)$_2$Cl is obtained as the *cis* dihydride isomer, as evident from the signals due to inequivalent hydrides and *t*-Bu groups in the ^{1}H NMR spectrum as well as its X-ray structure (Figure 3.10).

Figure 3.10 X-ray structure of *cis*-(^{tBu}xanPOP)RhH_2Cl

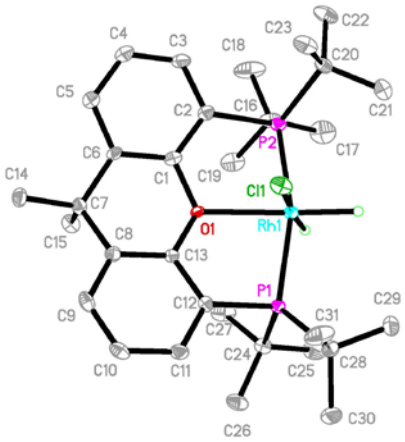

In contrast with the ^{tBu}xanPOP complex, when an atmosphere of H_2 is added to a toluene solution of (^{tBu}furPOP)RhCl at 25 °C, ^{1}H and ^{31}P NMR spectroscopy reveal full conversion to a 7:3 mixture of *cis*:*trans* dihydride isomers (see experimental section). DFT calculations of model PH_2-substituted complexes show that the *cis* isomer is more thermodynamically stable and indeed, heating the mixture for 12 h at 110 °C in toluene results in complete conversion to the *cis* isomer. Net *trans*-addition of H_2 has been reported with (PNP)Ir(Ph) by Milstein[29] and with (PONOP)Ir(CH_3) by Brookhart[30]. Milstein has proposed that addition to (PNP)Ir(Ph) proceeds via initial proton transfer from the PNP ligand to the metal center to form the dearomatized pincer complex (PNP*)Ir(H)(Ph), followed by H_2 addition across the metal and PNP* ligand (*trans* to the hydride ligand) to form *trans*-(PNP)Ir$(H)_2$(Ph). The PONOP ligand cannot undergo a similar deprotonation; hence protonation to give [(PNP)Ir(H)(CH_3)]X was proposed. Subsequent coordination of H_2 is then followed by deprotonation by X^- to form the product. In the present case, we have neither a ligand capable of undergoing Milstein-type dearomatization, nor a protic solvent presumably required for the Brookhart mechanism. A possible explanation is that (^{tBu}furPOP)RhCl is hemilabile under the reaction conditions, undergoing reversible

decoordination of one of the coordinating groups, most likely the weakly bound furan group (although dissociation of a phosphino group is also possible). Addition of H_2 to a three-coordinate (κ^2-^{tBu}furPOP)RhCl intermediate (Figure 3.11) is expected to be much faster than addition to the four-coordinate κ^3 complex,[31] and would result in a five-coordinate species to which the furan oxygen could recoordinate to afford the *trans* adduct. Initial formation of the *cis* adduct (ca. 30% of the kinetic distribution) might also occur via this three-coordinate intermediate, or via a conventional mechanism of concerted *cis* addition to the four-coordinate (κ^3-^{tBu}furPOP) complex, or a combination of these two possibilities.

Figure 3.11 Proposed mechanism for *trans* H_2 addition to (^{tBu}furPOP)RhCl, and potential mechanism for isomerization.

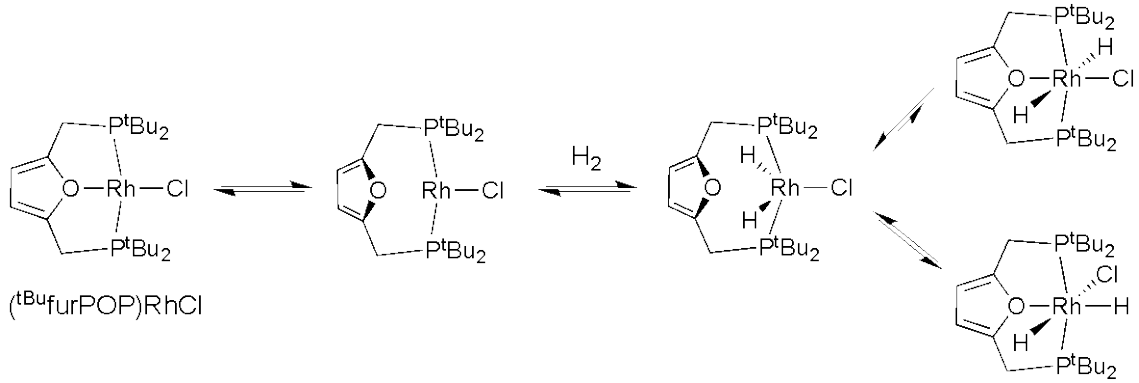

With convenient access to (^{tBu}xanPOP)Rh(H)$_2$Cl and (^{tBu}furPOP)Rh(H)$_2$Cl we targeted formation of the (POP)RhH_2^+ cationic complexes which are isoelectronic to the catalytically active complexes (PCP)IrH_2.[4, 6] Both (^{tBu}furPOP)Rh$(H)_2^+$ and (^{tBu}xanPOP)Rh$(H)_2^+$ can be formed in high yield by chloride abstraction with $AgBF_4$ or $AgSbF_6$ in acetone, THF, or CH_2Cl_2 (Figure 3.12).

Figure 3.12 Formation of the cationic hydrides (POP)Rh(H)$_2^+$

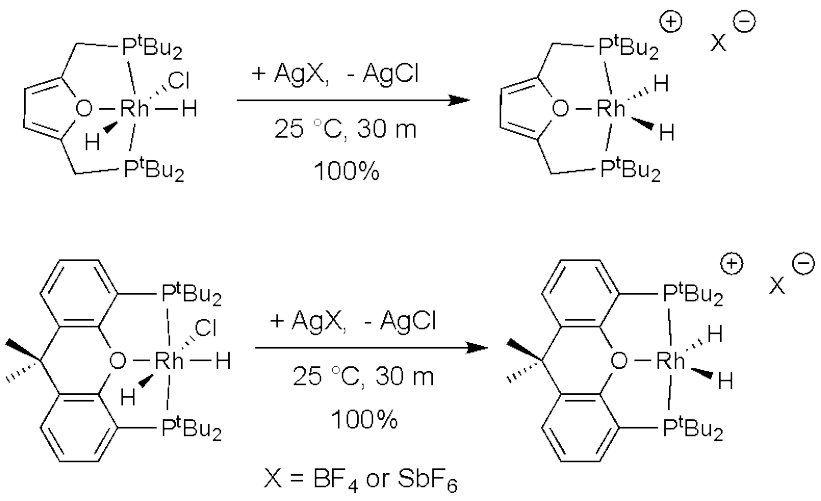

Both complexes feature a *dt* at ca. δ -21 ppm in the ^{1}H NMR spectrum, attributable to the equivalent hydride ligands, with similar values of J_{PH} (ca. 11 Hz) and particularly high values of J_{RhH} (ca. 40 Hz). These parameters are all indicative of classical dihydride complexes with strong Rh-H bonds, in contrast with the analogous neutral PCP [9,32] and POCOP[14], and cationic PNP[13] and PONOP[14] rhodium dihydrogen complexes, all of which have pincer ligands with central coordinating groups more strongly sigma-donating (stronger *trans*-influence) than the POP oxygen atoms. Indeed, the addition of H_2 to the [(^{tBu}xanPOP)Rh]$^+$ fragment is calculated (DFT) to be extremely exothermic; ΔH = -37.2 kcal/mol. This compares with a value of -27.0 kcal/mol calculated for H_2 addition to the archetypal pincer-ligated dehydrogenation catalyst, the *iridium* complex (^{tBu}PCP)Ir.

The *t*-Bu groups of the respective POP complexes each afford a single signal in the ^{1}H NMR spectra indicating their equivalency (see Supplementary Information). An X-ray structure of [(^{tBu}xanPOP)Rh(H)$_2$]SbF$_6$ (Figure 3.13) did not locate the hydride ligands with high certainty, but confirmed that no solvent or other ligand was coordinating to Rh.

Figure 3.13 X-ray structure of the cation of [(^{tBu}xanPOP)Rh(H)$_2$]SbF$_6$

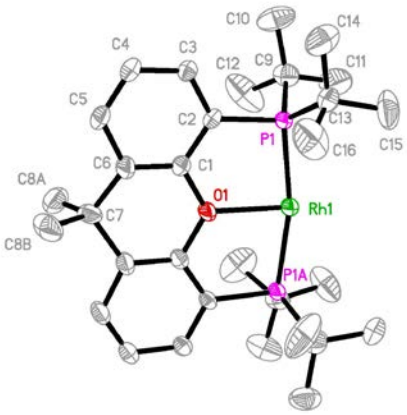

The chemical shift and coupling constant of the hydride ligands are not significantly affected by variations of solvent, including acetone, THF, or fluorobenzene, further supporting the conclusion that the complexes are coordinatively unsaturated dihydrides in these solutions as well as in the solid state. H_2O, however, does coordinate; *trans*-(^{tBu}xanPOP)Rh(OH_2)$(H)_2^+$ exhibits a broad singlet at δ -9 ppm in the ^{1}H NMR spectrum, suggesting that the hydrides are rapidly exchanging with the H_2O protons; the structure of this adduct was determined crystallographically (Figure 3.14).

Figure 3.14 X-ray structure of the cation of [*trans*-(^{tBu}xanPOP)Rh(H)$_2$(OH$_2$)]SbF$_6$

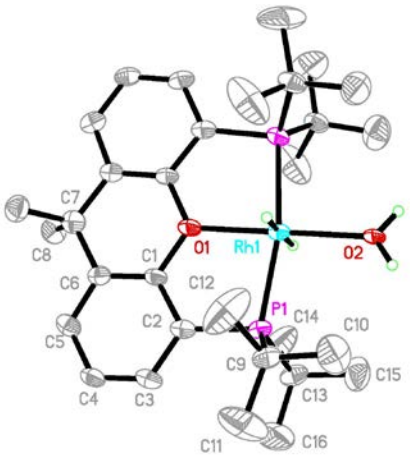

The cationic dihydrides are potential precursors to the corresponding 14-electron (POP)Rh$^+$ complexes; accordingly we investigated their reaction with common hydrogen acceptors. Surprisingly, neither (^{tBu}xanPOP)Rh(H)$_2^+$ nor (^{tBu}furPOP)Rh(H)$_2^+$ reacted with the commonly used acceptors TBE (*t*-butylethylene) or NBE (norbornene) (0.01 M - 0.2 M), even at temperatures up to 100 °C, in alkane or fluorobenzene solution. For comparison, (^{tBu}PCP)IrH$_2$ is readily dehydrogenated by NBE or TBE at ambient or near-ambient temperatures respectively.[33] Likewise (^{tBu}xanPOP)RhH$_2^+$ and (^{tBu}furPOP)RhH$_2^+$ underwent no reaction with 1-hexene (0.2 M) for over 48 hours at 100 °C (whereas (^{tBu}PCP)IrH$_2$ is dehydrogenated immediately upon mixing with 1-hexene at room temperature). However, we found that [(^{tBu}xanPOP)RhH$_2$]$^+$ reacts with ethylene to yield the cationic [(^{tBu}xanPOP)Rh(C$_2$H$_4$)]$^+$ (confirmed by independent synthesis from ^{tBu}xanPOP and Rh(C$_2$H$_4$)$_2$(solv)$_2^{+}$[34]) and ethane at room temperature within 1 hour. Conversely [(^{tBu}xanPOP)Rh(C$_2$H$_4$)]$^+$ also reacts with H$_2$ at room temperature to regenerate the dihydride complex, reaching completion after ca. 12 hours (Figure 3.15).

Figure 3.15 Reactions of (^{tBu}xanPOP)Rh(H)$_2^+$ with ethylene and (^{tBu}xanPOP)Rh(ethylene)$^+$ with dihydrogen.

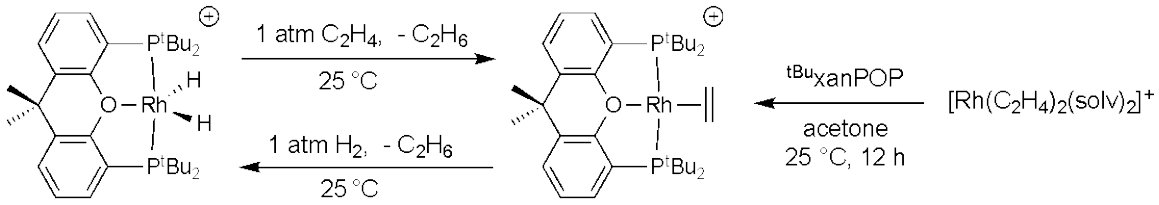

Propene, like 1-hexene, TBE and NBE, also fails to react with (^{tBu}xanPOP)Rh(H)$_2^+$. This exclusive selectivity for hydrogenation of ethylene (probably steric-based) is to our knowledge without close precedent.

Given the failure of both (^{tBu}xanPOP)Rh(H)$_2^+$and (^{tBu}furPOP)Rh(H)$_2^+$ to react with either TBE or 1-olefins, it is not surprising that neither is active for catalytic transfer-dehydrogenation of alkanes using these olefins. The use of ethylene as a hydrogen acceptor was also unsuccessful, also unsurprisingly in view of its ability to coordinate much more strongly than more bulky olefins.

In view of the unusual lack of reactivity of (^{tBu}furPOP)Rh(H)$_2^+$ and (^{tBu}xanPOP)Rh(H)$_2^+$ towards olefins bulkier than ethylene we investigated the less bulky ^{iPr}xanPOP ligand, reported recently by Asensio and Esteruelas.[21] *cis*-(^{iPr}xanPOP)Rh(H)$_2$Cl could be prepared analogously to the ^{tBu}xanPOP complex, although the product appears to be in slow equilibrium with a species that is possibly dimeric (or oligomeric). The monomeric *cis*-(^{iPr}xanPOP)Rh(H)$_2$Cl complex exhibits two *dtd* signals at δ -17.46 and -20.07 in the ^{1}H NMR spectrum, similar to the signals at δ -17.02 and -20.51 observed for (^{tBu}xanPOP)Rh(H)$_2$Cl. The suspected dimer or oligomer exhibits a very complex signal in both the ^{1}H and ^{31}P NMR spectra, which could not be effectively decoupled. We observed no *trans*-H$_2$ addition to (^{iPr}xanPOP), suggesting that this phenomenon derives from the flexibility of the methylene-linked backbone of (^{tBu}furPOP), rather than from the steric environment at the metal center.

The cationic dihydrides discussed above show limited solubility in alkane solvents at lower temperatures. Toward the goal of evaluating activity for alkane dehydrogenation in mind, we therefore employed the more lipophilic $B(C_6F_5)_4$ anion for this complex. Treatment of the mixture of *cis*-(^{iPr}xanPOP)Rh(H)$_2$Cl and the putative dimer with $LiB(C_6F_5)_4$•OEt_2 in CD_2Cl_2 lead to the clean formation of (^{iPr}xanPOP)Rh(H)$_2^+$ which exhibited a sharp *dt* at -23.93 ppm with J_{PH} = 15 Hz, and J_{RhH} = 44 Hz (2H), in good agreement with those values obtained with (^{tBu}xanPOP)Rh(H)$_2^+$ (Figure 3.16).

Figure 3.16 Preparation of (^{iPr}xanPOP)Rh(H)$_2^+$

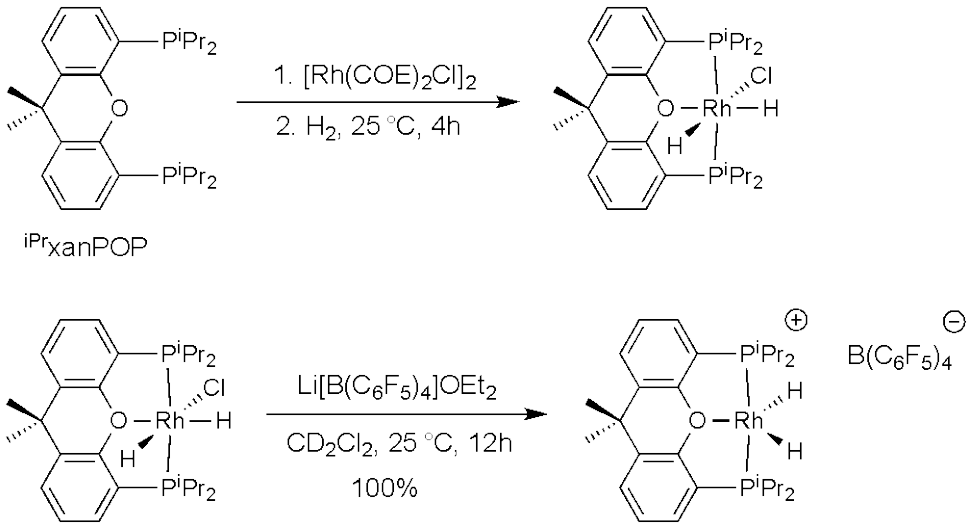

Unlike either of the ^{tBu}POP complexes, (^{iPr}xanPOP)Rh(H)$_2^+$ is catalytically active in the transfer dehydrogenation of COA. Under our most-commonly employed conditions, TBE (0.2 M) as an acceptor and 1 mM catalyst, 47 mM COE is observed after 10 h at 150 °C. (^{iPr}xanPOP)Rh(H)$_2^+$ is, to our knowledge, the first cationic pincer complex reported to catalyze alkane dehydrogenation.

A four-coordinate rhodium(I) monohydride. In part interested by the fact that (POP)Rh(H)$_3$ would be isoelectronic to Nozaki's (PNP)Ir(H)$_3$[28] catalyst for hydrogenation of CO_2, we investigated the dehydrohalogenation of (POP)Rh(H)$_2$Cl complexes. The reaction of

(^{tBu}xanPOP)Rh(H)$_2$Cl with KO^{t}Bu in benzene leads to a color change from orange to red within seconds.

Figure 3.17 Formation of a square-planar rhodium monohydride, (^{tBu}xanPOP)RhH

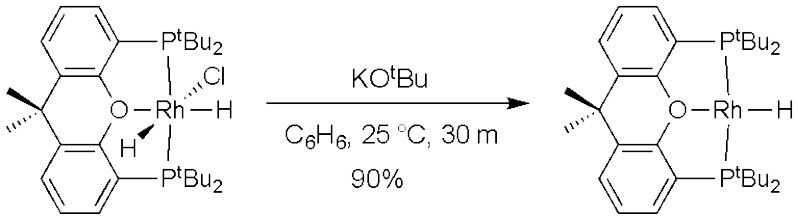

The ^{1}H NMR of the red product solution indicates that all 4 *t*-Bu groups are equivalent, and a single *dt* signal integrating to 1H is observed in the hydride region. The selectively hydride-coupled ^{31}P signal appears as a *dd*. These NMR data are all indicative of a product with a single hydride ligand *trans* to the POP oxygen atom. X-ray analysis of the product confirmed that no additional ligands are bound to the Rh center; the product is therefore assigned as the monohydride (^{tBu}xanPOP)RhH (Figures 17 and 18), which is a rare example of a 4-coordinate Group 9 metal hydride.[22, 35] The only other example of such a rhodium complex to our knowledge, (^{NHC}PCP)RhH, was recently reported by Fryzuk.[36] This complex was found to be thermally unstable above 70 °C,[36] whereas (^{tBu}xanPOP)RhH shows no appreciable decomposition in solutions at 150 °C for several hours.

Figure 3.18 X-ray structure of (^{tBu}xanPOP)RhH

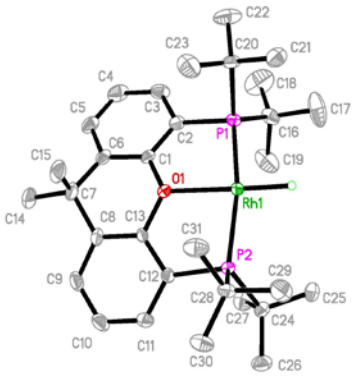

No evidence for addition of H_2 is observed upon the addition of 1 atm H_2 to a C_6D_6 solution of (^{tBu}xanPOP)RhH at room temperature. This result stands in marked contrast with the behavior of the chloride analog, (^{tBu}xanPOP)RhCl, which readily adds H_2, with no observable concentration of four-coordinate species remaining in solution, as discussed above. Accordingly, *cis* H_2 addition to (^{tBu}xanPOP)Rh(X) is calculated (DFT) to be favorable with $\Delta G°_{298K}$ = -5 kcal/mol for X = Cl, but unfavorable for X = H with $\Delta G°_{298K}$ = +5 kcal/mol. This large difference in reactivity represents another case where oxidative addition is strongly *disfavored* by increased sigma-donating ability of an ancillary ligand.

Addition of 1 atm ethylene to a solution of (^{tBu}xanPOP)RhH results in insertion into the Rh-H bond to give (^{tBu}xanPOP)RhEt within ca. 1 minute (eq 2). The methylene protons of the ethyl ligand appear as a *qd* (δ 2.21; $^2J_{RhH}$ = 2.4 Hz, $^3J_{HH}$ = 7.5 Hz).

(^{tBu}xanPOP)RhH $\xrightarrow[C_6D_6,\ 25°C,\ 1\ min]{1\ atm\ C_2H_4}$ (^{tBu}xanPOP)Rh(C_2H_5) (2)

A similar insertion reaction, in the case of the Rh(III) complex $(PPh_3)_2Rh(H)Cl_2$ was reported in 1967 by Wilkinson.[37] The resulting $(PPh_3)_2Rh(Et)Cl_2$ (eq 3) was found to be stable to air.

$$(PPh_3)_2Rh(H)Cl_2 + C_2H_4 \longrightarrow (PPh_3)_2Rh(C_2H_5)Cl_2 \quad (3)$$

In contrast, the Rh(I) complex (^{tBu}xanPOP)RhEt species loses ethylene when pumped dry, to reform (^{tBu}xanPOP)RhH.[38] This system thus afforded an unusual opportunity to determine the thermodynamics of insertion of an olefin into a late-metal hydride bond. The thermodynamics of olefin insertion into M-H bonds are of significance in the context of alkane dehydrogenation, olefin hydrogenation, and numerous transition-metal catalyzed additions of H-X to olefin. Yet reports of absolute thermodynamic data for olefin insertion into metal-hydride bonds are rare. The only other examples of which we are aware, reported by Chirik and Bercaw, are for insertion into a Zr-H bond of bis(cyclopentadienyl)ZrH_2 complexes.[39] For $(C_5Me_5)_2ZrH_2$ it was found that ΔG = -4.6 kcal/mol for insertion of isobutene and -6.9 kcal/mol for 1-butene; for the slightly less crowded $(C_5Me_5)(C_5Me_4H)ZrH_2$ the respective values are -8.5 kcal/mol and -10.6 kcal/mol.

$$(^{tBu}\text{xanPOP})Rh(C_2H_5) \underset{C_6D_6,\ 25\,^\circ C,\ 12h}{\overset{K_{eq} = 0.033\ M}{\rightleftharpoons}} (^{tBu}\text{xanPOP})RhH + C_2H_4 \quad (4)$$

A solution of (^{tBu}xanPOP)RhEt in C_6D_6 was prepared under ethylene atmosphere in a J-Young NMR tube. The solution was then frozen in pentane/liquid N_2 (-126 °C) and the headspace was evacuated on a high-vacuum line. The solution was thawed and an NMR spectrum was immediately (ca. 1 min) recorded, showing ca. 10% conversion into the (^{tBu}xanPOP)RhH complex and ethylene. After 12 h, the reaction had reached equilibrium with [(^{tBu}xanPOP)RhEt] = 3.8 mM, [(^{tBu}xanPOP)RhH] = 16 mM, and [C_2H_4] = 7.8 mM, corresponding to a K_{eq} = 0.033 M for deinsertion or K_{eq} = 30.5 M^{-1} for insertion of ethylene into the Rh-H bond, corresponding to $\Delta G_{insertion\ 298K}$ = -2.0 kcal/mol.

(^{tBu}xanPOP)RhH did not react with 1-hexene or propylene to yield any observable rhodium-containing products at temperatures ranging from ambient to 100 °C (eq 5). To determine if this failure to observe insertion products was due to kinetic or thermodynamic factors we reacted

(^{tBu}xanPOP)RhCl with approximately one half equivalent of *n*-BuLi, at 25 °C. Over the course of ca. 1 hour the reaction proceeded to completion (consuming all the *n*-BuLi), generating (^{tBu}xanPOP)Rh(*n*-Bu) (eq 6), the homologue of (^{tBu}xanPOP)RhEt.

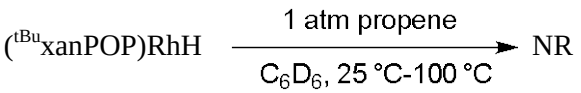

(5)

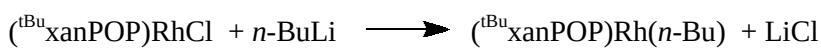

(6)

(^{tBu}xanPOP)Rh(*n*-Bu) underwent β-H elimination to give (^{tBu}xanPOP)RhH (eq 7), with a half-life on the order of 1 hour, the reaction proceeding to give complete conversion to the hydride within 18 hours. Thus, the failure of (^{tBu}xanPOP)RhH to insert higher olefins is due to thermodynamics, not kinetics. Addition across the double bond of a terminal alkene is generally less favorable than addition to ethylene (e.g. ΔH = -29.9 kcal/mol for hydrogenation of propene or 1-butene, vs. -32.6 kcal/mol for ethylene[40]). Given our determination of $\Delta G_{\text{insertion 298K}}$ = -2.0 kcal/mol for ethylene insertion, this difference of ca. 2.7 kcal/mol can largely explain the great difference in reactivity between ethylene and higher olefins toward (^{tBu}xanPOP)RhH. Note that the thermodynamics of insertion in this systems are much less favorable than those for the bis(cyclopentadienyl)ZrH_2 complexes noted above[39] (-6.9 kcal/mol and -10.6 kcal/mol for 1-butene insertion). Future studies will address the question of electronic and/or steric components of this difference.

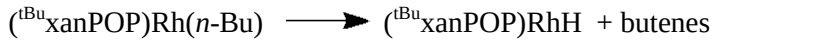

(7)

While (^{tBu}xanPOP)RhH does not react with 1-hexene to give an observable insertion product, it is highly active as an olefin isomerization catalyst (eq 8). For example, in a solution of 1 μmol (4 mM) (^{tBu}xanPOP)RhH in 2 mmol 1-hexene (neat), an initial TOF of 460 h^{-1} for

isomerization is obtained at 50 °C. After 16 hours, nearly 2000 TON were obtained. Moderate selectivity for formation of *trans*-2-hexene is observed.

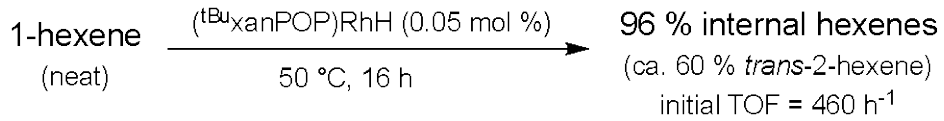

(8)

Summary

In conclusion, we have synthesized several (POP)Rh complexes and explored their reactivity including oxidative addition of hydrogen and hydrometalation of olefins. Using the bulky, neutral ligands, ^{tBu}xanPOP or ^{tBu}furPOP, monomeric pincer (POP)RhCl species can be obtained. These four-coordinate complexes add H_2 to afford the *cis* dihydrides as the thermodynamic products but (^{tBu}furPOP)RhCl gives a *trans* dihydride as a kinetic product; this likely proceeds via reversible decoordination and addition to a highly reactive three-coordinate intermediate. (^{tBu}furPOP)RhH_2^+ and (^{tBu}furPOP)RhH_2^+ were synthesized. Although they are isoelectronic to complexes (PCP)IrH_2 which are well known to catalyze alkane dehydrogenation,[4] these cationic rhodium complexes showed no such reactivity. The less crowded (^{iPr}xanPOP)RhH_2^+, however, is found to catalyze cyclooctane/TBE transfer-dehydrogenation. (^{iPr}xanPOP)Rh$(H)_2^+$ is the first cationic pincer complex reported to catalyze alkane dehydrogenation and it offers a relatively rare example of alkane dehydrogenation by a second row metal complex. Notably, this has been achieved not by increasing electron density on the metal center, but by the use of a very *poorly* sigma electron-donating group at the central coordinating position of the pincer ligand, i.e. an ether oxygen as compared with nitrogen donors or the anionic aryl groups found in pincer ligands of the PCP type. Presumably related to this is the observation that, unlike cationic PNP or neutral PCP rhodium fragments, the (POP)Rh unit oxidatively cleaves H_2 rather than forming a dihydrogen complex. Indeed, it appears that the thermodynamics of H_2 oxidative addition (calculated as exothermic by ca. 37 kcal/mol) may be too favorable for optimal catalytic activity, and that the

thermodynamic difficulty of removing hydrogen from (^{iPr}xanPOP)Rh(H)$_2^+$ limits the rate of catalytic transfer-dehydrogenation. Work is currently underway on the application of new POP ligands with greater *trans* influence, which may more closely emulate the electronics of the $(PMe_3)_2RhCl$ system.[41]

In addition, we report the formation of the stable four-coordinate hydride (^{tBu}xanPOP)RhH. This complex reversibly hydrometalates ethylene, thus allowing an unusual direct determination of the thermodynamics of insertion of olefin into a metal-hydrogen bond.

Acknowledgements

This work was supported by NSF through the CCI Center for Enabling New Technologies through Catalysis (CENTC), CHE-1205189 and CHE-0650456. M.C.H. is a graduate training fellow in the NSF IGERT for Renewable and Sustainable Fuels. We thank Johnson-Matthey for a gift of rhodium salts, and Penn A Kem for a generous supply of 2,5-bis(hydroxymethyl)furan. We also wish to acknowledge Chen Cheng, Dr. Damien Guironnet, and Prof. Maurice Brookhart (University of North Carolina - Chapel Hill), and Dr. Montserrat Oliván, and Prof. Miguel A. Esteruelas (Universidad de Zaragoza) for helpful discussions and sharing unpublished work.

Chapter 3.1 References

(1) C. J. Moulton and B. L. Shaw, *J. Chem. Soc., Dalton Trans.* 1976, 1020-1024.

(2) (a) G. van Koten and D. Milstein in Organometallic Pincer Chemistry In *Top. Organomet. Chem.*, 2013; **40**, Springer GmbH, p. 356 (b) D. Morales-Morales and C. Jensen in *The Chemistry of Pincer Compounds*, Vol. Elsevier, Amsterdam, 2007. (c) M. Albrecht and G. van Koten, *Angew. Chem., Intl. Ed.* 2001, **40**, 3750-3781.

(3) (a) C. Gunanathan and D. Milstein, *Acc. Chem. Res.* 2011, **44**, 588-602. (b) C. Gunanathan and D. Milstein, *Top. Organomet. Chem.* 2011, **37**, 55-84. (c) D. Srimani, E. Balaraman, B. Gnanaprakasam, Y. Ben-David and D. Milstein, *Adv. Synth. Catal.* 2012, **354**, 2403-2406, S2403/2401-S2403/2421.

(4) (a) J. Choi, A. H. R. MacArthur, M. Brookhart and A. S. Goldman, *Chem. Rev.* 2011, **111**, 1761-1779. (b) M. C. Haibach, S. Kundu, M. Brookhart and A. S. Goldman, *Acc. Chem. Res.* 2012, **45**, 947-958.

(5) B. C. Gruver, J. J. Adams, S. J. Warner, N. Arulsamy and D. M. Roddick, *Organometallics* 2011, **30**, 5133–5140.

(6) A. S. Goldman, A. H. Roy, Z. Huang, R. Ahuja, W. Schinski and M. Brookhart, *Science* 2006, **312**, 257-261.

(7) (a) J. A. Maguire and A. S. Goldman, *J. Am. Chem. Soc.* 1991, **113**, 6706-6708. (b) J. A. Maguire, A. Petrillo and A. S. Goldman, *J. Am. Chem. Soc.* 1992, **114**, 9492-9498. (c) K. Wang, M. E. Goldman, T. J. Emge and A. S. Goldman, *J. Organomet. Chem.* 1996, **518**, 55-68.

(8) S. Nemeh, C. Jensen, E. Binamira-Soriaga and W. C. Kaska, *Organometallics* 1983, **2**, 1442-1447.

(9) W. Xu, G. P. Rosini, M. Gupta, C. M. Jensen, W. C. Kaska, K. Krogh-Jespersen and A. S. Goldman, *Chem. Commun.* 1997, 2273-2274.

(10) D. Y. Wang, Y. Choliy, K. Krogh-Jespersen, J. F. Hartwig and A. S. Goldman, *Abstracts of Papers, 240th ACS National Meeting, Boston, MA, United States, August 22-26*, 2010, INOR-5.

(11) D. Hermann, M. Gandelman, H. Rozenberg, L. J. W. Shimon and D. Milstein, *Organometallics* 2002, **21**, 812-818.

(12) (a) L. Fan, B. M. Foxman and O. V. Ozerov, *Organometallics* 2004, **23**, 326-328. (a) L. Fan, L. Yang, C. Guo, B. M. Foxman and O. V. Ozerov, *Organometallics* 2004, **23**, 4778-4787. (c) O. V. Ozerov, C. Guo, L. Fan and B. M. Foxman, *Organometallics* 2004, **23**, 5573-5580. (d) O. V. Ozerov, C. Guo, V. A. Papkov and B. M. Foxman, *J. Am. Chem. Soc.* 2004, **126**, 4792-4793.

(13) A. B. Chaplin and A. S. Weller, *Organometallics* 2011, **30**, 4466-4469.

(14) M. Findlater, K. M. Schultz, W. H. Bernskoetter, A. Cartwright-Sykes, D. M. Heinekey and M. Brookhart, *Inorg. Chem.* 2012, **51**, 4672-4678.

(15) M. Brookhart, C. Chang, B. G. Kim, A. Goldman and D. Y. Wang, *Abstracts of Papers, 243rd ACS National Meeting , San Diego, CA, United States, March 25-29*, 2012, INOR-1007.

(16) K. Timmer, D. H. M. W. Thewissen and J. W. Marsman, *Recueil des Travaux Chimiques des Pays-Bas* 1988, **107**, 248-255.

(17) R. Dallanegra, A. B. Chaplin and A. S. Weller, *Organometallics* 2012, **31**, 2720–2728.

(18) G. L. Williams, C. M. Parks, C. R. Smith, H. Adams, A. Haynes, A. J. H. M. Meijer, G. J. Sunley and S. Gaemers, *Organometallics* 2011, **30**, 6166-6179.

(19) L. D. Julian and J. F. Hartwig, *J. Am. Chem. Soc.* 2010, **132**, 13813-13822.

(20) C. Mispelaere-Canivet, J.-F. Spindler, S. Perrio and P. Beslin, *Tetrahedron* 2005, **61**, 5253-5259.

(21) G. Asensio, A. B. Cuenca, M. A. Esteruelas, M. Medio-Simon, M. Olivan and M. Valencia, *Inorg. Chem.* 2010, **49**, 8665-8667.

(22) In the course of this work we became aware of independent work by Esteruelas and co-workers which included the synthesis of ^{iPr}furPOP as well as the synthesis of (^{iPr}xanPOP)RhCl, *cis*-(^{iPr}xanPOP)RhH_2Cl and (^{iPr}xanPOP)RhH. For the ^{iPr}xanPOP complexes see: M. A. Esteruelas, M. Olivan and A. Velez, *Inorg. Chem.* 2013, **52**, 5339-5349.

(23) a) M. W. Haenel, D. Jakubik, E. Rothenberger and G. Schroth, *Chem. Ber.* 1991, **124**, 1705-1710; b) E. M. Vogl, J. Bruckmann, M. Kessler, C. Kruger and M. W. Haenel, *Chem. Ber./Recl.* 1997, **130**, 1315-1319; c) M. Kranenburg, d. B. Y. E. M. van, P. C. J. Kamer, L. P. W. N. M. van, K. Goubitz and J. Fraanje, *Organometallics* 1995, **14**, 3081-3089.

(24) M. A. Esteruelas, N. Honczek, M. Olivan, E. Onate and M. Valencia, *Organometallics* 2011, **30**, 2468-2471.

(25) a) H. Kumobayashi, H. Taketomi and S. Akutagawa in *Isomenthone, Vol.* (Takasago Perfumery Co., Ltd., Japan). Application: JP, **1980**, p. 10 pp; b) H. Kumobayashi, H. Taketomi and S. Akutagawa in *Isomerization of piperitol, Vol.* (Takasago Perfumery Co., Ltd., Japan). Application: JP, **1980**, p. 10 pp.

(26) A. N. Cammidge, M. J. Cook, K. J. Harrison and N. B. McKeown, *J. Chem. Soc., Perkin Trans. 1* 1991, 3053-3058.

(27) K. Zhu, P. D. Achord, X. Zhang, K. Krogh-Jespersen and A. S. Goldman, *J. Am. Chem. Soc.* 2004, **126**, 13044-13053.

(28) R. Tanaka, M. Yamashita and K. Nozaki, *J. Am. Chem. Soc.* 2009, **131**, 14168-14169.

(29) a) E. Ben-Ari, G. Leitus, L. J. W. Shimon and D. Milstein, *J. Am. Chem. Soc.* 2006, **128**, 15390-15391; b) M. A. Iron, E. Ben-Ari, R. Cohen and D. Milstein, *Dalton Trans.* 2009, 9433-9439.

(30) M. Findlater, W. H. Bernskoetter and M. Brookhart, *J. Am. Chem. Soc.* 2010, **132**, 4534-4535.

(31) K. Tatsumi, R. Hoffmann, A. Yamamoto and J. K. Stille, *Bull. Chem. Soc. Jpn.* 1981, **54**, 1857-1867.

(32) W. C. Kaska, S. Nemeh, A. Shirazi and S. Potuznik, *Organometallics* 1988, **7**, 13-15.

(33) K. B. Renkema, Y. V. Kissin and A. S. Goldman, *J. Am. Chem. Soc.* 2003, **125**, 7770-7771.

(34) R. R. Schrock and J. A. Osborn, *J. Am. Chem. Soc.* 1976, **98**, 2134-2143.

(35) M. D. Millard, C. E. Moore, A. L. Rheingold and J. S. Figueroa, *J. Am. Chem. Soc.* 2010, **132**, 8921-8923.

(36) B. K. Shaw, B. O. Patrick and M. D. Fryzuk, *Organometallics* 2012, **31**, 783-786.

(37) M. C. Baird, J. T. Mague, J. A. Osborn and G. Wilkinson, *J. Chem. Soc. A* 1967, 1347-1360.

(38) In an even sharper contrast with the Wilkinson system of eq 3, Milstein and co-workers have reported that ethylene eliminates irreversibly from (^{tBu}PCP)IrEtI to give (^{tBu}PCP)IrHI; the kinetics of this system were investigated: M. E. Van der Boom, C. L. Higgitt and D. Milstein, *Organometallics* 1999, **18**, 2413-2419.

(39) P. J. Chirik and J. E. Bercaw, *Organometallics* 2005, **24**, 5407-5423.

(40) Afeefy, H. Y.; Liebman, J. F.; Stein, S.E. "Neutral Thermochemical Data" in NIST Chemistry WebBook, NIST Standard Reference Database Number 69, Eds. P.J. Linstrom and W.G. Mallard, National Institute of Standards and Technology, Gaithersburg MD, 20899, http://webbook.nist.gov, (retrieved January 26, 2013)

(41) M. C. Haibach and A. S. Goldman, manuscript in preparation.

Chapter 3.2 Experimental Section

General Information: All manipulations were carried out under argon, using standard Schlenk or glovebox techniques. Anhydrous grade hexane, pentane, benzene, octane, and toluene were bubbled with argon before use. C_6D_6, toluene-*d8*, *tert*-butylethylene (TBE), 1-hexene, and 1-octene were dried over NaK and vacuum distilled. Fluorobenzene was freeze-pump-thawed and distilled over CaH_2. Norbornene (NBE) was purified by sublimation. Et_2O and THF were distilled from sodium benzophenone under argon. $(CD_3)_2CO$ was dried over B_2O_3 and vacuum distilled. CD_2Cl_2 was dried over 4Å molecular sieves, freeze-pump-thawed, and stored over 4Å molecular sieves. ^{1}H, ^{13}C, and ^{31}P NMR were recorded on 300, 400, or 500 MHz Varian spectrometers and are reported in ppm. ^{1}H and ^{31}C NMR were referenced to the residual solvent signals. ^{31}P NMR were referenced to an external standard of 85% H_3PO_4. ^{tBu}xanPOP and di-*tert*-butylphosphine were purchased from Strem. 2,5-bis(hydroxymethyl)furan is commercially available from Pennakem and $[Rh(NBD)Cl]_2$ from Johnson-Matthey. ^{iPr}xanPOP[1], 2,5-bis(chloromethyl)furan[2] and $[Rh(COE)_2Cl]_2$[3] were prepared according to the literature.

Synthesis of Complexes

Synthesis of 2,5-bis((di-*tert*-butylphosphino)methyl)furan, ^{tBu}furPOP: 907 mg (5.40 mmol, 1.00 equiv) freshly prepared 2,5-bis(chloromethyl)furan was dissolved in 5.0 mL THF at room temperature. 2.00 mL (10.8 mmol, 2.00 equiv) di-*tert*-butylphosphine was added and the solution was stirred for 24 h at room temperature, leading to the formation of a yellow precipitate. The supernatant was removed via cannula filtration, and the precipitate was washed with pentane. The precipitate was suspended in MeOH and stirred with 1.00 mL Et_3N overnight. The supernatant was removed, dried in vacuo and the process was repeated twice to yield 1.04 g (2.70 mmol, 50%) of ^{tBu}furPOP as a tan oil which solidified upon standing. ^{1}H NMR (300 MHz, C_6D_6): δ 6.10 (s, 2H), 2.73 (s, 4H), 1.05 (d, $^2J_{PH}$ = 11 Hz, 36H). ^{13}C NMR (75 MHz, C_6D_6): δ 153.28 (d, J_{PC} = 18.3 Hz), 107.54 (d, J_{PC} = 7.7 Hz), 31.48 (d, J_{PC} = 24.9 Hz), 29.70 (d, J_{PC} = 13.8 Hz), 21.24 (d, J_{PC} = 25.9 Hz). ^{31}P NMR (121 MHz, C_6D_6): δ 27.6 (s).

(^{tBu}furPOP)RhCl: 23 mg (0.06 mmol) ^{tBu}furPOP and 20 mg (0.03 mmol) $[Rh(COE)_2(Cl)_2]_2$ were dissolved in 2 mL benzene and stored at room temperature overnight. The solvent was removed in vacuo and the light orange residue was extracted with 5 mL pentane. Removal of the pentane in vacuo afforded the title compound in 87% yield. Orange crystals suitable for X-ray diffraction were obtained by recrystallization from pentane. ^{1}H NMR (500 MHz, C_6D_6): δ 5.51 (s, 2H), 2.26 (s, 4H), 1.44 (vt, J_{PH} = 5.16 Hz, 36H). ^{13}C NMR (125 MHz, C_6D_6): δ 158.77, 104.82, 35.34 (t, J_{PC} = 5.1 Hz), 29.30 (t, J_{PC} = 3.7 Hz), 21.52 (t, J_{PC} = 2.8 Hz). ^{31}P NMR (C_6D_6, 202 MHz): δ 56.9 (d, J_{RhP} = 141 Hz).

***cis*-(^{tBu}furPOP)Rh(H)$_2$Cl:** 15 mg (0.04 mmol) (^{tBu}furPOP)RhCl is dissolved in 1 mL C_6D_6 in a J-Young tube to give a light orange solution. The solution is frozen, and the headspace evacuated and refilled with 1 atm H_2. The solution is gently warmed to room temperature, and the tube is shaken on an agitator table for 24 h. NMR indicates the formation of the *cis* and *trans* hydrides in

a 7:3 ratio. The solvent replaced with toluene-d_8 and the mixture is heated under 1 atm H_2 at 110°C for 2h, yielding the *cis* dihydride quantitatively.

Alternatively, 77 mg (0.2 mmol) ^{tBu}furPOP and 0.1 mmol $[Rh(NBD)Cl]_2$ were dissolved in 5 mL toluene and refluxed for 48 h under H_2 bubbling, yielding a red solution. The solvent was removed in vacuo and the residue redissolved in 2 mL benzene. Addition of 2 mL pentane caused the precipitation of 54 mg of a yellow solid, 51% yield of the title compound. Data for the *cis* complex: ^{1}H NMR (400 MHz, C_6D_6): δ 6.77 (s, 2H), 3.64 (s, 4H), 1.33 (vt, J_{PH} = 5.3 Hz), -22.40 (m, 2H). ^{13}C NMR (100 MHz, C_6D_6): δ 148.98, 107.59, 27.01 (m), 26.79 (m), 22.93. ^{31}P NMR (162 MHz, C_6D_6) δ 73.4 (d, J_{RhP} = 120 Hz). Selected data for the *trans* complex: ^{1}H NMR (400 MHz, C_6D_6): δ -22.59 (dt, J_{PH} = 16 Hz, J_{RhH} = 24 Hz).

(^{tBu}xanPOP)RhCl: 30 mg (0.06 mmol) ^{tBu}xanPOP and 20 mg (0.03 mmol) $[Rh(COE)_2Cl]_2$ were dissolved in 2 mL benzene and stored at room temperature overnight. The solvent was removed in vacuo and the light orange residue was extracted with 5 mL pentane. Removal of the pentane in vacuo afforded the title compound in 93% yield. Dark orange rods suitable for X-ray diffraction were obtained by slow evaporation from pentane. ^{1}H NMR (500 MHz, C_6D_6): δ 7.77 (m, 2H), 6.99 (m, 2H), 6.78 (m, 2H), 1.67 (vt, J_{PH} = 6.8 Hz, 36H), 1.15 (s, 6H). ^{13}C NMR (126 MHz, C_6D_6): δ 158.71, 133.90, 131.15, 125.65, 123.58, 37.44, 33.64, 32.32 ^{31}P NMR (202 MHz, C_6D_6): δ 48.8 (d, J_{RhP} = 141 Hz)

***cis*-(^{tBu}xanPOP)Rh(H)$_2$Cl:** 15 mg (^{tBu}xanPOP)RhCl is dissolved in 1 mL C_6D_6 in a J-Young tube to give an orange solution. The solution is frozen, and the headspace evacuated and refilled with 1 atm H_2. The solution is gently warmed to room temperature, and the tube is shaken for 24 h on an agitator table. During the reaction, the solution becomes yellow. NMR indicates full conversion into the title complex. Removal of the solvent affords the title compound as a yellow solid in quantitative yield. Orange needles suitable for X-ray diffraction were grown by slow diffusion of pentane into an acetone solution of the title compound.

Alternatively, a convenient one-pot preparation can be used for large scale reactions. 250 mg ^{tBu}xanPOP (0.50 mmol) and 175 mg $[Rh(COE)_2Cl]_2$ (0.50 mmol Rh) were dissolved in 5 mL benzene and stirred overnight. The resulting dark-red solution was gently bubbled with H_2 for 2 h at room temperature, causing the solution to become light orange. The solvent was removed in vacuo, affording the title complex as a yellow solid in quantitative yield. ^{1}H NMR (C_6D_6, 300 MHz): δ7.49-7.44 (m, 2H), 7.06 (dd, J = 3.2 Hz, J = 1.6 Hz, 2H), 6.86 (t, J_{PH} = 7.8 Hz, 2H), 1.76 (vt, J_{PH} = 7.0 Hz, 18H), 1.30 (vt, J_{PH} = 7.0 Hz, 18H), 1.23 (s, 3H), 1.20 (s, 3H), -17.02 (dtd, J_{RhH} = 23 Hz, J_{PH} = 14 Hz, J_{HH} = 9.2 Hz, 1H), -20.51 (dtd, J_{RhH} = 29 Hz, J_{PH} = 12 Hz, J_{HH} = 9.2 Hz, 1H). ^{13}C NMR (C_6D_6, 126 MHz): δ156.03 (t, J_{PC} = 6.5 Hz), 133.89, 132.71, 132.23 (t, J_{PC} = 2.5 Hz), 124.94 (t, J_{PC} = 8.6 Hz), 123.40 (t, J_{PC} = 2.1 Hz), 38.00 (t, J_{PC} = 5.6 Hz), 36.37 (m), 34.68 (m), 32.21, 30.27, 29.78 (m). ^{31}P NMR (C_6D_6, 162 MHz): δ79.1 (dt, J_{RhP} = 118 Hz, J_{HP} = 10 Hz). Analysis for $C_{31}H_{52}ClOP_2Rh$: calculated C 58.08, H 8.18. Found C 57.72, H 7.71.

[(^{tBu}xanPOP)Rh(H)$_2$]SbF$_6$/BF$_4$: 64 mg (0.15 mmol) *cis*-(^{tBu}xanPOP)Rh(H)$_2$Cl was dissolved in 3 mL acetone in a glass vial wrapped in aluminum foil. A solution of 34 mg (0.15 mmol) $AgSbF_6$ in 1 mL acetone was added dropwise and the reaction was stirred at room temperature. Over 30 min the reaction turns from yellow to orange and a grey precipitate forms. The solution is decanted, filtered to remove AgCl, and dried in vacuo to give the title complex as an orange solid in quantitative yield. The BF_4 salt is prepared similarly and has identical spectral data for the cation. ^{1}H NMR (400 MHz, CD_2Cl_2): δ7.85-7.80 (comp, 4H), 7.52 (m, 2H), 1.75 (s, 6H), 1.41 (vt, J_{PH} = 8.0 Hz, 36H), -21.53 (dt, J_{PH} = 12 Hz, J_{RhH} = 43 Hz). ^{13}C NMR (CD_2Cl_2, 100 MHz): δ 165.11, 133.70, 132.54, 126.48, 119.99, 36.96, 32.20, 30.81, 30.25. ^{31}P NMR (CD_2Cl_2, 162 MHz): δ80.1 (dt, J_{HP} = 11 Hz, J_{RhP} = 111 Hz). Analysis for {[(^{tBu}xanPOP)Rh(H)$_2$] BF_4}*½(CH_2Cl_2), $C_{31.5}H_{53}BF_4OP_2Rh$: calculated C 51.48, H 7.57. Found C 51.80, H 6.79. Alternatively, H_2 is bubbled through an acetone solution of [(^{tBu}xanPOP)Rh(C_2H_4)]BF_4 or [(^{tBu}xanPOP)Rh(C_2H_4)]SbF_6 for 1 h. NMR shows quantitative formation of

[(^{tBu}xanPOP)Rh(C_2H_4)]$^+$. Crystals suitable for X-ray diffraction were obtained by layering a solution of the title complex with pentane.

[(^{tBu}xanPOP)Rh(C_2H_4)]SbF_6/BF_4: 18 mg (0.025 mmol) $[Rh(COE)_2Cl]_2$ and 10 mg (0.05 mmol) $AgBF_4$ were dissolved in 2 mL acetone and stirred for 30 min at room temperature in a foil-wrapped vial. The solution is filtered and added to a solution of 25 mg (0.05 mmol) ^{tBu}xanPOP in 1 mL acetone. Ethylene is slowly passed through the solution for 24h. After removal of the solvent, the product is titurated with benzene to afford the title complex in 80% yield. The PF_6 salt is prepared similarly and has identical spectral data for the cation. ^{1}H NMR (400 MHz, acetone-d_6): δ 8.11-8.04 (comp, 4H), 7.57 (m, 2H), 3.95 (m, 4H), 1.81 (s, 6H), 1.52 (vt, J_{PH} = 14 Hz, 36H). ^{13}C NMR (acetone-d_6, 100 MHz): δ 165.11, 134.54, 131.87, 130.04, 128.49, 126.18, 43.10, 38.47 (dt, J_{PC} = 6.6 Hz, J_{RhC} = 71 Hz), 32.90, 30.43, 29.95. ^{31}P NMR (acetone-d_6, 162 MHz): δ 55.3 (d, J_{RhP} = 158 Hz).

Alternatively, ethylene is bubbled through an acetone solution of [(^{tBu}xanPOP)Rh(H_2)]BF_4 or [(^{tBu}xanPOP)Rh(H_2)]SbF_6 for 12h, affording the title complex in near quantitative yield.

[(^{tBu}furPOP)Rh($H)_2$]SbF_6: *cis*-(^{tBu}furPOP)Rh($H)_2$Cl or a *cis/trans* mixture was converted into the title complex in quantitative yield, following the same procedure as for [(^{tBu}xanPOP)Rh($H)_2$]SbF_6. The complex is a red solid. ^{1}H NMR (300 MHz, CD_2Cl_2): δ 6.26 (s, 2H), 3.28 (vt, J_{PH} = 3.3 Hz, 4H), 1.30 (vt, J_{PH} = 7.3 Hz, 36H), -20.12 (dt, J_{RhH} = 39 Hz, J_{PH} = 10 Hz, 2H). ^{13}C NMR (75 MHz, CD_2Cl_2): δ 127.76 (t, J_{PC} = 25 Hz), 108.89, 35.38 (t, J_{PC} = 8.3 Hz), 28.57 (t, J_{PC} = 3.3 Hz), 21.88 (t, J_{PC} = 6.6 Hz). ^{31}P NMR (CD_2Cl_2, 162 MHz): δ 83.9 (d, J_{RhP} = 113 Hz).

Attempted reaction of (^{tBu}PNP)RhCl with H_2: (^{tBu}PNP)RhCl was prepared according to the literature[4] and refluxed in toluene under H_2 bubbling for 48h. The title compound was recovered after removal of solvent. No hydrides were detected from 0 to -50 ppm in C_6D_6.

[*cis*-(^{tBu}xanPOP)Rh(H)$_2$(OH$_2$)]SbF$_6$: 10 mg of [(^{tBu}xanPOP)Rh(H)$_2$]SbF$_6$ was dissolved in undried CD_2Cl_2. Slow diffusion of pentane into this solution afforded crystals suitable for X-Ray diffraction. Selected NMR data: ^{1}H NMR (400 MHz, CD_2Cl_2): δ -9 ppm (br s).

(^{tBu}xanPOP)RhH: 20 mg *cis*-(^{tBu}xanPOP)Rh(H)$_2$Cl (0.031 mmol) was dissolved in 1 mL C_6D_6. 5 mg KO^{t}Bu was added and the orange solution immediately turned dark red. After 30 min, the solution was filtered through celite and characterized by NMR. The solvent was removed in vacuo, the residue extracted with pentane, and the pentane removed in vacuo to give the title complex as a red powder in 90% yield. ^{1}H NMR (300 MHz, C_6D_6): δ 7.78 (d, J = 6.6 Hz, 2H), 7.11 (d, J = 7.8 Hz, 2H), 6.90 (t, J = 7.5 Hz, 2H), 1.56 (vt, J_{PH} = 6.3 Hz, 36H), 1.28 (s, 6H), -18.95 (dt, J_{PH} = 18.9 Hz, J_{RhH} = 36.9 Hz, 1H). ^{13}C NMR (75 MHz, C_6D_6): δ 157.19, 132.55 (m), 131.154, 126.28, 122.92, 121.647, 35.53 (m), 34.14, 33.09, 31.31 (m). ^{31}P NMR (121 MHz, C_6D_6): δ 78.0 (dd, J_{HP} = 18.3 Hz, J_{RhP} = 173 Hz).

(^{tBu}xanPOP)RhEt: 15 mg (0.025 mmol) (^{tBu}xanPOP)RhH was dissolved in C_6D_6 in a J-Young NMR tube. The solution was frozen, the headspace evacuated and replaced with 1 atm ethylene. The solution was allowed to thaw and NMR was immediately recorded (~1 min reaction time). ^{1}H NMR (300 MHz, C_6D_6): δ 7.81 (m, 2H), 7.08, (m, 2H), 6.86 (t, J = 6.0 Hz, 2H), 2.21 (qd, J = 7.5 Hz and J_{RhH} = 2.4 Hz, 2H), 1.85 (t, J = 7.2 Hz, 3H). ^{13}C NMR (100 MHz, C_6D_6): δ 158.69, 133.18, 132.03, 132.29, 131.27, 125.15, 38.01, 37.74, 34.54, 31.43, 30.68, 18.32. ^{31}P NMR (121 MHz, C_6D_6): δ 46.3 (d, J_{RhP} = 194 Hz)

(^{iPr}xanPOP)RhH$_2$Cl: To an orange solution of 70 mg (0.20 mmol) [Rh(COE)$_2$Cl]$_2$ in 2 mL pentane is added 88 mg (0.2 mmol) ^{iPr}xanPOP in 10 mL pentane. The reaction mixture immediately becomes dark red, and is stirred at 25°C for 12 hours, resulting in the quantitative formation of (^{iPr}xanPOP)RhCl (^{31}P NMR (C_6H_6, 121 MHz): δ 38 ppm, d, J_{RhP} = 147 Hz). An additional 5 mL pentane is added, and the solution is bubbled with H_2 at 25°C. After 4h, the

solution had turned light orange. Removal of the solvent afforded the title complex, as a 1:1 mixture of the monomer and dimer in quantitative yield. Selected NMR data for the monomeric product: ^{1}H NMR (C_6D_6, 300 MHz): δ -17.46 (dtd, J_{HH} = 9.9 Hz, J_{PH} = 15 Hz, J_{RhH} = 24 Hz, 1H), -20.07 (dtd, J_{HH} = 9.9 Hz, J_{PH} = 14 Hz, J_{RhH} = 28 Hz, 1H). ^{31}P NMR (121 MHz, C_6D_6): δ 67.0 (dt, J_{HP} = 14 Hz, J_{RhP} = 115 Hz). Selected NMR data for the dimeric product: ^{1}H NMR (C_6D_6, 300 MHz): δ -22.03 (comp). ^{31}P NMR (121 MHz, C_6D_6): δ 61.5 (br d, J_{RhP} = 122 Hz).

[(^{iPr}xanPOP)Rh(H)$_2$]B(C$_6$F$_5$)$_4$: 0.1 mmol (^{iPr}xanPOP)RhH_2Cl was dissolved in 0.6 mL CD_2Cl_2 to give an orange solution. 0.1 mmol Li[B(C_6F_5)$_4$]*OEt_2 was added and the solution was kept at 25 °C for 12 h, yielding a red solution with a colorless precipitate. NMR indicated complete conversion into the title species, which was isolated as a red solid after filtration and drying in vacuo. ^{1}H NMR (CD_2Cl_2, 400 MHz): δ -23.93 (dt, J_{PH} = 15 Hz, J_{RhH} 44 Hz, 1H). ^{31}P NMR (CD_2Cl_2, 162 MHz): δ 79.3 (d, J_{RhP} = 206 Hz).

COMPUTATIONAL METHODS

DFT calculations[5] employed the M06-L exchange-correlation functionals[6] and the SDD-model effective core potentials/basis sets on all atoms.[7] Calculations were performed on the actual molecular species used in the experiments, where pincers retained their bulky *t*Bu groups on P, and on truncated model complexes (PR_2 = PH_2). Standard procedures were employed to obtain the geometries and electronic energies for stationary points on the potential energy surfaces. Normal mode analysis was performed for each species and the resulting set of vibrational frequencies was employed (without scaling) to determine zero-point energy corrections. Enthalpies (ΔH, $\Delta H^{\ddagger}$) and Gibbs' free energies (ΔG, $\Delta G^{\ddagger}$; T = 298.15 K, P = 1 atm) were obtained from the potential energies (ΔE, $\Delta E^{\ddagger}$) using standard thermodynamic corrections.[8] All calculations have been performed using the Gaussian09 collection of computer programs.[9]

Optimized geometries and absolute energies of molecular species relevant to the reactions of (^{tBu}xanPOP)RhX (X = Cl, H) and (^{tBu}xanPOP)Rh^{+} with H_2.

(tBuxanPOP)RhH

Charge = 0 Multiplicity = 1

Rh,0,-0.000011,-1.240756,-0.0471

P,0,2.278441,-0.969848,-0.010203

O,0,0.000013,0.994239,-0.058758

P,0,-2.278458,-0.969795,-0.010197

C,0,1.23439,1.697382,-0.030842

C,0,2.409255,0.908884,-0.014509

C,0,3.639255,1.584297,0.040529

C,0,3.703891,2.982854,0.05867

C,0,2.520727,3.724281,0.027005

C,0,1.261077,3.100353,-0.011889

C,0,-1.234348,1.697411,-0.030852

C,0,-2.409233,0.908939,-0.014526

C,0,-3.639218,1.584384,0.040485

C,0,-3.703819,2.982944,0.058621

C,0,-2.520637,3.72434,0.026973

C,0,-1.261002,3.100383,-0.011903

C,0,0.000048,3.96022,-0.03388

H,0,4.555059,1.00613,0.075586

H,0,4.663724,3.484397,0.099228

H,0,2.568978,4.809587,0.038013

H,0,-4.555037,1.006242,0.075524

H,0,-4.663641,3.484509,0.09916

H,0,-2.568862,4.809648,0.037975

C,0,0.000053,4.895387,1.203668

C,0,0.000066,4.826029,-1.321476

H,0,0.00004,4.314397,2.129599

H,0,0.882921,5.541285,1.202017

H,0,-0.882796,5.54131,1.202007

H,0,0.88566,5.468333,-1.352617

H,0,0.000062,4.195848,-2.214737

H,0,-0.885509,5.468358,-1.352626

C,0,3.262955,-1.533121,-1.59368

C,0,3.203105,-1.503306,1.625688

C,0,-3.203115,-1.503243,1.625693

C,0,-3.263017,-1.533089,-1.593631

C,0,2.720379,-2.93273,1.942126

H,0,3.072759,-3.661569,1.205574

H,0,3.103561,-3.232713,2.926608

H,0,1.62598,-2.971454,1.953463

C,0,4.736331,-1.469802,1.577011

H,0,5.129993,-0.469434,1.366406

H,0,5.13077,-1.773646,2.556105

H,0,5.138225,-2.167154,0.834112

C,0,2.681121,-0.554924,2.721403

H,0,3.015335,-0.914666,3.702532

H,0,3.049397,0.467221,2.584604

H,0,1.583001,-0.531281,2.716216

C,0,2.326908,-1.182036,-2.766878

H,0,2.174966,-0.098474,-2.841921

H,0,2.770259,-1.533218,-3.708129

H,0,1.344656,-1.64996,-2.631155

C,0,4.629466,-0.874862,-1.833181

H,0,4.52864,0.196719,-2.030225

H,0,5.324082,-1.014253,-0.999483

H,0,5.087036,-1.328655,-2.722817

C,0,3.410584,-3.061846,-1.498506

H,0,4.136319,-3.353588,-0.730819

H,0,2.449412,-3.534835,-1.268968

H,0,3.766959,-3.452797,-2.459722

C,0,-3.410619,-3.061813,-1.498418

H,0,-3.767048,-3.452789,-2.459605

H,0,-2.449426,-3.534782,-1.268929

H,0,-4.136302,-3.353548,-0.730677

C,0,-4.629554,-0.874864,-1.833059

H,0,-4.528764,0.196721,-2.030104

H,0,-5.08716,-1.328665,-2.722673

H,0,-5.324124,-1.014275,-0.999323

C,0,-2.327027,-1.181999,-2.766875

H,0,-2.770417,-1.533194,-3.708103

H,0,-2.175105,-0.098434,-2.841934

H,0,-1.34476,-1.649906,-2.631197

C,0,-4.736342,-1.469788,1.576981

H,0,-5.130033,-0.469429,1.366391

H,0,-5.138188,-2.167135,0.834049

H,0,-5.130795,-1.773671,2.556056

C,0,-2.681167,-0.554827,2.721396

H,0,-1.583047,-0.531147,2.716213

H,0,-3.049477,0.467305,2.584581

H,0,-3.015374,-0.914566,3.702529

C,0,-2.720355,-2.93265,1.942143

H,0,-1.625954,-2.971342,1.9535

H,0,-3.103545,-3.232641,2.92662

H,0,-3.072702,-3.661502,1.205586

H,0,-0.000028,-2.827641,-0.054658

SCF Done: E(RM06L) = -2078.96163130 A.U. after 1 cycles

Zero-point correction= 0.737926 (Hartree/Particle)

Thermal correction to Energy= 0.778230

Thermal correction to Enthalpy= 0.779174

Thermal correction to Gibbs Free Energy= 0.670495

Sum of electronic and zero-point Energies= -2078.223705

Sum of electronic and thermal Energies= -2078.183402

Sum of electronic and thermal Enthalpies= -2078.182457

Sum of electronic and thermal Free Energies= -2078.291136

(tBuxanPOP)RhCl

Charge = 0 Multiplicity = 1

Rh,0,-0.0000101478,-1.1933887044,0.0387982936

P,0,2.2995179313,-0.9556548407,0.005640696

O,0,0.0000050415,0.9760434429,0.031691394

P,0,-2.2995303599,-0.9556203577,0.0056408202

C,0,1.2385354504,1.6907824958,0.0038834154

C,0,2.4180333252,0.913754047,-0.0313761367

C,0,3.645907062,1.5967636326,-0.0325140784

C,0,3.7023655898,2.9941334647,-0.0042536111

C,0,2.5138283365,3.7253425649,0.0228521101

C,0,1.257669022,3.0937477331,0.0260617636

C,0,-1.2385136117,1.6907998796,0.0038016508

C,0,-2.4180207301,0.9137881756,-0.0315292716

C,0,-3.6458810631,1.5968200445,-0.0329449982

C,0,-3.7023195784,2.9941921747,-0.0047658271

C,0,-2.5137746065,3.7253821317,0.0225156272

C,0,-1.2576264586,3.0937660545,0.0259307178

C,0,0.0000257232,3.9530787869,0.0666468841

H,0,4.5670042662,1.0271110681,-0.0503165036

H,0,4.6593897058,3.5021046201,-0.0020160333

H,0,2.5530226868,4.8105732136,0.0464181773

H,0,-4.5669867452,1.0271873233,-0.0509030233

H,0,-4.6593356417,3.5021794718,-0.0027276558

H,0,-2.552954285,4.8106146294,0.0460182496

C,0,-0.000034661,4.7914833408,1.3723317278

C,0,0.0000960732,4.9134200898,-1.151756461

H,0,-0.0000919525,4.1429821068,2.2522835498

H,0,0.8849678761,5.4333427061,1.4170963822

H,0,-0.8850234789,5.4333680419,1.416999491

H,0,0.8830379424,5.5588368774,-1.1363755318

H,0,0.0001451481,4.3520510568,-2.0896426479

H,0,-0.882842767,5.558843292,-1.1364717613

C,0,3.188784715,-1.57572306,-1.6090805734

C,0,3.2836172732,-1.4584291048,1.6093513158

C,0,-3.2835692193,-1.4583080134,1.6094205032

C,0,-3.1888789734,-1.5757757803,-1.6089801178

C,0,2.8477468017,-2.8933206046,1.9649814673

H,0,3.1688368606,-3.6252430535,1.2189649112

H,0,3.2959494633,-3.1683162264,2.9288337625

H,0,1.7589390546,-2.9671073595,2.0434136696

C,0,4.8121075625,-1.3876059033,1.488654763

H,0,5.1681700592,-0.3763701852,1.2663810072

H,0,5.2571178774,-1.6866620069,2.4468422559

H,0,5.1954405673,-2.069682533,0.7231133326

C,0,2.790677064,-0.5063487659,2.7158937872

H,0,3.1796505083,-0.847891156,3.6828746663

H,0,3.129255337,0.522398696,2.5532312806

H,0,1.6942685972,-0.5077488146,2.7665565101

C,0,2.1530963405,-1.3507711818,-2.728841122

H,0,1.88247933,-0.2912817167,-2.8210064607

H,0,2.5756462247,-1.6832587571,-3.6859052994

H,0,1.2382481746,-1.9172072112,-2.5248359641

C,0,4.489700944,-0.8431069383,-1.9663691457

H,0,4.3079247284,0.2113117028,-2.1954676169

H,0,5.2438973108,-0.9065513298,-1.1752604985

H,0,4.9162465476,-1.3070303114,-2.8656152352

C,0,3.4413372747,-3.0855202288,-1.4502910303

H,0,4.2377701133,-3.2940720492,-0.7273535397

H,0,2.5312558157,-3.6089267367,-1.1381039489

H,0,3.75799339,-3.4940213759,-2.418268631

C,0,-3.4414557985,-3.0855567319,-1.4500696326

H,0,-3.7581685418,-3.4941178609,-2.4180031399

H,0,-2.5313703719,-3.6089608273,-1.1378899926

H,0,-4.2378574063,-3.2940394117,-0.7270771574

C,0,-4.4897991028,-0.8431372531,-1.9662104632

H,0,-4.3080181954,0.2113000965,-2.1952276836

H,0,-4.9163573852,-1.306999901,-2.8654815867

H,0,-5.2439861102,-0.9066320903,-1.1750970539

C,0,-2.1532429325,-1.3509046336,-2.7288067214

H,0,-2.5758472935,-1.6834395569,-3.6858304033

H,0,-1.8826131117,-0.2914245947,-2.821046348

H,0,-1.2383942207,-1.9173445374,-2.5248168351

C,0,-4.8120640242,-1.387469174,1.4887850831

H,0,-5.1681255134,-0.3762265375,1.2665511961

H,0,-5.195430183,-2.0695234433,0.7232389627

H,0,-5.2570421745,-1.6865445318,2.4469811119

C,0,-2.7905547672,-0.5062078203,2.7159147814

H,0,-1.6941427698,-0.5076155177,2.7665121572

H,0,-3.1291359484,0.5225396417,2.5532594779

H,0,-3.1794727667,-0.8477322522,3.6829243938

C,0,-2.8477146213,-2.8931984087,1.9650683182

H,0,-1.7589047571,-2.9670035196,2.0434616204

H,0,-3.2958869372,-3.1681633672,2.9289433206

H,0,-3.168849091,-3.6251308312,1.219079224

Cl,0,-0.0000448115,-3.6121410841,-0.1605636179

SCF Done: E(RM06L) = -2538.60143553 A.U. after 3 cycles

Zero-point correction= 0.732929 (Hartree/Particle)

Thermal correction to Energy= 0.774519

Thermal correction to Enthalpy= 0.775463

Thermal correction to Gibbs Free Energy= 0.663985

Sum of electronic and zero-point Energies= -2537.868507

Sum of electronic and thermal Energies= -2537.826917

Sum of electronic and thermal Enthalpies= -2537.825973

Sum of electronic and thermal Free Energies= -2537.937451

---

dihydrogen

Charge = 0 Multiplicity = 1

H,0,0.,0.,0.0025489349

H,0,0.,0.,0.7474510651

SCF Done: E(RM06L) = -1.16824931834 A.U. after 1 cycles

Zero-point correction= 0.009924 (Hartree/Particle)

Thermal correction to Energy= 0.012284

Thermal correction to Enthalpy= 0.013228

Thermal correction to Gibbs Free Energy= -0.001569

Sum of electronic and zero-point Energies= -1.158326

Sum of electronic and thermal Energies= -1.155965

Sum of electronic and thermal Enthalpies= -1.155021

Sum of electronic and thermal Free Energies= -1.169818

(tBuxanPOP)Rh-H-H-H

Charge = 0 Multiplicity = 1

Rh,0,0.0001187538,-1.2667873654,0.0123638939

P,0,2.2921342826,-0.9598788093,0.1135619257

O,0,-0.0000512846,1.0074048885,-0.2921368695

P,0,-2.2920356357,-0.9602987578,0.1127100645

C,0,1.2193679798,1.6832637604,0.0131946595

C,0,2.3606540432,0.9060411782,0.2823880856

C,0,3.5353587573,1.5964041172,0.6348830996

C,0,3.5651209884,2.9935968949,0.7044997949

C,0,2.4229328727,3.7328121431,0.3688752885

C,0,1.2346996903,3.0886142073,-0.0031298215

C,0,-1.2197305515,1.6830430317,0.0126459042

C,0,-2.3609925152,0.9056201838,0.2813612046

C,0,-3.5359899824,1.5957720659,0.6332701233

C,0,-3.5660725882,2.9929632635,0.702764016

C,0,-2.423864417,3.732381787,0.3676500574

C,0,-1.2353268516,3.0883901228,-0.0037313062

C,0,-0.0002550094,3.8164245788,-0.5272181778

H,0,4.4304095848,1.0280392116,0.8688647274

H,0,4.4763396915,3.5022630073,0.9970175823

H,0,2.4606703445,4.8162454777,0.388462319

H,0,-4.4310216869,1.0272379517,0.8669126985

H,0,-4.4775428269,3.5014681172,0.9947762481

H,0,-2.4618200679,4.8158104267,0.3871289282

C,0,-0.000483603,5.3073149663,-0.1707626055

C,0,0.0001374023,3.6711713935,-2.0802718978

H,0,-0.0007595301,5.4677643116,0.9116750613

H,0,0.87667803,5.8034413654,-0.5954359322

H,0,-0.8775338372,5.8032826828,-0.595854842

H,0,0.8907939671,4.1480868338,-2.5019809

H,0,0.0002376407,2.6167371857,-2.3758524335

H,0,-0.8903380189,4.1480353703,-2.5024186516

C,0,3.3279773096,-1.2400201684,-1.5224470523

C,0,3.2069732755,-1.6924506581,1.6756121369

C,0,-3.2072506445,-1.6928531258,1.6745303246

C,0,-3.3271633266,-1.2408180455,-1.5236902762

C,0,2.6259393392,-3.1093090639,1.8652289187

H,0,2.8235863573,-3.7550732047,1.0022703379

H,0,3.0883973962,-3.5679886365,2.7487494128

H,0,1.5430718512,-3.0640251943,2.0110866471

C,0,4.7366507272,-1.7911017898,1.5700822136

H,0,5.2164822414,-0.8211212965,1.4034934708

H,0,5.1222086467,-2.1909914608,2.5168581025

H,0,5.0491863893,-2.4746474404,0.7740553422

C,0,2.8211625127,-0.8321187141,2.8914813652

H,0,3.1379091402,-1.3513257883,3.804676495

H,0,3.3050097747,0.1494867943,2.8733505901

H,0,1.7364621704,-0.687891624,2.9313123585

C,0,2.5441948921,-0.5272037793,-2.640699597

H,0,2.5496132519,0.5610004306,-2.4963928546

H,0,3.0241251017,-0.7430076424,-3.603639184

H,0,1.5063219907,-0.8706092415,-2.6746013092

C,0,4.7588485346,-0.677656392,-1.5233462108

H,0,4.765782177,0.4051751699,-1.3623615179

H,0,5.4138719538,-1.1475426498,-0.7889040562

H,0,5.1961229913,-0.8584574342,-2.5143647801

C,0,3.3285426998,-2.7580752271,-1.7698360678

H,0,3.933000079,-3.290742485,-1.0254715463

H,0,2.3069952577,-3.1527368964,-1.7403729341

H,0,3.7534438525,-2.9706613611,-2.7584776578

C,0,-3.3274292275,-2.7589098786,-1.7708771313

H,0,-3.7519078544,-2.9716617194,-2.7596675973

H,0,-2.3058490375,-3.1534492803,-1.7409686519

H,0,-3.9321151239,-3.2915638791,-1.0266929498

C,0,-4.7581238245,-0.6786645128,-1.5252815772

H,0,-4.7652745372,0.4042302983,-1.3647095126

H,0,-5.1950404121,-0.8599154456,-2.5163781312

H,0,-5.4133340008,-1.1483617686,-0.7908881894

C,0,-2.5430273234,-0.5280743199,-2.641726881

H,0,-3.022608272,-0.7440399099,-3.6048050911

H,0,-2.5485650349,0.5601391774,-2.4975446415

H,0,-1.505126018,-0.8714360185,-2.6752016887

C,0,-4.736881718,-1.7916979291,1.5685760738

H,0,-5.2167794795,-0.821769523,1.4018483218

H,0,-5.0491023809,-2.4752798028,0.7724598238

H,0,-5.122664951,-2.1916259442,2.5152409636

C,0,-2.8219157881,-0.8323162292,2.8904098868

H,0,-1.7372369871,-0.6880558629,2.9305798859

H,0,-3.3057720586,0.1492795529,2.8719468427

H,0,-3.1389866741,-1.3514153342,3.8035509202

C,0,-2.6260689551,-3.1096121062,1.8644550358

H,0,-1.5432228435,-3.0641903529,2.0104229707

H,0,-3.0885648247,-3.5681968987,2.7480070261

H,0,-2.8235680778,-3.755543724,1.0015883964

H,0,0.0002728041,-2.8013834071,0.2126629718

H,0,0.0004891608,-1.7110900827,-1.5916614408

H,0,-0.0001955153,-1.0095157061,1.6841198983

SCF Done: E(RM06L) = -2080.14333814 A.U. after 3 cycles

Zero-point correction= 0.753984 (Hartree/Particle)

Thermal correction to Energy= 0.794681

Thermal correction to Enthalpy= 0.795625

Thermal correction to Gibbs Free Energy= 0.686996

Sum of electronic and zero-point Energies= -2079.389354

Sum of electronic and thermal Energies= -2079.348657

Sum of electronic and thermal Enthalpies= -2079.347713

Sum of electronic and thermal Free Energies= -2079.456342

(tBuxanPOP)Rh-Cl-H-H, H's cis

Charge = 0 Multiplicity = 1

Rh,0,0.0001869985,-1.2567482572,0.3560697427

P,0,2.319242503,-0.9715100989,0.1538342642

O,0,-0.0001308818,0.9760891959,-0.1431301043

P,0,-2.3189485838,-0.9722606057,0.1533784772

C,0,1.2309639345,1.6734319853,-0.0150936565

C,0,2.4052912855,0.8943173295,0.0842848028

C,0,3.6367438304,1.563764913,0.145688522

C,0,3.7026299225,2.9615508726,0.1140809472

C,0,2.5196727088,3.6991066457,0.0377791803

C,0,1.2606936305,3.0759050272,-0.0202383389

C,0,-1.2314779743,1.6730316559,-0.0153358859

C,0,-2.4055712182,0.893539302,0.083837616

C,0,-3.637253269,1.562593996,0.1449959293

C,0,-3.703583035,2.9603578705,0.1133670859

C,0,-2.52084844,3.6982937892,0.0372830495

C,0,-1.2616630542,3.0754943099,-0.0205059229

C,0,-0.0006225855,3.9347706142,-0.0697825909

H,0,4.5487290283,0.9819132257,0.2396359419

H,0,4.6608277363,3.464680178,0.1633457961

H,0,2.5682971706,4.7841328391,0.0282130578

H,0,-4.5490688556,0.9804493944,0.2387814656

H,0,-4.6619521284,3.4631790286,0.1624460411

H,0,-2.569814271,4.7833054335,0.0277178568

C,0,-0.0009383117,4.8900451862,1.1534362363

C,0,-0.0006228329,4.7731287806,-1.3744376857

H,0,-0.0009070147,4.3208545006,2.0861929447

H,0,0.8810706993,5.5367530351,1.141915895

H,0,-0.8832251428,5.5363732054,1.1417450505

H,0,0.8845547449,5.415334707,-1.418545424

H,0,-0.0004070177,4.1254826787,-2.2554955475

H,0,-0.8860179677,5.4150208025,-1.4187483762

C,0,3.0236216313,-1.4825735433,-1.5967149671

C,0,3.4708999795,-1.5620950072,1.6237341326

C,0,-3.4707574752,-1.5632605462,1.6229937475

C,0,-3.022774831,-1.4834894835,-1.5973580464

C,0,2.7648859777,-2.8186026831,2.1759192462

H,0,2.667306654,-3.6024357755,1.4155433956

H,0,3.3556722987,-3.2192212013,3.0092868594

H,0,1.7641840268,-2.565891663,2.5386564437

C,0,4.9083021826,-1.9160156487,1.2167361635

H,0,5.4567750685,-1.0530532,0.8242837186

H,0,5.4385545503,-2.2613370511,2.1134914931

H,0,4.9495172226,-2.724134172,0.479127908

C,0,3.5027869579,-0.4836550084,2.7222319467

H,0,3.9614963416,-0.9273506047,3.6153987474

H,0,4.1047633438,0.3831462337,2.4345536097

H,0,2.4963056685,-0.1482493538,2.9838665649

C,0,2.1243480489,-0.7836876247,-2.6355449445

H,0,2.2840705973,0.3004716915,-2.629210037

H,0,2.3790956033,-1.1582982444,-3.6346982581

H,0,1.0648341312,-0.9783085943,-2.4504468554

C,0,4.4718640951,-1.0568130235,-1.8938850608

H,0,4.6052306399,0.0253426425,-1.7968008424

H,0,5.2094963129,-1.5637595394,-1.2721731323

H,0,4.6926577514,-1.3140465679,-2.9381534276

C,0,2.8735393475,-3.0098030636,-1.7035856894

H,0,3.536744586,-3.5338332302,-1.0051774097

H,0,1.8428028984,-3.3159343489,-1.4963443507

H,0,3.1349671417,-3.333398927,-2.7184897559

C,0,-2.8721704407,-3.0106669792,-1.7042497002

H,0,-3.1333277085,-3.334311078,-2.7192090293

H,0,-1.8413701209,-3.3164648369,-1.4968438517

H,0,-3.5353201936,-3.5349361464,-1.0059673329

C,0,-4.4710888914,-1.0582220648,-1.8948512013

H,0,-4.6048931908,0.0238683027,-1.7976410516

H,0,-4.691503274,-1.3153760803,-2.9392192783

H,0,-5.208693161,-1.5655410445,-1.2734142195

C,0,-2.1235016173,-0.7842508954,-2.6359630592

H,0,-2.3778487006,-1.1589569165,-3.6351816477

H,0,-2.2836638919,0.2998432242,-2.6296565292

H,0,-1.0639568105,-0.9784556989,-2.4506119322

C,0,-4.9079380358,-1.9176428566,1.2156181253

H,0,-5.4566195837,-1.0548330572,0.8231202987

H,0,-4.9486877397,-2.7257036082,0.4779159254

H,0,-5.4382841277,-2.2632360331,2.112214006

C,0,-3.5032852722,-0.4848802828,2.7215304671

H,0,-2.4969844918,-0.1491238339,2.9834110739

H,0,-4.1055080859,0.3817211656,2.4337588074

H,0,-3.9620418342,-0.9287801511,3.6145710872

C,0,-2.7644654867,-2.819557871,2.1753082603

H,0,-1.7639323176,-2.5665308317,2.5382983326

H,0,-3.3553237671,-3.2203931233,3.0085208684

H,0,-2.6664504444,-3.6033394295,1.414932835

H,0,0.0003851153,-2.7501102977,0.7587304053

H,0,0.0004369301,-1.9652390366,-1.0372670348

Cl,0,-0.0002601074,-0.2174771211,2.7358496056

SCF Done: E(RM06L) = -2539.79959978 A.U. after 4 cycles

Zero-point correction= 0.750333 (Hartree/Particle)

Thermal correction to Energy= 0.792592

Thermal correction to Enthalpy= 0.793536

Thermal correction to Gibbs Free Energy= 0.681034

Sum of electronic and zero-point Energies= -2539.049267

Sum of electronic and thermal Energies= -2539.007008

Sum of electronic and thermal Enthalpies= -2539.006064

Sum of electronic and thermal Free Energies= -2539.118565

(tBuxanPOP)Rh-H-Cl-H, H's trans

Charge = 0 Multiplicity = 1

Rh,0,0.0000597823,-1.1532505429,-0.1384742291

P,0,2.3173752321,-0.9475102671,-0.1008102223

O,0,-0.0000516806,0.9960859158,0.0266996616

P,0,-2.3172748184,-0.9477392096,-0.1010360394

C,0,1.2403972215,1.6996669198,-0.0142854498

C,0,2.4184809074,0.9243807705,-0.1005402924

C,0,3.6458818532,1.6072755073,-0.091211064

C,0,3.7019781743,3.0026155129,-0.0104621477

C,0,2.5151959726,3.7319918551,0.0632055951

C,0,1.2592552258,3.1007875405,0.0619251914

C,0,-1.2405677636,1.6995460898,-0.0143891025

C,0,-2.4185719528,0.924145694,-0.1007351624

C,0,-3.6460376748,1.6069257167,-0.0914614594

C,0,-3.7022698224,3.0022608036,-0.010715966

C,0,-2.5155629474,3.7317510423,0.0630185962

C,0,-1.259563237,3.1006660214,0.0618249763

C,0,-0.0001992401,3.9543191715,0.1640927933

H,0,4.5668156447,1.040193438,-0.1369351118

H,0,4.659172466,3.5099326025,-0.000683746

H,0,2.5568894163,4.8149797254,0.1308716128

H,0,-4.5669182748,1.0397619493,-0.1372315774

H,0,-4.6595126244,3.5094874384,-0.000994859

H,0,-2.5573651203,4.8147342678,0.1306889728

C,0,-0.0002912889,4.6935481946,1.5289340344

C,0,-0.000202517,5.0009658559,-0.9808940488

H,0,-0.0002945001,3.9818730398,2.3586886343

H,0,0.885241425,5.3298673183,1.6205787975

H,0,-0.8858903909,5.3297853223,1.6205013636

H,0,0.8811900355,5.645229063,-0.9195004952

H,0,-0.000138367,4.5090512341,-1.9568826867

H,0,-0.8816604138,5.6451468363,-0.9195735814

C,0,3.3528975057,-1.6105404618,-1.6171650273

C,0,3.1893709524,-1.4365081998,1.5803947261

C,0,-3.1893666122,-1.4368571108,1.5800796682

C,0,-3.3525752526,-1.6108896558,-1.6175060903

C,0,2.7113577501,-2.8566377595,1.9384336274

H,0,3.0887352972,-3.6127899533,1.2456123856

H,0,3.0738725412,-3.1047856452,2.9443477856

H,0,1.6186180064,-2.9088972676,1.9317285822

C,0,4.7244418095,-1.380953285,1.5433298868

H,0,5.0999045907,-0.37589383,1.3199433473

H,0,5.1042154875,-1.6549709628,2.5360337032

H,0,5.1536647969,-2.0856736843,0.8253194449

C,0,2.6716039314,-0.4573095912,2.6501828328

H,0,3.0145438393,-0.8014455109,3.63358783

H,0,3.0480947761,0.5598471625,2.4947255115

H,0,1.5761772478,-0.4390993612,2.6563157307

C,0,2.4818987165,-1.4381829167,-2.8730900897

H,0,2.1978907141,-0.3923163869,-3.0318840785

H,0,3.0592035395,-1.7780107001,-3.7432666399

H,0,1.5641652008,-2.0254679313,-2.7986690604

C,0,4.6905711088,-0.8876232953,-1.8499464736

H,0,4.5354590414,0.1466660347,-2.1710003977

H,0,5.3460468392,-0.8933191737,-0.9746540583

H,0,5.2197277034,-1.4053543713,-2.6603293076

C,0,3.5856473789,-3.1162205983,-1.3848890103

H,0,4.3018375497,-3.3087884084,-0.5798421838

H,0,2.6468794609,-3.6320815808,-1.1589317912

H,0,3.9988290215,-3.5471401435,-2.3054303393

C,0,-3.5851761286,-3.1165949262,-1.3852552289

H,0,-3.9982026149,-3.5475603676,-2.3058461003

H,0,-2.6463713334,-3.6323404728,-1.1591901823

H,0,-4.3014318518,-3.309244158,-0.5802885186

C,0,-4.6903037556,-0.8881250254,-1.8504337424

H,0,-4.5352673075,0.1461672523,-2.1715143498

H,0,-5.2193304417,-1.4059396794,-2.6608478737

H,0,-5.3458623349,-0.8938532013,-0.9752018169

C,0,-2.4814683543,-1.4384341202,-2.8733438428

H,0,-3.0586419799,-1.7783427275,-3.7435762028

H,0,-2.1975840061,-0.3925314118,-3.0321172396

H,0,-1.5636684059,-2.0256024606,-2.7988336761

C,0,-4.7244447005,-1.3814978125,1.54287137

H,0,-5.1000083155,-0.3764916591,1.3194228022

H,0,-5.1535167334,-2.086287634,0.8248384951

H,0,-5.1042759213,-1.6555368536,2.535548286

C,0,-2.6718176677,-0.4575976865,2.6499167095

H,0,-1.5763931593,-0.4392329207,2.6561459994

H,0,-3.0484361741,0.5595069374,2.4944335928

H,0,-3.0147911135,-0.8017824377,3.6332924409

C,0,-2.7111883346,-2.8569193714,1.9381588547

H,0,-1.6184400458,-2.9090307325,1.9315570737

H,0,-3.0737597988,-3.1051193376,2.944040097

H,0,-3.0883977191,-3.6131193371,1.2453013518

H,0,0.0001149598,-0.9046208097,-1.774828149

Cl,0,0.0001841595,-3.5540162953,-0.5130361185

H,0,-0.0000801557,-1.3964336602,1.5303389863

SCF Done: E(RM06L) = -2539.75623615 A.U. after 3 cycles

Zero-point correction= 0.748274 (Hartree/Particle)

Thermal correction to Energy= 0.790144

Thermal correction to Enthalpy= 0.791088

Thermal correction to Gibbs Free Energy= 0.679842

Sum of electronic and zero-point Energies= -2539.007962

Sum of electronic and thermal Energies= -2538.966092

Sum of electronic and thermal Enthalpies= -2538.965148

Sum of electronic and thermal Free Energies= -2539.076394

(tBuxanPOP)Rh+

Charge = 1 Multiplicity = 1

Rh,0,-0.0000022209,-1.0176362059,0.085219743

P,0,2.2799085567,-0.7357677852,0.0826407999

O,0,-0.0000026192,1.1572128133,-0.1031784597

P,0,-2.2799132514,-0.7357691403,0.08264469

C,0,1.2206630603,1.8591155616,-0.0711571387

C,0,2.3890195448,1.0865523933,0.0180160335

C,0,3.6141166646,1.7553155498,0.0774245546

C,0,3.6755160906,3.1391170667,0.0200089125

C,0,2.5015088471,3.8637395352,-0.089537252

C,0,1.2470089201,3.2494480804,-0.1262202377

C,0,-1.2206684438,1.8591150782,-0.0711552727

C,0,-2.3890245904,1.0865514388,0.0180195792

C,0,-3.6141217674,1.7553146925,0.0774279352

C,0,-3.6755215551,3.1391161618,0.0200116511

C,0,-2.5015146127,3.8637388711,-0.0895351992

C,0,-1.2470146473,3.2494476371,-0.1262187899

C,0,-0.0000030765,4.1058902408,-0.2370468498

H,0,4.5281999154,1.1812197597,0.1721595375

H,0,4.6315344182,3.6478079852,0.0603943256

H,0,2.5506000356,4.9461742946,-0.1438682601

H,0,-4.5282050127,1.181219173,0.1721630848

H,0,-4.6315399927,3.6478068691,0.0603970062

H,0,-2.5506060805,4.9461735926,-0.1438667394

C,0,-0.0000026902,5.1537339212,0.8902093336

C,0,-0.0000040422,4.8184497637,-1.6017010313

H,0,-0.0000020352,4.6785601896,1.873883011

H,0,0.8766108751,5.8007492571,0.8270959694

H,0,-0.8766166428,5.8007488305,0.8270969347

H,0,0.8820517046,5.4547509167,-1.707794585

H,0,-0.0000043058,4.1010007193,-2.4259163189

H,0,-0.8820602868,5.4547503989,-1.7077935876

C,0,3.144593325,-1.3624234708,-1.4723775554

C,0,3.0879733802,-1.290104349,1.6971965402

C,0,-3.0879706432,-1.2901053365,1.6972060318

C,0,-3.1445955233,-1.3624240787,-1.4723766852

C,0,2.4738728568,-2.6586527834,2.0210461481

H,0,2.7297983902,-3.4256923195,1.2871667001

H,0,2.8364710597,-3.0033959072,2.9948527151

H,0,1.3799787378,-2.593926257,2.0833419501

C,0,4.6097827879,-1.3940149905,1.681975382

H,0,5.0952503873,-0.4410711764,1.4588309251

H,0,4.9584358669,-1.7022838176,2.6735707553

H,0,4.9714762588,-2.1400269105,0.97079809

C,0,2.6365085968,-0.294397541,2.7700228008

H,0,2.9133215566,-0.6767084208,3.7574732761

H,0,3.1014818148,0.6866325689,2.6500818221

H,0,1.5483808361,-0.1591767642,2.7589594351

C,0,2.2193228736,-0.9444387366,-2.6217492023

H,0,2.1169588254,0.1433343995,-2.688112002

H,0,2.6328093244,-1.2954018721,-3.5728733102

H,0,1.216659106,-1.3708889783,-2.5082785141

C,0,4.5403717864,-0.8002381515,-1.733030757

H,0,4.517368479,0.2734232719,-1.9290416937

H,0,5.2426842458,-0.991176552,-0.9197948812

H,0,4.9499316576,-1.2780348914,-2.6295116488

C,0,3.1963727675,-2.8897523396,-1.3956882238

H,0,3.9050331187,-3.2462878397,-0.6442594759

H,0,2.2152020082,-3.3241010256,-1.1760895522

H,0,3.5211309288,-3.2914974249,-2.3605708219

C,0,-3.1964054404,-2.8897514746,-1.3956754923

H,0,-3.5211528159,-3.2914980342,-2.3605611108

H,0,-2.2152469015,-3.3241167371,-1.1760549289

H,0,-3.905086599,-3.2462684987,-0.644257888

C,0,-4.5403585833,-0.8002122827,-1.7330566406

H,0,-4.5173294024,0.273446308,-1.9290799083

H,0,-4.9499147355,-1.278010255,-2.6295385826

H,0,-5.2426878831,-0.9911260731,-0.9198301403

C,0,-2.2193025458,-0.9444696238,-2.6217410714

H,0,-2.6327829672,-1.2954361882,-3.5728665066

H,0,-2.1169177331,0.1433008454,-2.6881151406

H,0,-1.2166481235,-1.3709369705,-2.5082523614

C,0,-4.6097799238,-1.394021546,1.6819995291

H,0,-5.0952533359,-0.4410823731,1.4588485002

H,0,-4.9714781597,-2.1400437696,0.9708361692

H,0,-4.9584221862,-1.7022794835,2.6736021047

C,0,-2.6365021478,-0.2943947464,2.7700270444

H,0,-1.5483747581,-0.1591716966,2.7589571222

H,0,-3.1014781077,0.6866340275,2.6500858491

H,0,-2.9133087192,-0.6767034271,3.7574801707

C,0,-2.4738633689,-2.6586504081,2.0210569608

H,0,-1.3799691148,-2.5939199757,2.0833448756

H,0,-2.8364537426,-3.0033907967,2.9948674027

H,0,-2.7297912663,-3.4256937866,1.287182415

SCF Done: E(RM06L) = -2077.71595038   A.U. after   1 cycles

Zero-point correction= 0.720477 (Hartree/Particle)

Thermal correction to Energy= 0.761116

Thermal correction to Enthalpy= 0.762061

Thermal correction to Gibbs Free Energy= 0.650693

Sum of electronic and zero-point Energies= -2076.995473

Sum of electronic and thermal Energies= -2076.954834

Sum of electronic and thermal Enthalpies= -2076.953890

Sum of electronic and thermal Free Energies= -2077.065257

(tBuxanPOP)Rh+, SQP, H apical

Charge = 1 Multiplicity = 1

Rh,0,0.0020887359,-1.2397126496,-0.0096136167

P,0,-2.2977516475,-0.9446788175,-0.0448578068

O,0,-0.0000534775,1.011147994,0.125026047

P,0,2.3008952685,-0.9392815804,-0.0625083914

C,0,-1.219170531,1.6879976257,0.0143969909

C,0,-2.3806767206,0.8956913156,-0.0575444782

C,0,-3.6063179228,1.5613491798,-0.1497679477

C,0,-3.6764316331,2.9459790241,-0.1586140588

C,0,-2.5091122689,3.6860929673,-0.0812561154

C,0,-1.2540887986,3.0793747092,-0.0011563038

C,0,1.2166538491,1.6908554569,0.0057713865

C,0,2.3794806879,0.9012873997,-0.074586045

C,0,3.6028749519,1.5698453086,-0.1753363667

C,0,3.6696740775,2.9546386571,-0.1843397022

C,0,2.5011915808,3.6919939684,-0.098677577

C,0,1.2481929616,3.082313612,-0.0098651707

C,0,-0.0035946179,3.9372945129,0.0972280947

H,0,-4.5199212932,0.9833470443,-0.2123440012

H,0,-4.6368955155,3.4436567773,-0.2236254822

H,0,-2.5677798518,4.7692957858,-0.0792833767

H,0,4.5173686973,0.9940182716,-0.2445447559

H,0,4.6284878141,3.4545832702,-0.2559815272

H,0,2.5573167135,4.7753329723,-0.0969843673

C,0,-0.0087188358,4.9799159156,-1.0338878759

C,0,0.0002779636,4.6569429075,1.4584829122

H,0,-0.0115847919,4.501028657,-2.0157095038

H,0,-0.8845900441,5.6275147758,-0.9705131758

H,0,0.8660924322,5.6295123384,-0.9765970187

H,0,-0.8831477675,5.2918211852,1.5638349029

H,0,0.0039903137,3.943986443,2.2868942011

H,0,0.882909476,5.2939084924,1.5577166063

C,0,-3.056254862,-1.4531668727,1.6073170841

C,0,-3.2565111524,-1.5645026641,-1.5506143984

C,0,3.249499608,-1.5556146067,-1.5760968728

C,0,3.0730256144,-1.4474856167,1.5834349034

C,0,-2.7619314061,-2.9859955098,-1.8465693597

H,0,-2.9610606973,-3.6823170358,-1.0294629036

H,0,-3.2822102749,-3.3639122705,-2.7321523243

H,0,-1.6893332613,-3.0067445352,-2.0493715875

C,0,-4.7760968304,-1.5932334773,-1.3824478854

H,0,-5.2086238071,-0.6095651719,-1.191185137

H,0,-5.2238475708,-1.9576401946,-2.3127351255

H,0,-5.0966326359,-2.2719751821,-0.5896045927

C,0,-2.8791470865,-0.6579113851,-2.7250652631

H,0,-3.2712999397,-1.0901270113,-3.6506367697

H,0,-3.2924181672,0.3482062166,-2.6259891623

H,0,-1.7937378581,-0.5692767119,-2.839166553

C,0,-1.9931013193,-1.0529384982,2.6375617691

H,0,-1.7677120817,0.0187629204,2.6107545936

H,0,-2.3423110657,-1.2887617648,3.6480944978

H,0,-1.0626526792,-1.613153612,2.4819523703

C,0,-4.3762828535,-0.7749780018,1.9641894178

H,0,-4.2641784247,0.3049774272,2.0797746022

H,0,-5.1661577137,-0.9653216277,1.235451437

H,0,-4.725595085,-1.1668216476,2.9253393491

C,0,-3.2139436265,-2.9747210873,1.6228348703

H,0,-4.015573732,-3.317736395,0.9651600143

H,0,-2.2896571896,-3.4840851505,1.3338511029

H,0,-3.4687905531,-3.3003646906,2.6363165954

C,0,3.2346298117,-2.9686562393,1.5963333776

H,0,3.4977080578,-3.2945837246,2.607618848

H,0,2.3095188669,-3.480063462,1.3136750772

H,0,4.0322820445,-3.3090509012,0.9324923459

C,0,4.393977106,-0.7663795398,1.9312121608

H,0,4.2800277292,0.3131404809,2.049009694

H,0,4.7515232543,-1.1585304595,2.8892041658

H,0,5.178806034,-0.9538265663,1.1962870419

C,0,2.0165038828,-1.0509914329,2.6219164749

H,0,2.3738739888,-1.2865963742,3.6296447775

H,0,1.7879063046,0.0200963282,2.5976310381

H,0,1.0865181383,-1.6137555819,2.4727790473

C,0,4.7703965604,-1.5806078127,-1.4196447835

H,0,5.2018544032,-0.5959358798,-1.231138177

H,0,5.0987387488,-2.2589826889,-0.6296894478

H,0,5.2119158175,-1.9433325583,-2.3535605159

C,0,2.8608142614,-0.649012977,-2.7468418975

H,0,1.7743349738,-0.5631357162,-2.8525643407

H,0,3.2722081075,0.3580977183,-2.6500430052

H,0,3.2470122426,-1.0794132743,-3.6757571982

C,0,2.7561812051,-2.9780834006,-1.86942587

H,0,1.6820432888,-3.0013752805,-2.063631512

H,0,3.2702819738,-3.3538368662,-2.7595260449

H,0,2.9636490599,-3.674668939,-1.0546329473

H,0,0.0035917985,-2.7840441593,-0.1043079534

H,0,-0.003765815,-1.4074340567,-1.5268735047

SCF Done: E(RM06L) = -2078.95091020 A.U. after 1 cycles

Zero-point correction= 0.737429 (Hartree/Particle)

Thermal correction to Energy= 0.778545

Thermal correction to Enthalpy= 0.779489

Thermal correction to Gibbs Free Energy= 0.668729

Sum of electronic and zero-point Energies= -2078.213481

Sum of electronic and thermal Energies= -2078.172365

Sum of electronic and thermal Enthalpies= -2078.171421

Sum of electronic and thermal Free Energies= -2078.282181

Chapter 3.3 Experimental Section References

(1) Asensio, G.; Cuenca, A. B.; Esteruelas, M. A.; Medio-Simon, M.; Olivan, M.; Valencia, M. *Inorg. Chem.* **2010**, *49*, 8665-8667.
(2) Cammidge, A. N.; Cook, M. J.; Harrison, K. J.; McKeown, N. B. *J. Chem. Soc., Perkin Trans. 1* **1991**, 3053-3058.
(3) van der Ent, A.; Onderlinden, A. L.; Schunn, R. A. *Inorg. Synth. 28*, 90-92.
(4) Hermann, D.; Gandelman, M.; Rozenberg, H.; Shimon, L. J. W.; Milstein, D. *Organometallics* **2002**, *21*, 812-818.
(5) R. G. Parr, W. Yang, *Density-Functional Theory of Atoms and Molecules*; University Press: Oxford, 1989.
(6) Y. Zhao, D. G. Truhlar, *Theo. Chem. Acc.* **120**, 215 (2008).
(7) (a) Dolg, M.; Stoll, H.; Preuss, H.; Pitzer, R.M. *J. Phys Chem.* **1993**, *97*, 5852. (b) Dunning, T. H. Jr.; Hay, P. in *Modern Theoretical Chemistry*, Ed. H. F. Schaefer III, Vol. 3 (Plenum, New York, 1976) 1-28.
(8) A. McQuarrie, *Statistical Thermodynamics*; Harper and Row: New York, 1973.
(9) Gaussian 09, Revision A.02, M. J. Frisch, G. W. Trucks, H. B. Schlegel, G. E. Scuseria, M. A.Robb, J. R. Cheeseman, G. Scalmani, V. Barone, B. Mennucci, G. A. Petersson, H. Nakatsuji, M. Caricato, X. Li, H. P. Hratchian, A. F. Izmaylov, J. Bloino, G. Zheng, J. L. Sonnenberg, M. Hada, M. Ehara, K. Toyota, R. Fukuda, J. Hasegawa, M. Ishida, T. Nakajima, Y. Honda, O. Kitao, H. Nakai, T. Vreven, J. A. Montgomery, Jr., J. E. Peralta, F. Ogliaro, M. Bearpark, J. J. Heyd, E. Brothers, K. N. Kudin, V. N. Staroverov, R. Kobayashi, J. Normand, K. Raghavachari, A. Rendell, J. C. Burant, S. S. Iyengar, J. Tomasi, M. Cossi, N. Rega, N. J. Millam, M. Klene, J. E. Knox, J. B. Cross, V. Bakken, C. Adamo, J. Jaramillo, R. Gomperts, R. E. Stratmann, O. Yazyev, A. J. Austin, R. Cammi, C. Pomelli, J. W. Ochterski, R. L. Martin, K. Morokuma, V. G. Zakrzewski, G. A. Voth, P. Salvador, J. J. Dannenberg, S. Dapprich, A. D. Daniels, Ö. Farkas, J. B. Foresman, J. V. Ortiz, J. Cioslowski, D. J. Fox, Gaussian, Inc., Wallingford CT, 2009.

Chapter 4

Catalytic Formation of C–O Bonds: Olefin Hydroaryloxylation

Olefin Hydroaryloxylation Catalyzed by Pincer–Iridium Complexes

Michael C. Haibach, Changjian Guan, David Y. Wang, Bo Li, Nicholas Lease, Andrew M. Steffens, Karsten Krogh-Jespersen, and Alan S. Goldman

Journal of the American Chemical Society **2013** *135* (40), 15062-15070.

Introduction

The addition of H-X bonds across olefinic double bonds catalyzed by transition metal complexes represents a reaction class of great importance in organic chemical synthesis.[1-3] Recent years have seen significant developments in catalytic hydroamination;[4-6] however, progress toward the development of transition metal complexes for catalytic addition of O-H bonds to olefins has been much more limited.[1-3,6,7] Such additions of alcohol O-H bonds, especially intermolecular, remain a particularly important and attractive challenge.

Alkyl aryl ethers are an important class of commodity chemicals, with applications ranging from solvents, to fragrances, to pharmaceutical building blocks.[8] They are currently synthesized primarily via the very classical[9] Williamson ether synthesis, whereby an alkali salt of the appropriate phenol (preformed or generated *in situ*) is coupled with an alkyl halide or alkyl sulfonate ester, typically in a polar aprotic solvent (Scheme 4.4.1).

Scheme 4.4.1. Alternative syntheses of alkyl aryl ethers (shown for the addition of phenol to propene)

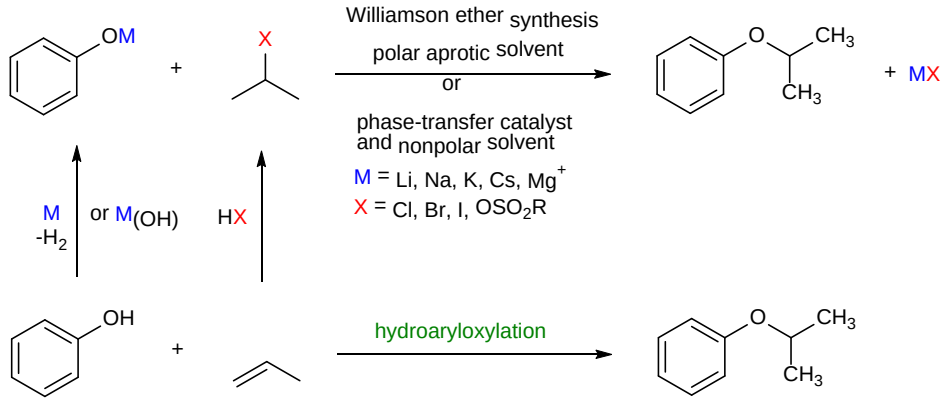

In some cases, phase transfer catalysis can be used to avoid the requirement of a polar aprotic solvent. The use of alkyl alcohols in place of alkyl halides typically requires a gas-phase reaction or dehydrating agent. For the industrially preferred route, one equivalent of alkali halide or alkali

sulfonate waste is generated per equivalent of product produced, in addition to the waste associated with preparation of the alkali phenoxide and the alkyl halide, which is typically prepared from the corresponding olefin.

Despite these drawbacks, the Williamson ether synthesis is widely used for both industrial and small-scale applications, rather than the atom economical olefin hydroaryloxylation route shown in Scheme 4.1. This is due at least in part to the fact that, until quite recently, the known catalysts for olefin hydroaryloxylation were all strong Brønsted or Lewis acids such as H_2SO_4 or BF_3•OEt_2. While this class of catalysts is highly active, its use suffers from competing Friedel-Crafts alkylations and very poor chemoselectivity. For example, the reaction of propene with phenol catalyzed by BF_3•OEt_2 affords comparable amounts of both *C* and *O*-isopropylphenol, even at 0 °C.[10] Beginning with He's report in 2005,[11] significant attention has been focused on transition metal precatalysts for hydroaryloxylation, such as (PPh_3)Au(OTf). Despite early evidence that triflic acid was the catalytically active species,[12,13] researchers continued to identify numerous transition metal "precatalysts" that were later shown by Hintermann to be Brønsted acid delivery systems (with Ag(OTf) in chlorinated solvents serving as the most common source).[14,15] Many recent and classic examples employing Lewis acid catalysts, particularly lanthanide triflates, are also proposed to operate via Yamamoto's Lewis-assisted Brønsted acid[16] mode of activation.[12,14,15] Indeed, to our knowledge, at the outset of this work there were no well-defined examples of intermolecular addition of alcohol O-H bonds across the double bond of simple olefins directly catalyzed by a transition metal complex.[7,14,17] In this communication, we report the first such catalysts, specifically for the reaction of phenols, and support for a likely mechanism based on experimental and computational evidence.[18] These catalysts offer selectivity much greater than, and in some cases orthogonal to, that of previously reported acid catalysts.

Results and Discussion

We have previously reported that precursors of the fragment (^{tBu}PCP)Ir (^{R}PCP = κ^3-C_6H_3-2,6-$(CH_2PR_2)_2$) could cleave aryl-sp^3 C-O bonds stoichiometrically via an initial C-H oxidative addition step.[19,20] In the case of ethyl phenyl ether, for example, this led to dehydroaryloxylation and formation of the iridium adducts of ethylene and phenol (Scheme 4.2). The potential ability of such species to undergo kinetically facile olefin loss and phenol elimination suggested the possibility of a catalytic cycle; in the thermodynamically favorable reverse direction such a cycle would constitute olefin hydroaryloxylation.

Scheme 4.2. Stoichiometric dehydroaryloxylation of ethyl phenyl ether by (^{tBu}PCP)Ir

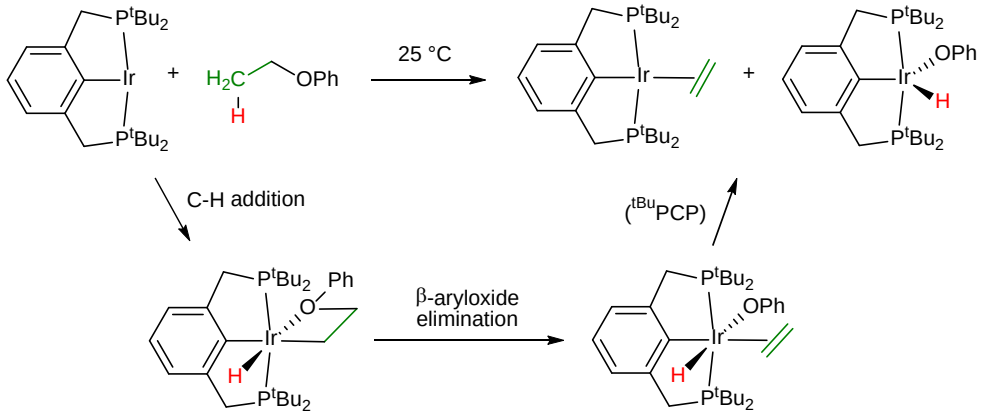

Attempts to effect catalytic hydroaryloxylation by (^{tBu}PCP)Ir (10 mM (^{tBu}PCP)IrH_4 catalyst precursor, 500 mM phenol, 1 atm ethylene or propene, *p*-xylene solvent, 100 - 150 °C) were unsuccessful, yielding no new organic products. Investigation of some previously reported derivatives of (^{tBu}PCP)Ir, however, successfully identified several catalysts active for the addition of propene to 3,5-dimethylphenol at 150 °C (Figure 4.1).[21] The three most active derivatives identified were (^{tBu3Me}PCP)Ir,[22] (MeO-^{iPr}PCP)Ir,[23] and (^{iPr}PCOP)Ir.[24]

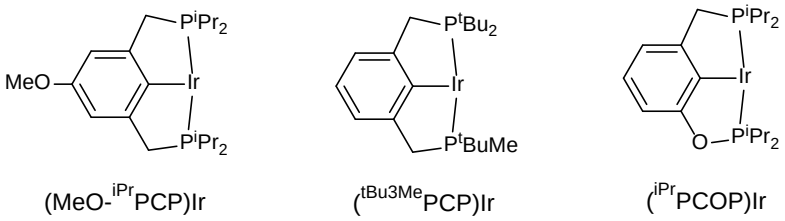

Figure 4.1. Species found to be active for catalytic hydroaryloxylation.

This group of sterically less congested catalysts is about an order of magnitude more active for alkane dehydrogenation than (^{tBu}PCP)Ir.[25,26] As in alkane dehydrogenation, the catalytically active species can be generated from the iridium tetrahydride or ethylene complexes under the reaction conditions, or from the corresponding (pincer)IrHCl complex and a base.[27] Presumably due to inhibition resulting from strong binding by ethylene, the catalytic activity for each (pincer)Ir precatalyst followed the trend (pincer)Ir(C_2H_4) < (pincer)IrH_4 ≈ (pincer)Ir(H)(Cl)/NaO^{t}Bu.

Scheme 4.3. Hydroaryloxylation of olefins catalyzed by (^{iPr}PCOP)IrH_4

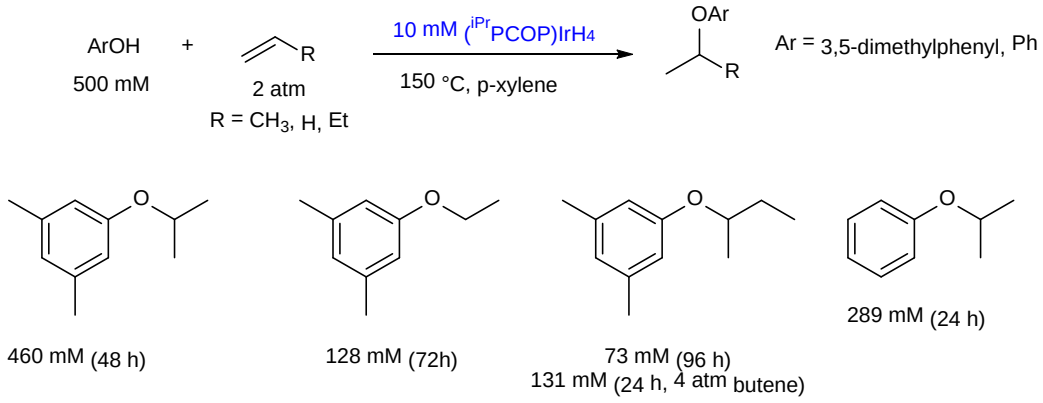

In a typical experiment, *p*-xylene solutions (100 μL) of 10 mM (^{iPr}PCOP)IrH_4[28] and 500 mM 3,5-dimethylphenol are heated at 150 °C in glass ampoules sealed with 2 atm propene. (Each ampoule has a total volume of 1.2 mL which holds 1.8 equivalents propene in the gas phase per equivalent alcohol, plus any propene which may have dissolved in solution prior to sealing.) After

24 hours the appearance of 400 mM isopropyl aryl ether (40 catalytic turnovers (TO)) was observed (by GC), while in another ampoule 460 mM was observed after 48 hours (Scheme 4.3). No *n*-propyl aryl ether or other alkylphenols were detectable 4.by GC, indicating that the reaction is fully regio- and chemoselective. The analogous reaction with ethylene yields exclusively ethyl aryl ether (47 mM after 24 h, 128 mM after 72 h). 1-butene also yields only the *iso* product, albeit with lower conversion than either ethylene or propene (Scheme 4.3). Running the same reaction at 4 atm of 1-butene affords higher conversion. Importantly, when (unsubstituted) phenol and propene are allowed to react, only isopropyl phenyl ether (289 mM) is observed after 24 hours. Note that any catalyst operating by the "hidden Brønsted acid" mechanism proposed by Hintermann is expected to afford at least some *C*-alkyl phenol. Indeed, the reaction of phenol and propene using 10 mM Hintermann's Brønsted acid catalyst (10 mM AgOTf and 40 mM ^{t}BuCl) yields no isopropyl phenyl ether after 24 hours. Instead, 10 different products are observable by GC, with both phenol and the *p*-xylene solvent undergoing apparently unselective Friedel-Crafts alkylations and isomerizations.

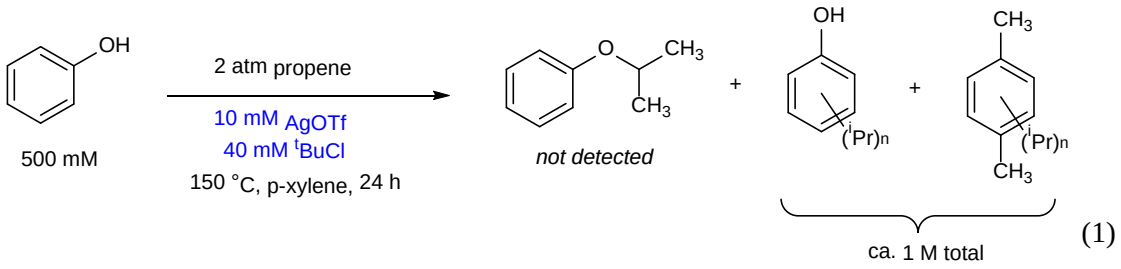

(1)

Further evidence of the non-acidic nature of the iridium catalyst system derives from a competition experiment between isobutene and propene. Isobutene forms a much more sTable 4.carbocation when protonated; hence an acidic catalyst would be expected to yield the *tert*-butyl phenyl ether as the major product. However, when a solution of 3,5-dimethylphenol and (^{iPr}PCOP)IrH_4 is subject to equal partial pressures of isobutene and propene, the aryl isopropyl

ether is formed with selectivity >40:1 (eq 2). The control experiment, using AgOTf/*t*-BuCl, gave no aryl isopropyl ether although only trace aryl *t*-butyl ether was observed (eq 3); the major products resulted from Friedel-Crafts alkylation of the arene rings as in the case of eq 1. Similarly arguing against any carbocation-derived selectivity, although propene reacts significantly faster with 3,5-dimethylphenol than does ethylene in independent experiments, ethylene reacts preferentially vs. propene with selectivity >3:1 in an internal competition experiment (eq 4).

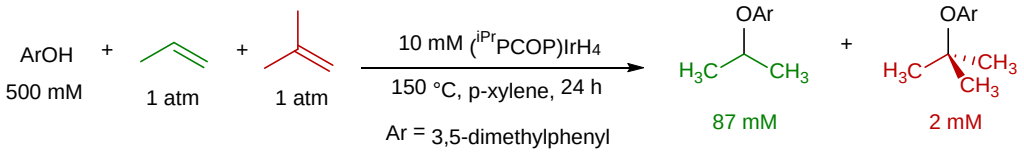

(2)

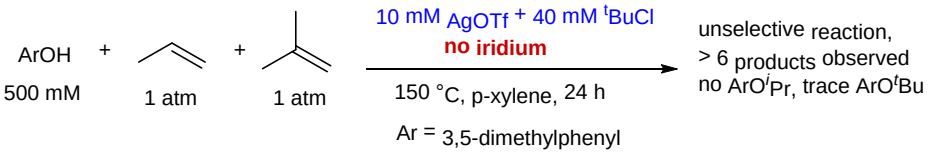

(3)

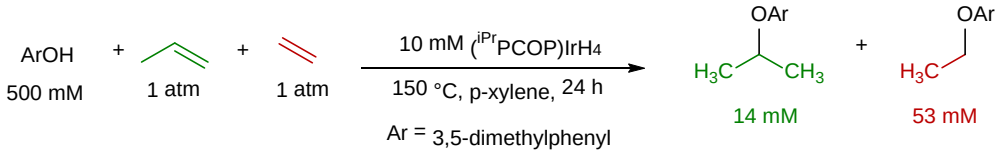

(4)

The apparently high regioselectivity for formation of *i*-PrOAr vs. *n*-PrOAr (Scheme 4.3) and the high chemoselectivity for hydroaryloxylation of propene vs. isobutene (eq 2) might be attributed, *a priori*, to thermodynamic rather than kinetic factors. In such a case the rate of the respective hydroaryloxylations might be comparable to or even more rapid than the reaction to

give *i*-PrOAr, but the respective dehydroaryloxylation back-reactions could be even faster. To test this hypothesis we investigated the possible back reactions.

A *p*-xylene solution of *i*-PrOAr (500 mM), *n*-PrOAr (500 mM) and (^{iPr}PCOP)Ir(C_2H_4) was sealed under vacuum (100 μL in a 1 mL ampoule) and heated to 150 °C. After 12 h, GC analysis revealed the disappearance of 48% of the *i*-PrOAr and 8% of the *n*-PrOAr, with commensurate appearance of ArOH (270 mM) and the appearance of propene.[29] Thus, both the rate of propene hydroaryloxylation to give *n*-PrOAr, and the dehydroaryloxylation of *n*-PrOAr are much slower than the corresponding reactions for *i*-PrOAr; this selectivity is therefore clearly a kinetic phenomenon.

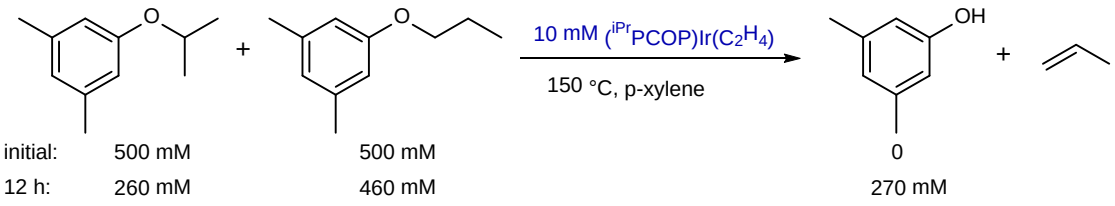

(5)

Note that the dehydroaryloxylation of *i*-PrOAr proceeds at least 6-fold more rapidly than that of *n*-PrOAr (eq 5). Both experimental data[30] and DFT calculations (discussed below) indicate that the free energy of *n*-PrOAr is ca. 3 kcal/mol higher than that of *i*-PrOAr. $\Delta\Delta G_H^{\ddagger}$ for the hydroaryloxylation of propene to give *n*-PrOAr must therefore be ca. 3 kcal/mol greater than $\Delta\Delta G_D^{\ddagger}$ for the dehydroaryloxylations (Scheme 4.4). In that case, a 6-fold rate difference for the latter, at 150 °C, would correspond to a rate difference of 6•exp(-3 kcal/mol/(RT)) ≈ 200 (i.e. $\Delta\Delta G_H^{\ddagger} \approx$ 4.5 kcal/mol), in accord with our conclusion of essentially complete kinetic selectivity for the formation of *i*-PrOAr in the hydroaryloxylation.

Scheme 4.4. Schematic free energy profile for hydroaryloxylation of propene to give *i*-PrOAr and *n*-PrOAr and the corresponding dehydroaryloxylations catalyzed by (^{iPr}PCOP)IrH$_4$ at 150 °C

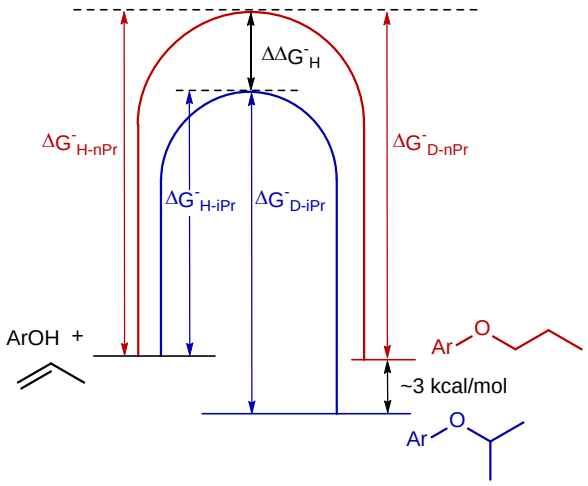

$\Delta\Delta G^{\ddagger}_{D} = \Delta G^{\ddagger}_{D\text{-}nPr} - \Delta G^{\ddagger}_{D\text{-}iPr} \approx RT(\ln 6) = 1.5$ kcal/mol (based on experimental results, eq 5)

$\Delta\Delta G^{\ddagger}_{H} + \Delta G^{\ddagger}_{D\text{-}iPr} = \Delta G^{\ddagger}_{D\text{-}nPr} +$ ~3 kcal/mol (see Scheme)

$\Delta\Delta G^{\ddagger}_{H} = \Delta G^{\ddagger}_{D\text{-}nPr} - \Delta G^{\ddagger}_{D\text{-}iPr} +$ ~3 kcal/mol = $\Delta\Delta G^{\ddagger}_{D}$ + ~3 kcal/mol ≈ 4.5 kcal/mol

A competition experiment under the same conditions as the experiment of eq 5 was also conducted with *i*-PrOAr and *t*-BuOAr. The dehydroaryloxylation of *i*-PrOAr was found to be more rapid (by a factor larger than 2; eq 6). Thus the much greater rate of hydroaryloxylation of propene vs. isobutene (> 40-fold; eq 2), like the regioselectivity to give *i*-PrOAr, is a kinetic phenomenon.

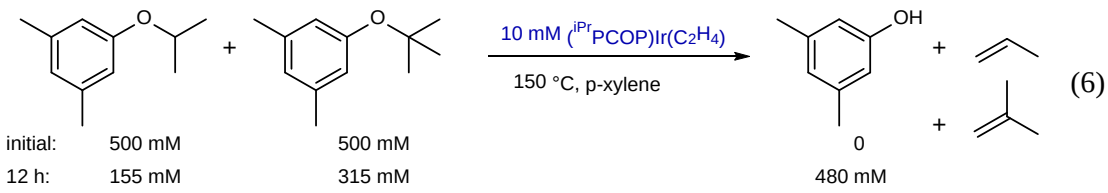

(6)

Finally, we note that even in the presence of a large excess of NaO^{t}Bu (125 mM), a solution of 3,5-dimethylphenol (0.5 M) under propene (2 atm) undergoes clean catalytic hydroaryloxylation by (^{tBu3Me}PCP)IrHCl (10 mM), yielding 250 mM *i*-PrOAr product after 24 h at 150 °C. This result argues strongly against any mechanism involving Brønsted acid.

Identification of the catalytic resting state. The reaction of phenol with propene using (^{iPr}PCOP)Ir as the catalyst was investigated in detail by ^{1}H and ^{31}P NMR. Addition of 1 atm propene to a J-Young NMR tube with either a 0.1 M or 0.01 M solution of (^{iPr}PCOP)Ir(H)(OPh)[19] in *p*-xylene-d_{10} (affording a solution propene concentration of ca. 1 M) results in quantitative conversion to the (^{iPr}PCOP)Ir(η^2-propene) complex (see Supporting Information for characterization of (^{iPr}PCOP)Ir(η^2-propene) and (^{iPr}PCOP)Ir(H)(OPh)) and free phenol within 15 minutes at 25 °C (Scheme 4.5). No change is observed upon heating to 120 °C in the NMR spectrometer. Importantly, no signals between 0 and -50 ppm in the ^{1}H NMR spectrum, characteristic of iridium hydrides, are observed, thus indicating the lack of formation of any appreciable amounts of either (^{iPr}PCOP)Ir(η^2-propene)(H)(OPh) or (^{iPr}PCOP)Ir[$CH_2CH(OAr)CH_3$](H) under these conditions.

Scheme 4.5. Identification of (^{iPr}PCOP)Ir(η^2-propene) as the catalytic resting state by NMR studies

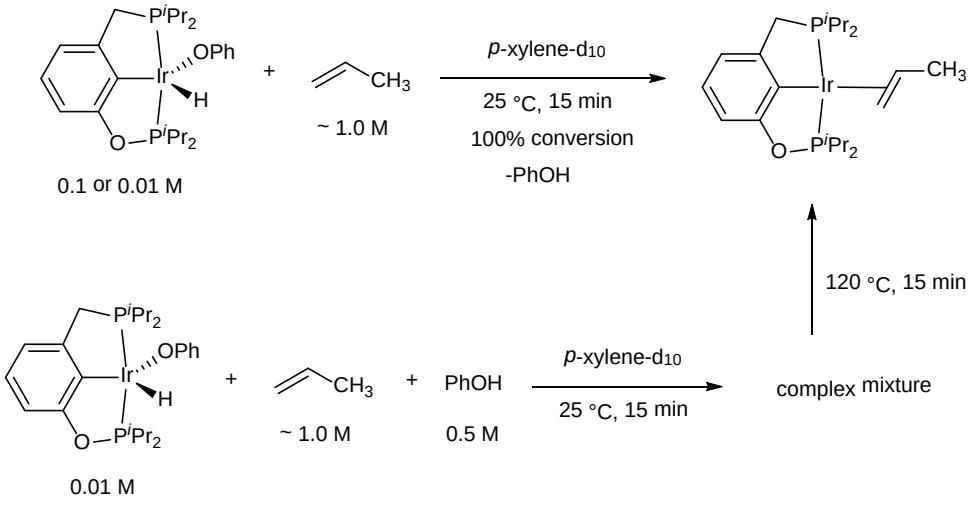

A solution otherwise similar to that described above was prepared, but with 0.5 M PhOH added (0.01 M (^{iPr}PCOP)Ir(H)(OPh), 0.5 M PhOH, ca. 1 M propene) to replicate the concentrations typically used for the catalytic runs. Under these conditions, the presence of PhOH resulted in a complex mixture of iridium-containing complexes at 25 °C (^{31}P and ^{1}H NMR). (^{iPr}PCOP)Ir(η^2-propene) is present, while several signals between [illegible]7 and -24 ppm (triplets with J values of ca. 15 Hz which is typical for $^{2}J_{PH}$) are also observed in the ^{1}H NMR spectrum. These signals are indicative of 6-coordinate iridium hydrides; it would seem likely that at least some of these are of the composition (^{iPr}PCOP)Ir(η^2-propene)(OPh)(H). The low symmetry of these complexes, however, apparently generates several isomers making assignment of their structures by NMR prohibitively difficult. (Note that even a single coordination isomer of (^{iPr}PCOP)Ir(η^2-propene)(OPh)(H) has at least four possible conformers depending upon the orientation of the propene ligand.) When this solution is heated to 120 °C,[31] however, a temperature at which there is catalytic activity, the only species observable in solution is (^{iPr}PCOP)Ir(η^2-propene). Thus the apparent equilibrium of (^{iPr}PCOP)Ir(η^2-propene)(OPh)(H) isomers with (^{iPr}PCOP)Ir(η^2-propene)

plus free phenol (eq 7) is driven toward the side with free phenol at higher temperature (as would be expected), and (^{iPr}PCOP)Ir(η^2-propene) is the resting state under catalytic conditions.

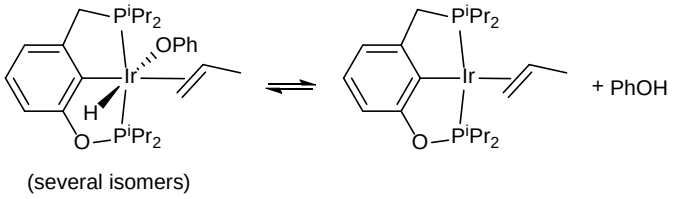

(7)

Computational investigation of the mechanism. Computational (DFT[21]) studies have been conducted which shed light on the mechanism and selectivity of the hydroaryloxylation reactions. We employed the widely used M06 and M06-L density functionals. Both functionals predicted regio- and chemoselectivity in full agreement with our experimental results. Since the M06-L functional provided slightly better quantitative agreement, we will primarily discuss M06-L energies and present those values in the figures shown here; energies obtained with the M06 functional are given in tables in the Supporting Information. We have focused on the reaction of phenol with propene by our most effective catalyst, (^{iPr}PCOP)Ir. Although the calculations assume idealized gas-phase conditions, free energies have been calculated at conditions (T,P) that are closer to those of the actual catalytic experiments than are standard conditions (T = 298.15 K, P = 1.0 atm). Specifically, we use T = 150 °C = 423.15 K, and, in order to approximate the concentrations of reagents in solution, partial pressures of 34.7 atm were assumed, which correspond to concentrations of 1 mol/liter at 150 °C.

Experimentally, as noted above, (^{iPr}PCOP)Ir(η^2-propene) (**1a**) was found to be the only major species in solution at the standard reaction conditions. Using the M06 functional and the above noted thermodynamic conditions (T = 150 °C, P = 34.7 atm), (^{iPr}PCOP)Ir(η^2-propene) was indeed computed to be the lowest energy species, 1.7 kcal/mol lower in free energy than (^{iPr}PCOP)Ir(H)(OPh) (**3**) (Table 4.S4) and 3.9 kcal/mol below (^{iPr}PCOP)Ir(H)(η^2-propene)(OPh) (**4**) (the lowest energy conformer, with propene coordinated trans to the pincer aryl group; Table

4.S-5). The corresponding M06-L values for (^{iPr}PCOP)Ir(H)(OPh) and (^{iPr}PCOP)Ir(H)(η^2-propene)(OPh), relative to **1a**, are -2.3 kcal/mol and -0.1 kcal/mol at 150 °C, respectively (Table 4.S1). In both cases, we judge the differences to be within the error margins of the calculations when comparing species that are significantly different (e.g. an Ir(I) complex and an Ir(III) complex, σ- vs. π-coordination, 4-coordination vs. 5- or 6-coordination). Accordingly, we will only consider energies relative to the experimentally observed resting state, the olefin π-complex **1a.**

Under typical reaction conditions, (^{iPr}PCOP)Ir(η^2-propene) (**1a**) is calculated to be the major resting state (the kinetically accessible species of lowest free energy) in the (^{iPr}PCOP)Ir/phenol/propene system using the M06 functional. However, at 25 °C the free energy of (^{iPr}PCOP)Ir(H)(η^2-propene)(OPh) is calculated to be -0.6 kcal/mol below the four-coordinate propene adduct, whereas (^{iPr}PCOP)Ir(H)(OPh) remains higher in energy than **1a** by 2.0 kcal/mol. The corresponding M06-L values for (^{iPr}PCOP)Ir(H)(OPh) and (^{iPr}PCOP)Ir(H)(η^2-propene)(OPh), relative to **1a,** are -2.1 kcal/mol and -4.5 kcal/mol at 25 °C. These results are consistent (at least within the limits of precision of the calculations) with the observation that a mixture of (^{iPr}PCOP)Ir(η^2-propene), (^{iPr}PCOP)Ir(H)(OPh), and (^{iPr}PCOP)Ir(H)(η^2-propene)(OPh) appear to be present in a typical reaction solution at 25 °C, whereas only (^{iPr}PCOP)Ir(η^2-propene) is observed at 120 °C.

The results of the selectivity experiments discussed above argue strongly against a Brønsted-acid catalyzed pathway, or any pathway involving a carbocationic or carbocation-like intermediate, and instead favor a genuinely "organometallic-catalyzed" mechanism. Generally speaking, "organometallic" mechanisms for hydrofunctionalization (addition of species H-X across multiple bonds) may proceed via insertion of olefin into a M-H bond followed by alkyl-X elimination (Figure 4.2a); known examples include X = SiR_3, BR_2, and CN[1]. Such mechanisms can favor formation of anti-Markovnikov products (e.g. CH_2X-CH_2R from CH_2=CHR plus HX). It is generally assumed that such selectivity is attribuTable 4.to the preference of transition metals

for less substituted alkyl ligands[32-35] (e.g. primary vs. secondary) reflected in the TS preceding or perhaps following the intermediate species $L_nM(alkyl)X$.

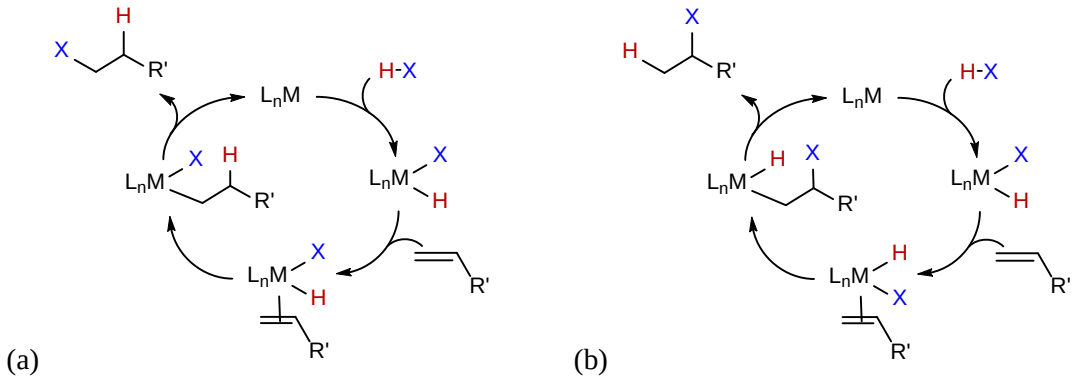

Figure 4.2. Typical "organometallic" pathways (proceeding via H-X addition, olefin insertion, and C-X or C-H elimination) for generic hydrofunctionalization of an olefin (addition of H-X). Cycle (a) is shown giving anti-Markovnikov product and cycle (b) is shown giving the Markovnikov product. This represents the regioselectivity commonly expected of each pathway, but neither mechanism is necessarily limited to either type of regioselectivity.

In the case of the present system, the free energy calculated for the TS for the key step of C-X elimination as per Figure 4.2a (L_nM = (^{iPr}PCOP)Ir; X = OPh; alkyl = *i*-Pr) is 47.3 kcal/mol above that of the calculated resting state, (^{iPr}PCOP)Ir(propene) (M06-L; Table 4.S-1). This value is substantially greater than the overall barrier indicated by experiment, $\Delta G^{\ddagger} \sim 32$ kcal/mol (based on ca. 1.2 turnovers per hour). The pathway of Figure 4.2a is thus calculated not to be viable in this case, regardless of the energies of any other intermediates and transition states in that pathway. This result is consistent with and closely related to our previous work in which it was found that the barrier to direct C-O bond oxidative addition to (^{tBu}PCP)Ir is prohibitively high.[19,20]

Interestingly, although the pathway of Figure 4.2a is precluded by the high barrier to C-O bond elimination, the initial steps appear to be quite favorable. Addition of ArOD (0.5 M) and (perprotio) propene (1 atm) to a *p*-xylene-d_{10} solution of (^{iPr}PCOP)IrH_4, to give the mixture of

species indicated in eq 6 (and isotopologues thereof), results in rapid H/D exchange between propene and ArOD (50% conversion to ArOH within 15 minutes at room temperature as revealed in the ^{1}H NMR spectrum). This is most easily explained in terms of reversible insertion of propene into the Ir-H/D bond of (^{iPr}PCOP)Ir(η^2-propene)(OPh)(H/D). The thermodynamics of this insertion are calculated to be quite allowable for such an exchange mechanism (ΔG = +7.3 kcal/mol and +8.6 kcal/mol for 1,2- and 2,1-Ir-H addition, respectively) although we have been unable to locate appropriate low-energy TS's for these insertions.

Rather than the mechanism indicated in Figure 4.2a, the calculations are instead consistent with the hypothesis that led to this work, namely, that the mechanism indicated in Scheme 4.2 could be implemented catalytically in the reverse direction (as shown explicitly in Figure 4.2b). The mechanism of Figure 4.2b proceeds via olefin insertion into the M-X (Ir-O) bond, rather than insertion into the M-H bond as in Figure 4.2a, and is followed by C-H rather than C-X (C-O) elimination. There are relatively few well characterized examples of insertion of olefins into transition metal-oxygen bonds, but the reaction is certainly not without precedent.[36-40]

Figure 4.3 shows results of calculations of the catalytic cycle (as per Figure 4.2b) for the (^{iPr}PCOP)Ir-catalyzed reaction of propene and phenol to give *i*-PrOPh and *n*-PrOPh (all free energies are expressed relative to the free three-coordinate pincer iridium complex and free propene and phenol). 1,2-Addition of the Ir-OPh bond of (^{iPr}PCOP)IrH(OPh)(η^2-propene) (**4a**) across the double bond of coordinated propene is calculated to have a barrier of only ca. 16 kcal/mol, with a transition state (TS; **TS-4a-5a**) that is 21.5 kcal/mol above the propene complex resting state (**1a**). This is in agreement with a theoretical study[39] by Hartwig on olefin insertion into the Rh-X bond (X = CH_3, NH_2, OH) of $(PMe_3)_2RhX$, in which it was calculated that the barrier to 1,2 insertion of coordinated propene into a Rh-O bond was 19.3 kcal/mol. Moreover, also in accord with Hartwig's results,[39] in the present system the metal-oxygen bond remains largely intact during and even after the insertion step. The Ir-O bond distances in *trans*-(^{iPr}PCOP)IrH(OPh)(propene) (**4a**), **TS-4a-5a**, and the insertion product **5a**, are 2.30 Å, 2.33 Å and

2.42 Å, respectively (Figure 4.4); thus the Ir-O bond appears to transition smoothly from formally covalent to dative.[39] A conformer of **5a** in which there is no significant Ir-O interaction (d_{Ir-O} = 4.4 Å) is a local minimum with a free energy 7.0 kcal/mol above the lowest free energy conformer of **5a**; this value presumably represents the approximate strength of the dative interaction.

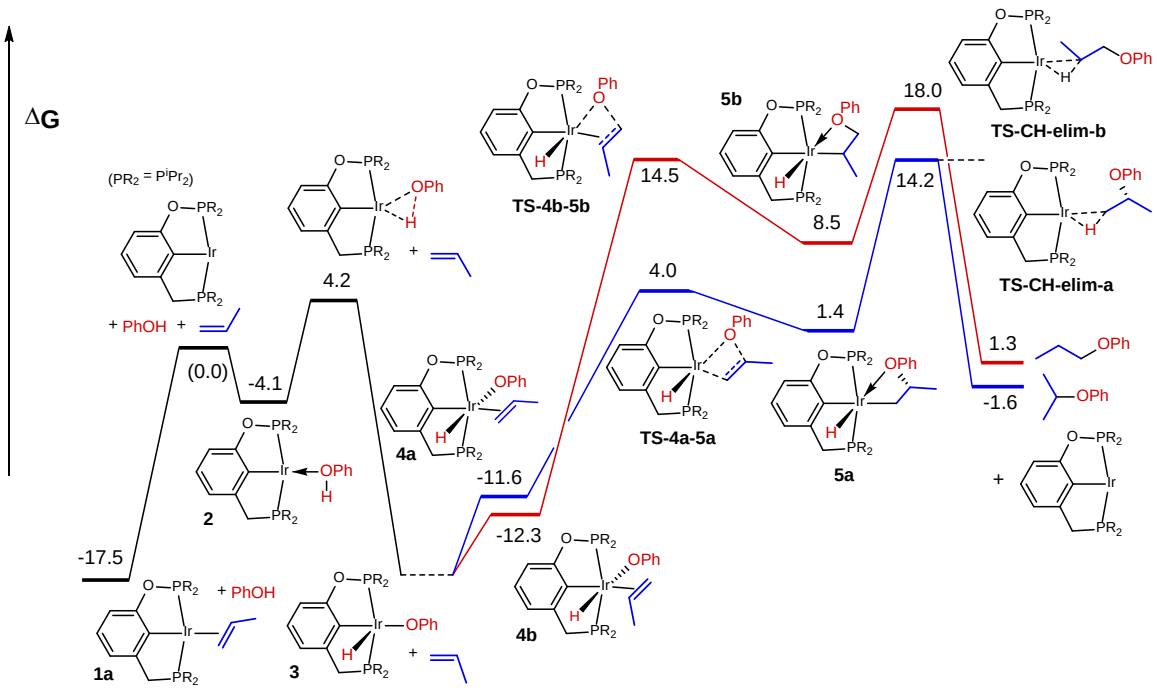

Figure 4.3. Free energy diagram (M06-L; values of ΔG in kcal/mol) for the proposed 1,2-Ir-O addition pathway for hydrophenoxylation of propene by (^{iPr}PCOP)Ir to give *i*-PrOAr (observed product; blue lines) and *n*-PrOAr (not observed; red lines).

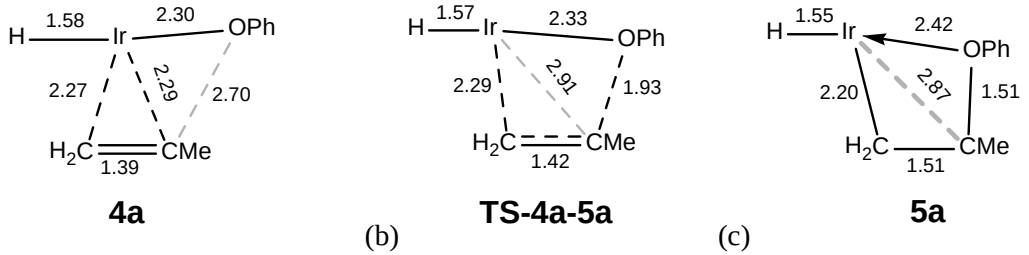

(a) (b) (c)

Figure 4.4. Calculated distances (Å) for the H-Ir-C-C(propene)-O(phenoxide) unit for the 1,2-Ir-O insertion step. (a) *trans*-(^{iPr}PCOP)IrH(OPh)(propene) (**4a**) (b) TS for propene insertion (**TS-4a-5a**) (c) insertion product (^{iPr}PCOP)IrH[$CH_2CH(CH_3)$OPh] (**5a**)

The product of the 1,2-Ir-OPh addition to propene, (^{iPr}PCOP)Ir[$CH_2CH(OPh)CH_3$](H) (**5a**), is 18.9 kcal/mol above the propene resting state **1a** (Figure 4.3). The TS for C-H elimination from

this species (**TS-CH-elim-a**), to give *i*-PrOPh, is calculated to have a free energy 31.7 kcal/mol above the resting state (i.e. 14.2 kcal/mol above the reference); this TS leads to a C-H sigma-bond complex (not shown in Figure 4.3) that is 22.9 kcal/mol above the resting state (i.e. 5.4 kcal/mol above the reference). We have been unable to locate a proper TS for dissociation of this sigma-bond complex. However, it seems likely (although not certain) that loss of the sigma-C-H-bound ether product (which may proceed dissociatively or via displacement by solvent, phenol, or propene) is fast relative to the back-reaction, C-H addition. In that case, the C-H elimination is the rate-determining step for formation of *i*-PrOPh, with an overall calculated barrier height of 31.7 kcal/mol (**TS-CH-elim-a**), in complete (and presumably fortuitously excellent) agreement with the approximate experimental barrier, $\Delta G^{\ddagger} \sim 32$ kcal/mol.

Figure 4.3 also shows a pathway that proceeds via a 2,1-Ir-O addition which would lead to *n*-PrOPh; this represents the mechanism shown in Figure 4.2b but with the reverse regioselectivity. The 2,1-Ir-O addition has a calculated barrier substantially higher than the 1,2 Ir-O addition; **TS-4b-5b** is 32.0 kcal/mol above the resting state vs. 21.5 kcal/mol for **TS-4a-5a**. The energy of the resulting phenoxy-substituted secondary alkyl hydride, **5b**, is 7.1 kcal/mol above that of the primary alkyl hydride, **5a**, derived from the 1,2-addition (26.0 kcal/mol above the resting state vs. 18.9 kcal/mol). This is also in agreement with Hartwig's study in which it was found that 1,2 addition of the M-O bond was much more favorable than 2,1 addition (with the difference being much greater than that found for M-C addition).[39] But, while these 1,2 Ir-O addition energies are higher than the corresponding values for the 2,1-Ir-O addition, they are not so high as to necessarily preclude formation of the *n*-propyl ether at a rate comparable to that observed for formation of *i*-PrOAr.

The calculations illustrated in Figure 4.3 predict that the subsequent C-H elimination, not insertion into the Ir-OAr bond, is both rate- and product-determining. The TS for the C-H elimination, **TS-CH-elim-b**, is of higher energy for the secondary alkyl hydride than for the primary, **TS-CH-elim-a**, by a substantial margin of 3.8 kcal/mol. This difference would

correspond to a factor greater than 90 in the rates for formation of *i*-PrOAr ($\Delta G^{\ddagger}_{calc}$ = 31.7 kcal/mol) vs. *n*-PrOAr ($\Delta G^{\ddagger}_{calc}$ = 35.5 kcal/mol) at 150 °C. The calculations thus fully account for the observed rate of formation of *i*-PrOAr and for the absence of *n*-PrOAr. Moreover, the same energy diagram illustrates that the barrier to the back reaction (dehydroaryloxylation) is calculated to be slightly higher for the reaction of *i*-PrOPh than for *n*-PrOPh (by 0.9 kcal/mol). This is also in excellent agreement with experimental observations noted above.

The free energy difference between the two rate-determining C-H elimination TS's, which may determine the very high regioselectivity for formation of *i*-PrOAr vs. *n*-PrOAr, can perhaps be most simply explained by considering the reaction proceeding in the *reverse* direction. The difference of 3.8 kcal/mol can then be viewed as resulting from a combination of two simple factors: (i) The energy of free *i*-PrOAr is lower than that of free *n*-PrOAr (2.9 kcal/mol calculated difference, 3.35 ± 0.43 kcal/mol experimental[30]). (ii) The barrier for the oxidative cleavage of primary C-H bonds is generally less than for secondary C-H bonds;[34] in this case addition of the primary C-H bond of *i*-PrOPh is calculated to be 0.9 kcal/mol lower than that for the secondary C-H (C2) bond of *n*-PrOPh.

Overall, the calculated results presented above, obtained with the use of the M06-L functional, strongly indicate that C-H elimination is the rate-determining step in the cycle. The calculations are in excellent agreement with experimental results, including the absolute rate and the selectivities for formation of *i*-PrOAr vs. *n*-PrOAr (very high) and for dehydroaryloxylation of *i*-PrOAr vs. *n*-PrOAr (ca. 6-fold). Calculations using the M06 functional lead to essentially the same predictions, including the rate-determining nature of C-H elimination. However, whereas the use of M06-L leads to barrier heights for C-H elimination that are much higher than for insertion (by 10.2 kcal/mol and 3.5 kcal/mol for 1,2-addition and 2,1 addition, respectively) the differences are much less pronounced using M06 (3.5 kcal/mol and 0.7 kcal/mol for 1,2-addition and 2,1 addition, respectively; see Tables S4-5 and Figure 4.S4). Thus, while DFT calculations obtained using either functional indicate that C-H elimination is rate-determining for

hydroaryloxylation (and C-H addition rate-determining for dehydroaryloxylation), future studies to test this important conclusion seem warranted.

It should be noted that two geometrically distinct variants of either the 1,2- or 2,1-Ir-O addition pathways have been calculated. For each pathway there is the variant in which the olefin is initially coordinated trans to the PCP aryl of (^{iPr}PCOP)Ir(OPh)H (shown in Figure 4.3), and another in which olefin coordinates cis to the PCP aryl, while the phenoxy group is coordinated trans (shown in Figure 4.5 for 1,2-addition leading to *i*-PrOPh). The olefin-trans variant has a lower-energy TS for insertion of olefin into the Ir-O bond in for both 1,2- and 2,1-additions. Each variant gives rise to a different isomer of (^{iPr}PCOP)Ir(phenoxypropyl)(H) upon Ir-O addition (**5a** vs. **5c** in the case of the 1,2-addition shown in Figure 4.5). In both cases the olefin-trans insertion TS is of higher energy than the olefin-cis TS (**TS-4c-5c** vs. **TS-4a-5a** in the case of 1,2-addition). However, the intermediates resulting from Ir-O addition can probably interchange readily (the barrier to decoordination of the phenoxy group, as noted above, is only 7 kcal/mol). Thus even if the olefin-cis insertion were more facile than the olefin-trans, since the insertion step is not rate-determining the distinction between these pathways would not necessarily be significant.

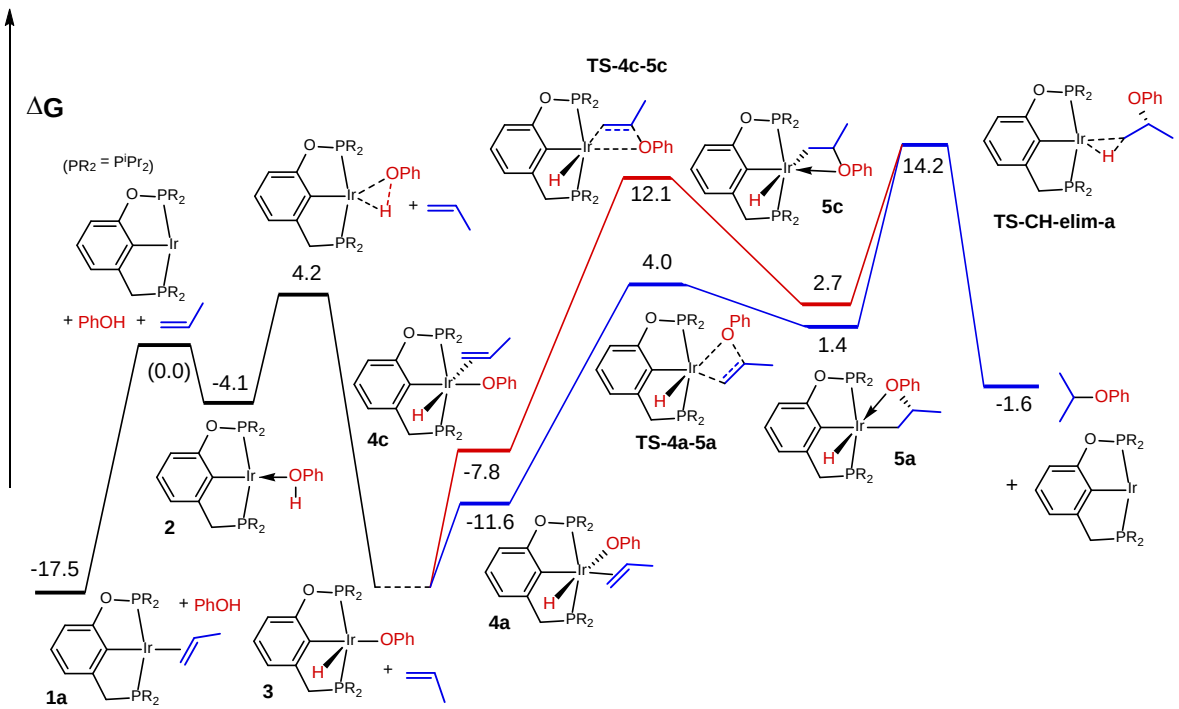

Figure 4.5. Free energy diagram (M06-L; values of ΔG in kcal/mol) for the proposed 1,2-Ir-O addition pathway for hydrophenoxylation of propene by (^{iPr}PCOP)Ir to give *i*-PrOAr proceeding via "olefin-trans" (blue) and "olefin-cis" (red) pathways.

Finally, Figure 4.6 illustrates the results of calculations for the addition of PhOH to ethylene proceeding via the mechanism of Figure 4.2b, along with the calculated values for the addition to propene in the presence of ethylene, thereby modeling the competition experiment of eq 4. The overall barrier for PhOH addition to ethylene (which is not affected by the presence of propene) is calculated to be 35.6 kcal/mol (the difference between the free energy of **TS-CH-elim-d** and the free energy of (^{iPr}PCOP)Ir(ethene), **1c**). The overall barrier for hydroaryloxylation of propene, *in the presence of ethylene* (which results in an ethylene bound resting state), is calculated to be 37.7 kcal/mol (the free energy of **TS-CH-elim-a** minus the free energy of the resting state ethene complex **1c**) as compared with 31.7 kcal/mol above the propene-bound resting state. Thus these calculations successfully capture both the greater reactivity of ethylene in competition

experiments *and* the greater reactivity of propene in independent runs, providing additional support for the proposed mechanism of Figure 4.2b. Interestingly, the TS for ethene insertion **TS-4d-5d** is slightly higher than that for propene insertion, **TS-4a-5a**. If that is in fact the case (although the small difference of 0.9 kcal/mol is arguably not meaningful), and if insertion into the Ir-O bond, not C-H elimination, were rate-determining, then the competition experiment of eq 4 would have yielded more *i*-PrOAr than EtOAr, in contrast with the experimental result.

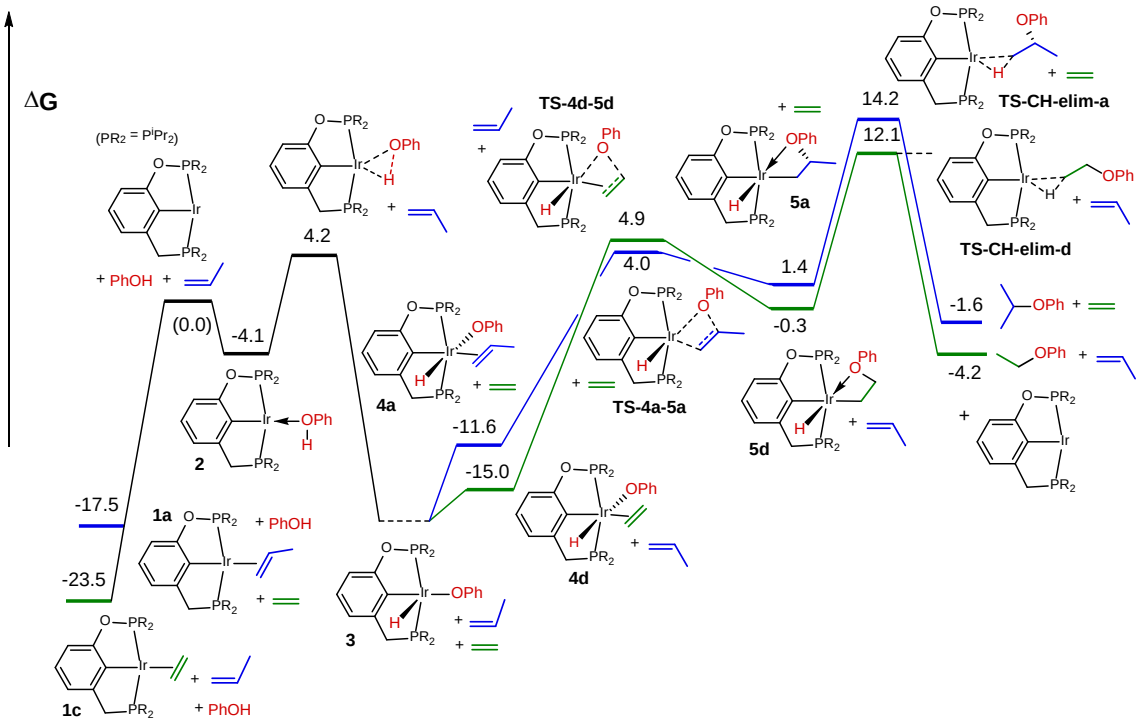

Figure 4.6. Free energy diagram (values in kcal/mol) for proposed pathway for hydrophenoxylation of ethylene (green lines) and propene (blue lines) by (^{iPr}PCOP)Ir. From a common resting state (as in a competition experiment) the barrier to the reaction of ethylene is lower, but in individual experiments, the overall barrier is lower for the reaction of propene.

Conclusions

We report iridium pincer complexes that catalyze olefin hydroaryloxylation with simple olefins and phenols. These catalysts do not operate via a "hidden Brønsted acid" mechanism, common to previously reported precatalysts for this reaction, as their high selectivity for *O- vs. C*-alkylation and the preference for addition to less-substituted olefins make clear. DFT calculations are strongly supportive of a mechanism proceeding via insertion of olefin into the iridium-aryloxide Ir-O bond. A very high degree of regioselectivity is observed. DFT calculations indicate that this is determined by the energy of the respective TS's for C-H bond elimination; this derives in part from the same factors that control selectivity for C-H bond addition.

The nature of the sterically congested and geometrically well-defined pincer-metal unit, and the formation of secondary alkyl ethers, suggest an entry into the development of olefin hydroaryloxylation catalysis that may display unusual selectivity or enantioselectivity. More generally, the discovery of these well-defined non-acid catalysts suggests the possibility of catalytic intermolecular O-H addition across multiple bonds with a scope broader than phenols and simple olefins. Finally, we find that the catalysts are also effective for the reverse, C-O bond cleavage reaction, dehydroaryloxylation. Further research efforts in these contexts are underway.

Chapter 4.1 References

(1) Hartwig, J. F. In *Organotransition Metal Chemistry*; University Science Books: Sausalito, CA, 2010, p 667-699.
(2) Yadav, J. S.; Antony, A.; Rao, T. S.; Subba Reddy, B. V. *J. Organomet. Chem.* **2011**, *696*, 16-36.
(3) Ananikov, V. P.; Beletskaya, I. P. In *Hydrofunctionalization*; Ananikov, V. P., Tanaka, M., Eds.; Springer Berlin Heidelberg: 2013; Vol. 43, p 1-19.
(4) Muller, T. E.; Hultzsch, K. C.; Yus, M.; Foubelo, F.; Tada, M. *Chem. Rev.* **2008**, *108*, 3795-3892.
(5) Julian, L. D.; Hartwig, J. F. *J. Am. Chem. Soc.* **2010**, *132*, 13813-13822.
(6) Julian, L. D.; Springer Berlin Heidelberg: 2013, p 1-47.
(7) For examples of lanthanide catalyzed intramolecular O-H addition to multiple bonds see (a) Seo, S.; Yu, X.; Marks, T. J. *J. Am. Chem. Soc.* **2008**, *131*, 263-276. (b) Dzudza, A.; Marks, T. J. *Org. Lett.* **2009**, *11*, 1523-1526. (c) Dzudza, A.; Marks, T. J. *Chem.-Eur. J.* **2010**, *16*, 3403-3422.
(8) Fiege, H.; Voges, H.-W.; Hamamoto, T.; Umemura, S.; Iwata, T.; Miki, H.; Fujita, Y.; Buysch, H.-J.; Garbe, D.; Paulus, W. In *Ullmann's Encyclopedia of Industrial Chemistry*; Wiley-VCH Verlag GmbH & Co. KGaA: 2000.
(9) Williamson, A. *Philosophical Magazine* **1850**, *37*, 350-356.
(10) Sowa, F. J.; Hinton, H. D.; Nieuwland, J. A. *J. Am. Chem. Soc.* **1932**, *54*, 3694-3698.
(11) Yang, C.-G.; He, C. *J. Am. Chem. Soc.* **2005**, *127*, 6966-6967.
(12) Rosenfeld, D. C.; Shekhar, S.; Takemiya, A.; Utsunomiya, M.; Hartwig, J. F. *Org. Lett.* **2006**, *8*, 4179-4182.
(13) Li, Z.; Zhang, J.; Brouwer, C.; Yang, C.-G.; Reich, N. W.; He, C. *Organic Letters* **2006**, *8*, 4175-4178.
(14) Hintermann, L. In *C-X Bond Formation*; Vigalok, A., Ed.; Springer Berlin Heidelberg: 2010; Vol. 31, p 123-155.
(15) Dang, T. T.; Boeck, F.; Hintermann, L. *J. Org. Chem.* **2011**, *76*, 9353-9361.
(16) Yamamoto, H.; Futatsugi, K. *Angew. Chem., Intl. Ed.* **2005**, *44*, 1924-1942.
(17) After this manuscript was submitted for publication, a report by Sevov and Hartwig on a Segphos-iridium catalyzed olefin hydroaryloxylation appeared: Sevov, C. S.; Hartwig, J. F. *J. Am. Chem. Soc.* **2013**, 135, 9303-9306.
(18) Some of this work has been presented preliminarily: Haibach, M. C.; Li, B.; Wang, D. Y.; Guan, C.; Krogh-Jespersen, K.; Goldman, A. S. Abstracts of Papers, 245th ACS National Meeting & Exposition, New Orleans, LA, United States, April 7-11, 2013, INOR-130.
(19) Choi, J.; Choliy, Y.; Zhang, X.; Emge, T. J.; Krogh-Jespersen, K.; Goldman, A. S. *J. Am. Chem. Soc.* **2009**, *131*, 15627-15629.
(20) Kundu, S.; Choi, J.; Wang, D. Y.; Choliy, Y.; Emge, T. J.; Krogh-Jespersen, K.; Goldman, A. S. *J. Am. Chem. Soc.* **2013**, *135*, 5127-5143.
((21) See Supporting Information for details.
(22) Kundu, S.; Choliy, Y.; Zhuo, G.; Ahuja, R.; Emge, T. J.; Warmuth, R.; Brookhart, M.; Krogh-Jespersen, K.; Goldman, A. S. *Organometallics* **2009**, *28*, 5432-5444.
(23) Zhu, K.; Achord, P. D.; Zhang, X.; Krogh-Jespersen, K.; Goldman, A. S. *J. Am. Chem. Soc.* **2004**, *126*, 13044-13053.
(24) Ahuja, R.; Punji, B.; Findlater, M.; Supplee, C.; Schinski, W.; Brookhart, M.; Goldman, A. S. *Nature Chem.* **2011**, *3*, 167-171.
(25) Choi, J.; MacArthur, A. H. R.; Brookhart, M.; Goldman, A. S. *Chem. Rev.* **2011**, *111*, 1761-1779.

(26) Haibach, M. C.; Kundu, S.; Brookhart, M.; Goldman, A. S. *Acc. Chem. Res.* **2012**, *45*, 947-958.
(27) Pincer iridium dihydrides and tetrahydrides are well known to undergo dehydrogenation by olefin, and are therefore presumed to act simply as precursors of the corresponding (pincer)Ir fragment. Likewise, the ethylene adducts and the hydrido chlorides in the presence of strong base are known precursors of the same fragment. (a) Gupta, M.; Hagen, C.; Kaska, W. C.; Cramer, R. E.; Jensen, C. M. *J. Am. Chem. Soc.* **1997**, *119*, 840-841. (b) Renkema, K. B.; Kissin, Y. V.; Goldman, A. S. *J. Am. Chem. Soc.* **2003**, *125*, 7770-7771. (c) Göttker-Schnetmann, I.; White, P.; Brookhart, M. *J. Am. Chem. Soc.* **2004**, *126*, 1804 - 1811.
(28) (^{iPr}PCOP)IrH_4 was generated from the reported (^{iPr}PCOP)Ir(C_2H_4) complex and H_2 at room temperature. See the Supporting Information for experimental details and spectral data.
(29) Dehydroalkoxylation, catalyzed by lanthanide triflates and thermodynamically driven by hydrogenation of the olefin product catalyzed by Pd nanoparticles (at 110 °C in the case of acyclic ethers) was recently reported by Marks and co-workers: Atesin, A. C.; Ray, N. A.; Stair, P. C.; Marks, T. J. *J. Am. Chem. Soc.* **2012**, *134*, 14682-14685.
(30) Afeefy, H. Y.; Liebman, J. F.; Stein, S.E. "Neutral Thermochemical Data" in NIST Chemistry WebBook, NIST Standard Reference Database Number 69, Eds. P.J. Linstrom and W.G. Mallard, National Institute of Standards and Technology, Gaithersburg MD, 20899, http://webbook.nist.gov, (retrieved February 11, 2013)
(31) Conversion from a mixture of products to exclusively (^{iPr}PCOP)Ir(η^2-propene) is observed upon raising the temperature from ambient to 120 °C. It seems safe to assume that at 150 °C, the temperature of most of our experimental runs, the major species is still predominantly the same propene complex. Unfortunately, however, the temperature limits of our NMR spectrometers did not allow observation at this temperature. (Note that when the temperature is taken back down to ambient in between intervals of heating at 150 °C, the original mixture is again observed, which, on warming to 120 °C in the NMR spectrometer, again yields exclusively (^{iPr}PCOP)Ir(η^2-propene)).
(32) Schwartz, J.; Labinger, J. A. *Angew. Chem., Int. Ed.* **1976**, *15*, 333-340.
(33) Reger, D. L.; Culbertson, E. C. *Inorg. Chem.* **1977**, *16*, 3104-3107.
(34) Some excellent lead references to organometallic C-H addition, with particular emphasis on selectivity: (a) Bennett, J. L.; Vaid, T. P.; Wolczanski, P. T. *Inorg. Chim. Acta.* **1998**, *270(1-2)*, 414-423 (b) Wick, D. D.; Jones, W. D. *Organometallics* **1999**, *18*, 495-505. (c) Asbury, J. B.; Hang, K.; Yeston, J. S.; Cordaro, J. G.; Bergman, R. G.; Lian, T. *J. Am. Chem. Soc.* **2000**, *122*, 12870 -12871 and references 4-11 therein. (d) Vetter, A. J.; Flaschenriem, C.; Jones, W. D. *J. Am. Chem. Soc.* **2005**, *127*, 12315-12322. (e) Balcells, D.; Clot, E.; Eisenstein, O. *Chem. Rev.* **2010**, *110*, 749-823.
(35) Hartwig, J. F. In *Organotransition Metal Chemistry*; University Science Books: Sausalito, CA, 2010, p 85-146.
(36) Bryndza, H. E. *Organometallics* **1985**, *4*, 406-8.
(37) Woerpel, K. A.; Bergman, R. G. *J. Am. Chem. Soc.* **1993**, *115*, 7888-7889.
(38) Zhao, P.; Incarvito, C. D.; Hartwig, J. F. *J. Am. Chem. Soc.* **2006**, *128*, 9642-9643.
(39) Tye, J. W.; Hartwig, J. F. *J. Am. Chem. Soc.* **2009**, *131*, 14703-14712.
(40) Hartwig, J. F. *Nature* **2008**, *455*, 314-322

Chapter 4.2 Experimental Section

General Information: All procedures involving organometallic complexes were carried out under argon atmosphere using standard glovebox and Schlenk techniques. Solvents were purchased as anhydrous grade and purged with Argon before use. *p*-Xylene-d_{10} was degassed via freeze-pump-thaw cycles and dried over activated Al_2O_3 prior to use. Ethylene, propylene, 1-butene and isobutene were purchased from various suppliers in the highest purity available and used as received. 3,5-dimethylphenol was purchased from Sigma-Aldrich and used as received. Phenol was sublimed before use. (MeO-^{iPr}PCP)IrH_4[1], (^{tBu3Me}PCP)Ir(H)(Cl)[2], and (^{iPr}PCOP)Ir(C_2H_4)[3] were prepared according to the literature.

^{1}H, ^{13}C, and ^{31}P NMR were recorded on 300, 400, and 500 MHz Varian spectrometers and chemical shifts are reported in ppm. ^{1}H and ^{13}C NMR are referenced to the residual solvent signals, and ^{31}P NMR is referenced to an external standard of 85% H_3PO_4. GC analyses (FID detection) were conducted on a Varian 430 instrument equipped with a Varian FactorFour capillary column (stationary phase = VF-1ms, dimensions = 15 m x 0.25 mm, film thickness = 0.25 µm). Response factors were obtained for the ether products relative to C_6Me_6. The following method parameters were used:

Starting temperature: 38 °C

Time at starting temperature: 1.4 min

Ramp 1: 20 °C per min up to 250 °C with hold time 15 min

Ramp 2: 30 °C per min up to 280 °C with hold time 36 min

Injector temperature: 300 °C

Detector temperature: 310 °C

Example GC Traces

Figure 4.S1: GC Trace showing product separation during the propene/isobutene competition study with (^{iPr}PCOP)IrH_4 as catalyst.

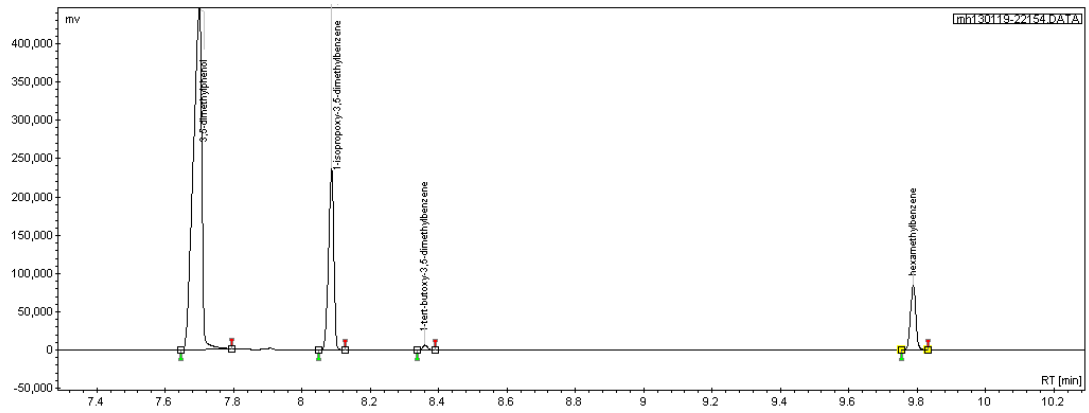

Figure 4.S2: GC Trace (blue) showing product separation during the propene/isobutene competition study with AgOTf/^{t}BuCl (Hintermann's acid) as catalyst. Overlays of GC traces (black and green) of the hydroaryloxylation products are shown to indicate their absence in this reaction.

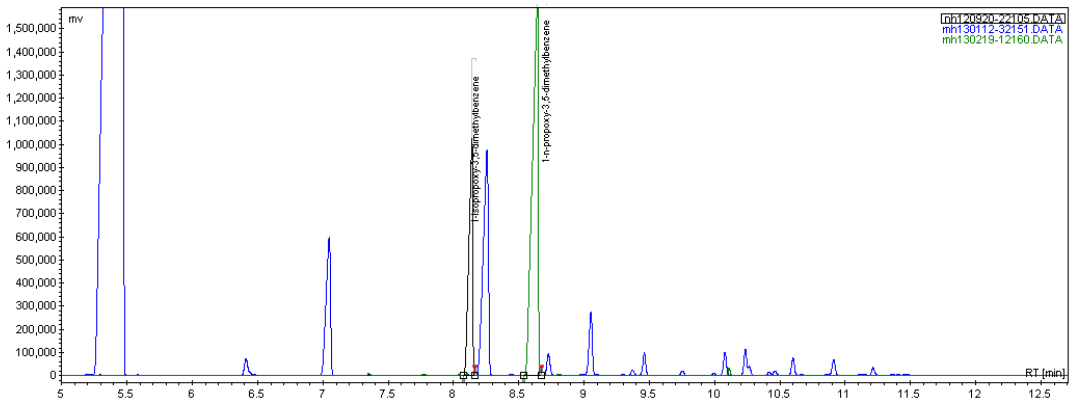

Figure 4.S3: GC Trace showing product separation during a reaction between propylene and 3,5-dimethylphenol, catalyzed by (MeO-^{iPr}PCP)IrH_4.

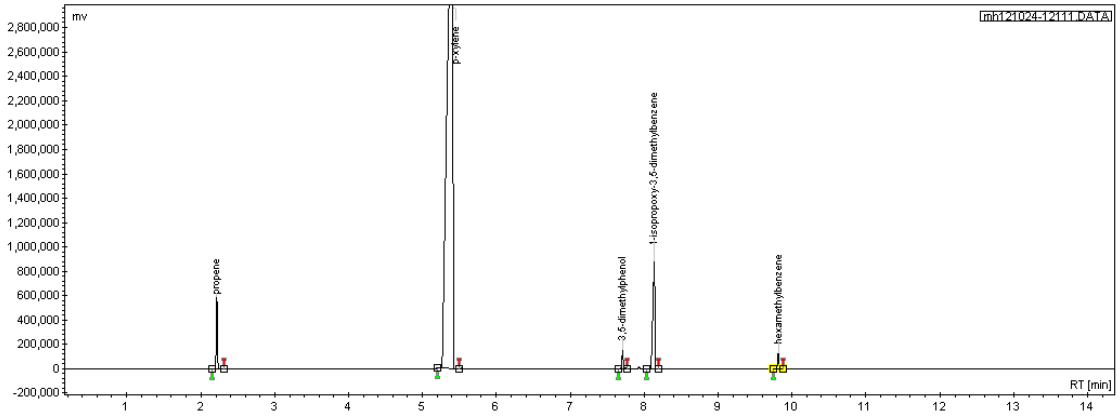

Additional Catalytic Optimization Results

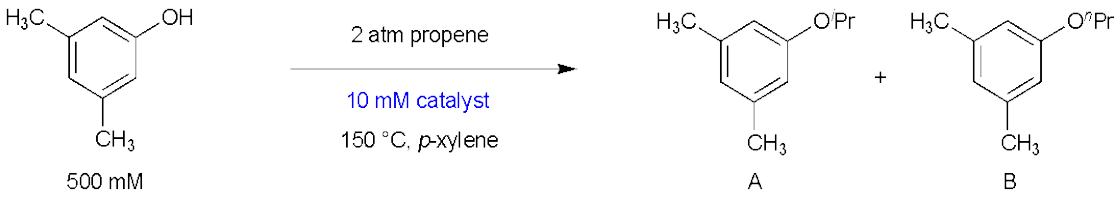

Catalyst (10 mM)	Co-catalyst (mM)	Time (h)	[A] (mM)	[B] (mM)
(^{tBu3Me}PCP)Ir(H)(Cl)	NaO^{t}Bu (125)	24	250	Not detected
(MeO-^{iPr}PCP)IrH$_4$	none	24	350	Not detected
(^{iPr}PCOP)IrH$_4$	none	24	400	Not detected
(^{iPr}PCOP)IrH$_4$	none	48	460	Not detected

Experimental Details

Synthesis of (^{iPr}PCOP)IrH$_4$: A stock solution containing 10 mM (^{iPr}PCOP)Ir(C_2H_4) in 10 mL *p*-xylene was stirred under an atmosphere of H_2. A color change from red to orange was observed. This solution was used directly for catalytic experiments. The same reaction is carried out in a J-Young NMR tube for spectroscopic analysis. ^{1}H NMR (500 MHz, *p*-xylene-d_{10}): δ 7.07 (t, J_{HH} = 7.6 Hz, 1H), 6.97 (t, J_{HH} = 7.0 Hz, 2H), 3.26 (d, J_{PH} = 10.1 Hz, 2H), 1.99 (sept of d, J_{HH} = 7.0 Hz, J_{PH} = 3.4 Hz, 2H), 1.64 (sept. of d, J_{HH} = 3.2 Hz, J_{PH} = 1.6 Hz, 2H), 1.27 (dd, J_{PH} = 15.1 Hz, J_{HH} = 6.9 Hz, 6H), 1.17 (dd, J_{PH} = 17.7 Hz, J_{HH} = 7.0 Hz, 6H), 1.14 (dd, J_{PH} = 15.7 Hz, J_{HH} = 6.9 Hz, 6H), 1.09 (dd, J_{PH} = 14.5 Hz, J_{HH} = 7.0 Hz, 2H), -8.97 (t, J_{PH} = 10.2 Hz, 4H). ^{31}P NMR (202 MHz, *p*-xylene-d_{10}): δ 177.19 (d, J_{PP} = 327.3 Hz), 57.81 (d, J_{PP} = 327.6 Hz).

General procedure for catalytic experiments: Inside the glovebox, a flame-dried glass vial was charged with 1.0 mL *p*-xylene solution 10 mM in (^{iPr}PCOP)IrH$_4$, 61 mg 3,5-dimethylphenol (0.50 mmol, 500 mM), and 5.0 mg C_6Me_6 (0.031 mmol, 31 mM). The orange solution was stirred until homogeneous, then divided into 0.20 mL aliquots into sealable glass ampoules (sealed volume 2.3 mL). The ampoules were attached to Kontes valves (total headspace volume 4.6 mL) and removed from the glovebox.

The Kontes valves were attached to a vacuum-gas manifold and the solutions inside were frozen with liquid N_2. The headspace was evacuated down to a pressure of 0.010 Torr and then placed under 1 atm propylene. The ampoule was fully immersed in liquid N_2, allowing the propylene to condense. After ~1 minute, the ampoule was sealed with an oxygen torch (this decreased the volume by 50% and brought the total pressure to 2 atm). Each sealed ampoule was carefully allowed to reach room temperature and then placed in a CG oven and heated to 150 °C.

At the desired times, the GC oven was cooled to room temperature and an ampoule was removed and immersed in liquid N_2 to condense the propylene. The ampoule was then cracked open and analyzed by GC, using C_6Me_6 as the internal standard.

Procedure for control experiments using Hintermann's Brönsted acid catalyst: A solution of 10 mM AgOTf and 40 mM ^{t}BuCl in *p*-xylene was stirred at room temperature for 15 minutes, during which time the solution became turbid. The solution was filtered through a 4 μm Teflon syringe filter to remove the AgCl and the phenol was added. The reaction was then carried out as in the general experimental procedure.

Procedure for competition experiments: Ampoules containing *p*-xylene solutions of 3,5-dimethylphenol, (^{iPr}PCOP)IrH_4, and C_6Me_6 were prepared according to the general procedure and attached to a vacuum gas manifold. 0.5 atm isobutene and 0.5 atm propylene were successively condensed into the ampoules, which were then sealed as in the general procedure. The ampoules were allowed to thaw, heated in a GC oven at 150 °C, and monitored by GC. The competition between propene and ethylene was carried out similarly. Experiments using the reaction products as starting materials were conducted in ampoules sealed under vacuum (0.010 Torr).

Synthesis of GC standards

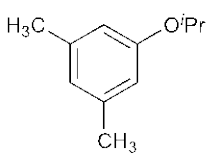

1

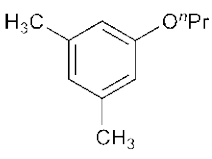

2

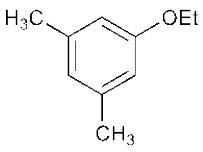

3

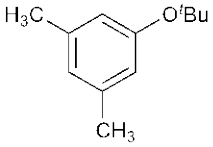

4

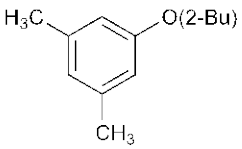

5

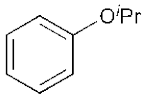

6

Compounds **1**[4], **2**[5], **4**[6], **5**[7] and **6**[8] have been previously reported and characterized by NMR in the literature. After preparing compounds **1–6**, we verified their identity by ^{1}H and ^{13}C NMR, and GC/MS before using them as GC standards or starting materials for selectivity experiments.

1-ethoxy-3,5-dimethylbenzene (3): 615 mg 3,5-dimethylphenol (5.0 mmol), 0.46 mL ethyl iodide (6.0 mmol), and 828 mg K_2CO_3 (6.0 mmol) were dissolved in 10 mL acetone. The suspension was stirred for 6 hours at reflux, at which time TLC indicates that the reaction is incomplete. Acetone and the remaining ethyl iodide were distilled off inside the hood, and the residue was extracted with 50 mL hexanes. The hexanes were washed with 40% aq. KOH (3 x 20 mL), H_2O, (20 mL), brine (20 mL), and then dried over anhydrous $CaCl_2$. Removal of the solvent afforded 240 mg of **3** as a clear colorless oil (1.6 mmol, 32% yield). ^{1}H NMR (500 MHz, $CDCl_3$): δ 6.68 (s, 1H), 6.63 (s, 2H), 4.08 (q, J = 6.9 Hz, 2H), 2.38 (s, 6H), 1.49 (t, J = 6.9 Hz, 3H). ^{13}C NMR (126 MHz, $CDCl_3$): δ 159.11, 139.16, 122.39, 66.22, 21.51, 15.00.

1-*tert*-butoxy-3,5-dimethylbenzene (4): Adapted from reference 9. 5.0 g 3,5-dimethylphenol (41 mmol) is dissolved in 100 mL dry CH_2Cl_2 and the mixture is cooled to –15 °C under argon. 0.5 mL H_2SO_4 is added to the stirred solution. Next, isobutene gas (bp. = –9 °C)

was bubbled into the reaction mixture for 15 minutes at a slow rate such that the reaction volume increases by about 20 mL. The reaction is stirred stirred for 30 minutes further, then neutralized with 25 mL sat. aq. $NaHCO_3$ while still at –15 °C. The reaction was warmed to room temperature to allow the excess isobutene to evaporate into the fume hood. Next, the reaction mixture was washed with H_2O (50 mL), 2 M NaOH (3 x 50 mL), and brine (50 mL). The organic layer was dried over anhydrous $MgSO_4$, filtered, and concentrated in vacuo to yield 1.9 g of **4** as a pale yellow oil. Characterization data was consistent with the literature.[6] Trace amounts of CH_2Cl_2 present in the material were removed by treatment with NaK under argon.

Characterization of (^{iPr}PCOP)Ir adducts of propene and phenol in solution

(^{iPr}PCOP)Ir(H)(OPh): A solution of (^{iPr}PCOP)Ir(H)(Cl)[3] and ca. 2 equiv NaOPh in *p*-xylene-d_{10} is heated to 100 °C for 2 hours in a J-Young NMR tube. The spectrum is then recorded. ^{1}H NMR (300 MHz, C_6D_6) δ 7.11 (t, J = 7.7 Hz, 2H), 6.95 (m, 2H), 6.81 (t, J = 7.7 Hz, 1H), 6.72 (t, J = 7.6 Hz, 3H), 2.83 (d, J = 9.8 Hz, 2H), 2.41-2.24 (m, 2H), 1.93-1.65 (m, 2H), 1.30-0.80 (m, 24H), -33.30 (t, J_{PH} = 13.9 Hz, 1H). ^{31}P NMR (121 MHz, C_6D_6): δ 167.99 (d, J_{PP} = 357.6 Hz), 62.32 (d, J_{PP} = 351.1 Hz).

(^{iPr}PCOP)Ir(η_2-propene): A solution of (^{iPr}PCOP)Ir(H)(OPh) or (^{iPr}PCOP)IrH_4 in *p*-xylene-d_{10} is placed under 1 atm propene in a J-Young NMR tube. After 15 minutes at room temperature, the spectrum is recorded. ^{1}H NMR (400 MHz, C_6D_6): δ 7.27 (d, J = 4.6 Hz, 1H), 7.21 (s, 2H), 3.41-3.21 (m, 2H), 2.94 (d, J = 7.7 Hz, 2H), 2.76-2.56 (m, 1H), 2.21 (ddt, J = 14.1, 9.8, 6.9 Hz, 2H), 1.68-1.58 (m, 2H), 1.53 (dd, J = 15.0, 7.1 Hz , 6H), 1.43 (dd, J = 15.0, 7.1 Hz, 6H), 1.31 (dd, J = 14.2, 6.9 Hz, 6H), 1.26- 1.06 (m, 9H). ^{31}P NMR (162 MHz, C_6D_6): δ 177.45 (d, J_{PP} = 314.5 Hz), 58.52 (d, J_{PP} = 314.5 Hz).

Evidence for reversible olefin insertion into the Ir–H bond: A J-Young NMR tube is charged with 500 mM 3,5-dimethylphenol-*O*–*D* and 10 mM (^{iPr}PCOP)Ir(η_2-propene) in *p*-xylene-d_{10} and placed under 1 atm propene. The signal corresponding to the phenolic proton begins appearing within minutes at 25 °C.

Chapter 4.3 Experimental Section References

1. Zhu, K.; Achord, P. D.; Zhang, X.; Krogh-Jespersen; K.; Goldman, A. S. *J. Am. Chem. Soc.* **2004**, *126*, 13044-13053.
2. Kundu, S; Choliy, Y.; Zhuo, G.; Ahuja, R.; Emge, T. J.; Warmuth, R.; Krogh-Jespersen, K.; Goldman, A. S. *Organometallics* **2009**, *28*, 5432-5444.
3. Ahuja, R.; Punji, B.; Findlater, M.; Supplee, C.; Schinski, W.; Brookhart, M.; Goldman, A. S. *Nature Chem.* **2011**, *3*, 167-171.
4. Wolter, M.; Nordmann, G.; Job, G. E.; Buchwald; S. L. *Org. Lett.* **2002**, *4*, 973-976.
5. Villa, G.; Povie, G.; Renaud, P. *J. Am. Chem. Soc.* **2011**, *133*, 5913-5920.
6. Parrish, C. A.; Buchwald, S. L. *J. Org. Chem.* **2001**, *66*, 2498-2500.
7. Vorogushin, A. V.; Huang, X.; Buchwald, S. L. *J. Am. Chem. Soc*. **2005**, *127*, 8146-8149.
8. Quach, T. D.; Batey, R. A. *Org. Lett.* **2003**, *5*, 1381-1384.
9. Chi, Y.; English, E. P.; Pomerantz, W. C.; Horne, S.; Joyce, L. A.; Alexander, L. R.; Fleming, W. S.; Hopkins, E. A.; Gellman, S. H. *J. Am. Chem. Soc*. **2007**, *129*, 6050-6055.

Chapter 5

Catalytic Cleavage of Ether C–O Bonds by Pincer Iridium Complexes

Reproduced with permission from

Catalytic Cleavage of Ether C–O Bonds by Pincer Iridium Complexes

Michael C. Haibach, Nicholas Lease, Alan S. Goldman

Angewandte Chemie Inernational Edition **2014**, *53*, 10160-10163.

The relative inertness of the C(alkyl)–O bond of aryl alkyl ethers both contributes to the stability of lignocellulosic biomass[1] and leads to its value as a protecting group for phenols[2]. In both cases, less-than-ideal conditions are required to break this unreactive bond. Many current processes for cleavage of the C–O bonds in lignin require the use of H_2 which presently invokes a non-renewable carbon-based input. Deprotection of alkyl (typically methyl) aryl ethers typically uses stoichiometric quantities of strong Lewis acids[2] (BBr_3, TMSI) or strong nucleophiles[3] (typically thiols or their salts) (Fig. 1). Thus the development of systems that can effect the redox or atom-economic[4] catalytic cleavage of ether C–O bonds currently represents a major goal in the field of catalysis.

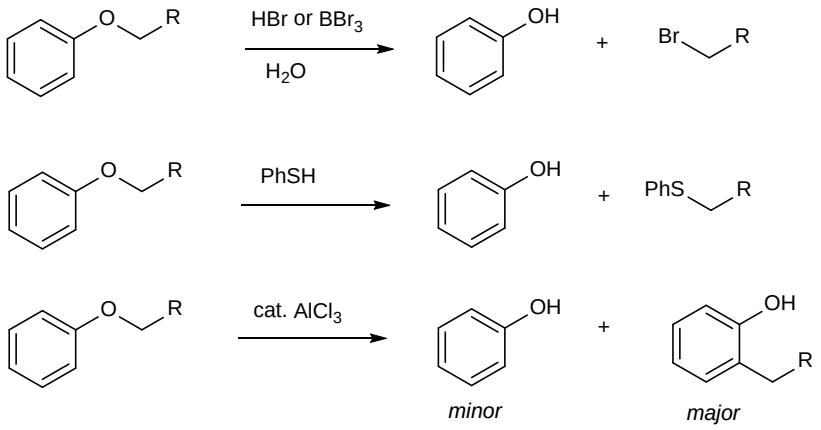

Figure 1. Classical methods for ether C–O bond cleavage.

Friedel-Crafts catalysts have classically been shown to rearrange phenol alkyl ethers to 2-(alkyl)phenols[5] (Fig. 1). Although not a true net cleavage reaction, advances in acid catalysis have allowed this process to be become synthetically useful for the production of *o*-alkylphenols[6].

The use of H_2 represents the most widely studied catalytic method to cleave ethers. Most classical examples require pressures and temperatures higher than typically accessible under common laboratory condition to cleave alkyl ethers, with an important exception: the Pd-catalysed hydrogenolysis of benzyl ethers is a standard transformation in organic synthesis[7].

More recently, some notable examples have advanced the scope of ether C–O bonds cleavable with H_2 under more accessible conditions. Hartwig and co-workers have developed Ni-based catalysts that selectively cleave the aryl C–O bond of ethers under only 1 atm H_2 (Fig. 2).[8a–b] In studies by Marks and co-workers, cyclic alkyl ethers are catalytically cleaved using $Yb(OTf)_3$ via dehydroalkoxylation[9]. In order to overcome the endergonic ring opening, the initially generated alkenols were hydrogenated using palladium nanoparticles. Ellman and Bergman reported a Ru-catalyzed cleavage of alkyl aryl ethers where an adjacent alcohol group serves as the internal H_2 donor.[1d] Aside from that work, we are not aware of any reported method whereby the C–O bond of an ether can be cleaved catalytically in a fully atom-economic fashion, i.e. without the use of additional reagents (including H_2). We report here the first such example, an iridium-catalysed dehydroaryloxylation of alkyl aryl ethers.

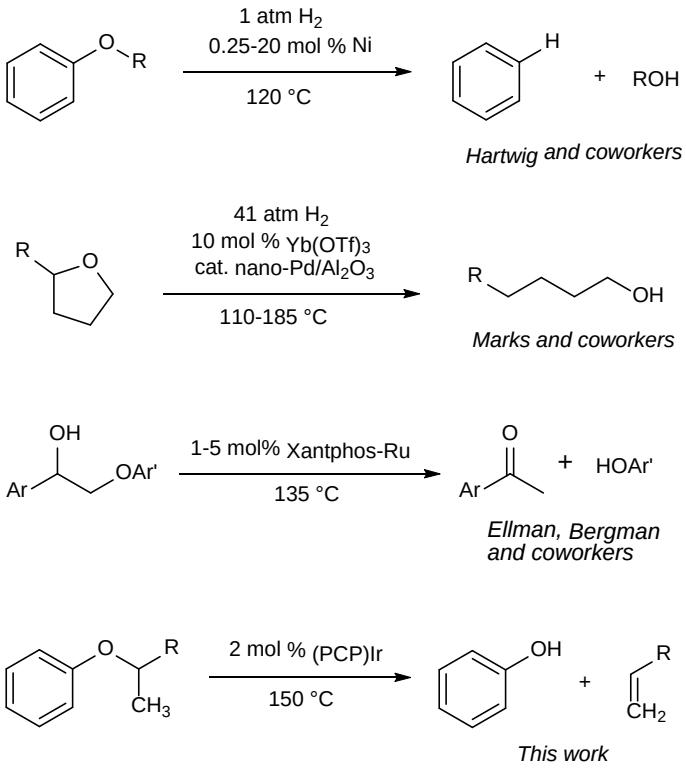

Figure 2. Recent advances in catalytic ether C–O bond cleavage

Recently, our group and that of Hartwig independently developed methods for the formation of ether C–O bonds via iridium-catalyzed olefin hydroaryloxylation.[10] In our system, iridium complexes of PCP-type pincers catalyze the O–H addition of phenols across olefins at 150 °C. The reaction is understood to proceed via formation of 6-coordinate (pincer)Ir(H)(OAr)(olefin), insertion of olefin into the Ir-OAr bond, and then C–H reductive elimination. In the course of our investigation of the reaction mechanism, we observed that the catalysts could also effect the "back-reaction," i.e. ether dehydroaryloxylation. We had previously reported that (^{tBu}PCP)Ir and EtOPh or *i*-PrOPh underwent such a reaction in a stoichiometric fashion to give (^{tBu}PCP)Ir(H)(OPh) and the corresponding free olefin[11]. However, heating a 500 mM solution of (3,5-$Me_2C_6H_3$)O-*i*-Pr in the presence of 2 mol% (^{tBu}PCP)IrH_2/TBE[12] results in negligible catalytic activity (4% conversion to (3,5-$Me_2C_6H_3$)OH after 16 h at 150 °C). As is the case in the hydroaryloxylation reaction, the use of less sterically congested (^{iPr}PCP)Ir[13] and (^{iPr}PCOP)Ir[14] precursors is found to lead to much higher conversions (88% and 92% respectively; Table 1, entries 2 and 3b) under identical conditions. No organic products other than the phenol and olefin are detected during the reaction. In particular, the dehydroaryloxylation process does not suffer from a competing Friedel-Crafts alkylation reaction between the olefin and the phenol.

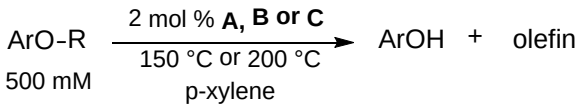

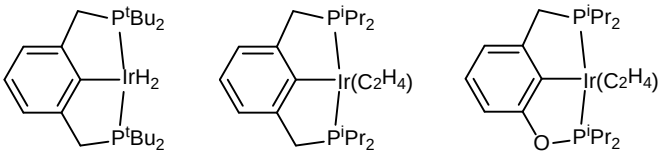

(^{tBu}PCP)IrH$_2$ **A** (^{iPr}PCP)Ir(C$_2$H$_4$) **B** (^{iPr}PCOP)Ir(C$_2$H$_4$) **C**

Table 1. Optimization and scope of the dehydroaryloxylation.[a]

Entry	T(°C)	Ar	R	cat	Time(h)	%Conv
1	150	3,5-Me$_2$Ph	*i*-Pr	A[b]	16	4
2	150	3,5-Me$_2$Ph	*i*-Pr	B	16	88
3a	150	3,5-Me$_2$Ph	*i*-Pr	C	4	72
3b	150	3,5-Me$_2$Ph	*i*-Pr	C	16	92
3c	150	3,5-Me$_2$Ph	*i*-Pr	C	48	97 (83)[c]
4a	150	3,5-Me$_2$Ph	2-Bu	C	4	41
4b	150	3,5-Me$_2$Ph	2-Bu	C	20	77
4c	150	3,5-Me$_2$Ph	2-Bu	C	48	85
4d	150	3,5-Me$_2$Ph	2-Bu	C	240	99
5	150	4-MeOPh	*i*-Pr	C	44	62 (55)[c]
6	150	4-FPh	*i*-Pr	C	36	76 (52)[c]
7a	150	2-naphthyl	*i*-Pr	C	16	80
7b	150	2-naphthyl	*i*-Pr	C	48	88 (72)[c]
8	150	Ph	*i*-Pr	C	48	78 (63)[c]
9	150	4-MePh	*i*-Pr	C	48	90
10	150	3,5-Me$_2$Ph	*n*-Oct	C	48	23
11	200	3,5-Me$_2$Ph	*i*-Pr	C	1	97
12a	200	Ph	*i*-Pr	C	16	55
12b	200	Ph	*i*-Pr	C	48	55
13a	200	3,5-Me$_2$Ph	*n*-Oct	C	16	57
13b	200	3,5-Me$_2$Ph	*n*-Oct	C	240	68
13c	200	3,5-Me$_2$Ph	*n*-Oct	B	16	52
13d	200	3,5-Me$_2$Ph	*n*-Oct	B	240	72
14a	200	3,5-Me$_2$Ph	*n*-Bu	C	4	66
14b	200	3,5-Me$_2$Ph	*n*-Bu	C	48	69
15a	200	3,5-Me$_2$Ph	2-Bu	C	1	64
15b	200	3,5-Me$_2$Ph	2-Bu	C	16	96

a 2 mol% catalyst (500 mM ether and 10 mM catalyst). Reactions were carried out in glass ampoules sealed under vacuum (0.01 Torr), headspace/solvent volume = 50, on a 0.05 mmol scale and were monitored by GC using C_6Me_6 as an internal standard. b 1.0 equivalent tert-

butylethylene added to dehydrogenate (^{tBu}PCP)IrH_2. c Isolated yield on an 0.25 mmol scale indicated in parentheses.

The scope of the dehydroaryloxylation by (^{iPr}PCOP)Ir, as initially determined, is shown in Table 1, entries 3–10. Reactions were conducted in glass ampoules sealed under vacuum to facilitate loss of gaseous olefins from the liquid phase.[15] In most cases, >70% conversion was obtained with 2 mol% catalyst within 16–48 h at 150 °C. In the case of *p*-methoxyphenyl isopropyl ether, no cleavage of the methyl C–O bond is observed (entry 5). (3,5-$Me_2C_6H_3$)O-2-Bu undergoes 99% conversion after an extended period (240 h; entry 4d), along with the detection of a mixture of butenes. Thus, despite a slower initial rate when compared with the corresponding aryl isopropyl ether (41% vs 72% after 4 h), the 2-butyl ether reaction also eventually proceeds to full conversion (entries 4c,d).

While we have not yet conducted extensive optimization of reaction conditions, we note that the reaction proceeds at a much faster rate at 200 °C. In the case of (3,5-$Me_2C_6H_3$)O*i*-Pr, 97% conversion is observed after only 1 hour (entry 11), corresponding to an average TOF of 0.81 min^{-1}. The higher reaction temperature allows for the conversion of an aryl *n*-octyl ether (entries 13a, b), a substrate that was found to react only slowly at 150 °C (entry 10).[16]

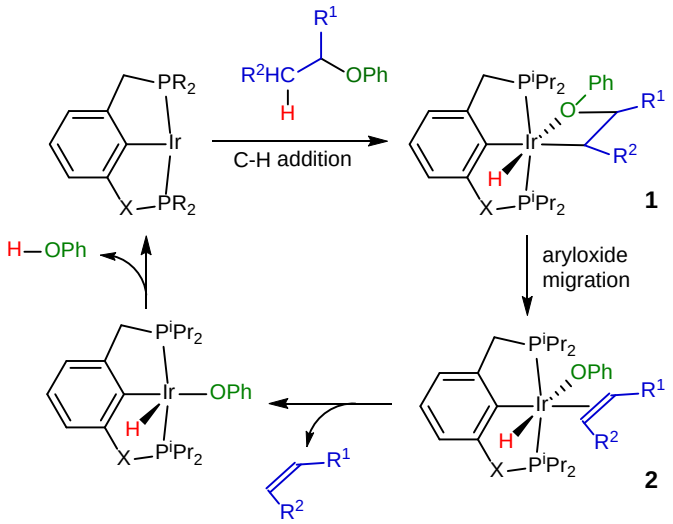

Scheme 5.1. Proposed mechanism for the dehydroaryloxylation.

The mechanism of the dehydroaryloxylation reaction is proposed to occur via the same set of steps as does the stoichiometric variant with (^{tBu}PCP)Ir and EtOPh or *i*-PrOPh studied previously by our group[11b] (Scheme 1). The initial step is addition of a C–H bond to yield **1**, followed by aryloxide migration to form the six-coordinate intermediate **2**. Loss of the olefin and phenol from **2** regenerates the active (pincer)Ir species and completes the catalytic cycle. The apparent relative reactivity levels observed for the ethers investigated (Table 1) is consistent with aryloxide migration being the rate-determining step, assuming that the transition state would have some character of both species **1** and **2**. Primary alkyl transition metal complexes are generally thermodynamically favoured over secondary alkyls;[17] thus R^2 = H would be favoured over R^2 = alkyl, accounting for the much greater reactivity of *i*-PrOAr and 2-BuOAr compared with *n*-BuOAr and *n*-OctOAr. The binding of propene would be less sterically demanding than the binding of 1-butene, contributing to greater reactivity for *i*-PrOAr vs. 2-BuOAr. *i*-PrOAr would also enjoy a statistical advantage of a factor of two, having two methyl groups bound to the α-

carbon (this point is equally applicable if C-H addition or β-aryloxide elimination is rate-determining).

The dehydroaryloxylations do not appear to be limited by thermodynamic factors under our reaction conditions. Thus even at 150 °C the reaction of 2-BuOAr and *i*-PrOAr can proceed essentially to completion (Table 1, entries 3c and 4d); the equilibrium would of course be shifted significantly further right by higher temperature. In these cases with gaseous olefin product the equilibrium has been favoured by employing a high ratio (50:1) of head space to solution volume. Note that at equilibrium *n*-BuOAr and 2-BuOAr would achieve the same distribution of products (in fact, no interconversion between these two ethers is observed) and that the less reactive ether, *n*-BuOAr, (see entry 14) is thermodynamically *higher* in energy.[18] Thus the relatively low reactivity of *n*-BuOAr (and by extrapolation, *n*-OctOAr) is not a thermodynamic effect.

Pincer complexes **A**–**C** are known to be thermally robust in the context of alkane dehydrogenation; nevertheless, we sought to determine the nature of the iridium-containing species present after completion of reactions run at 200 °C.[19] The conditions of entry 11 were approximated inside an NMR tube sealed under vacuum (500 mM ether, 20 mM **C**) (Scheme 2). After 1 hour at 200 °C, the major organometallic product identifiable in the ^{31}P NMR spectrum, **D**, [20] was distinct from **C**, (^{iPr}PCOP)Ir(propene), or (^{iPr}PCOP)Ir(H)(OAr). We hypothesized that as the reaction proceeds, the increasing concentration of propene (a hydrogen acceptor) could favour the dehydrogenation of the isopropoxy group by (^{iPr}PCOP)Ir. The resulting vinyl ether might strongly bind to the three-coordinate Ir centre to give species **D**.

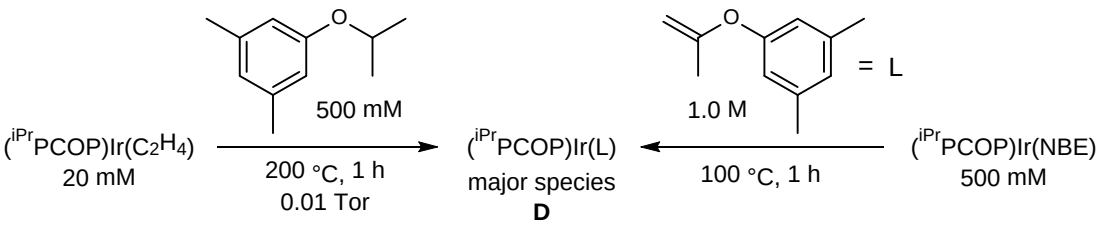

Scheme 2. Evidence of a vinyl ether addition product as the major iridium-containing species present after completion of reactions run at 200 °C.

To test this hypothesis, we prepared 2-(3,5-dimethylphenoxy)propene independently and treated it with a solution of the labile olefin complex (^{iPr}PCOP)Ir(NBE).[20] The ^{31}P NMR spectrum corresponding to the unknown **D** was observed, [20] confirming that **D** is a product of addition of (^{iPr}PCOP)Ir(vinyl ether). This result indicates that the catalyst remains homogenous throughout the reaction.

In conclusion, we report a unique process whereby the C–O bonds of ethers are catalytically cleaved, by (PCP)Ir-type catalysts, with complete atom-economy. This dehydroaryloxylation reaction proceeds in moderate to excellent conversion for a variety of substituted alkyl aryl ethers. Efforts are currently underway to increase the catalytic efficiency and functional group tolerance of this transformation.

Chapter 5.1 References

(1) a) J. Zakzeski, P. C. A. Bruijnincx, A. L. Jongerius, B. M. Weckhuysen, *Chem. Rev.* **2010**, *110*, 3552-3599; b) A. M. Ruppert, K. Weinberg, R. Palkovits, *Angew. Chem. Int. Ed.* **2012**, *51*, 2564-2601; For recent examples of catalytic approaches to C–O bond cleavage in lignin and model compounds, see: c) S. Son, F. D. Toste, *Angew. Chem. Int. Ed.* **2010**, *49*, 3791-3794; d) J. M. Nichols, L. M. Bishop, R. G. Bergman, J. A. Ellman *J. Am. Chem. Soc.* **2010**, *132*, 12554-12555; e) S. K. Hanson, R. Wu, L. A. Silks, *Angew. Chem. Int. Ed.* **2012**, *51*, 3410-3413; f) J. M. W. Chan, S. Bauer, H. Sorek, S. Sreekumar, K. Wang, F. D. Toste, *ACS Catal.*, **2013**, *3*, 1369-1377. (2) T. W. Greene, P. G. Wuts, J. Wiley, *Protective Groups in Organic Synthesis, Vol. 168*, Wiley New York, **1999**.

(3) A. Maercker, *Angew. Chem. Int. Ed.* **1987**, *26*, 972-989.

(4) a) B. M. Trost, *Science* **1991**, *254*, 1471-1477; b) B. M. Trost, *Angew. Chem. Int. Ed.* **1995**, *34*, 259-281.

(5) J.-i. Tateiwa, T. Nishimura, H. Horiuchi, S. Uemura, *J. Chem. Soc., Perkin Trans. 1* **1994**, 3367-3371.

(6) B. E. Firth, T. J. Rosen, *Vol. 4,447,675*, UOP Inc., Des Plaines, Ill., United States, **1984**.

(7) W. H. Hartung, R. Simonoff, *Org. React.* **1953**.

(8) a) A. G. Sergeev, J. F. Hartwig, *Science* **2011**, *332*, 439-443; b) A. G. Sergeev, J. D. Webb, J. F. Hartwig, *J. Am. Chem. Soc.* **2012**, *134*, 20226-20229; Other reports that may be mechanistically related: c) D.-G. Yu, X. Wang, R.-Y. Zhu, S. Luo, X.-B. Zhang, B.-Q. Wang, L. Wang, Z.-J. Shi, *J. Am., Chem. Soc.* **2012**, *134*, 14638-14641; d) Y. Ren, M. Yan, Z. C. Zhang, K. Yao, *Angew. Chem. Int. Ed.* **2013**, *52*, 12674-12678.

(9) a) A. C. Atesin, N. A. Ray, P. C. Stair, T. J. Marks, *J. Am. Chem. Soc.* **2012**, *134*, 14682-14685; b) R. S. Assary, A. C. Atesin, Z. Li, L. A. Curtiss, T. J. Marks, *ACS Catalysis* **2013**, *3*, 1908-1914; c) Z. Li, R. S. Assary, A. C. Atesin, L. A. Curtiss, T. J. Marks, *J. Am. Chem. Soc.* **2014**, *136*, 104-107.

(10) a) C. S. Sevov, J. F. Hartwig, *J. Am. Chem. Soc.* **2013**, *135*, 9303-9306; b) M. C. Haibach, C. Guan, D. Y. Wang, B. Li, N. Lease, A. M. Steffens, K. Krogh-Jespersen, A. S. Goldman, *J. Am. Chem. Soc.* **2013**, *135*, 15062-15070; For an extensive review of metal-catalyzed addition of C–O bonds across olefins, see: c) L. Hintermann, in *C-X Bond Formation*, A. Vigalok, Ed. Springer: Berlin, Heidelberg, **2010**, *31*, 123-155.

(11) a) J. Choi, Y. Choliy, X. Zhang, T. J. Emge, K. Krogh-Jespersen, A. S. Goldman, *J. Am. Chem. Soc.* **2009**, *131*, 15627-15629; b) S. Kundu, J. Choi, D. Y. Wang, Y. Choliy, T. J. Emge, K. Krogh-Jespersen, A. S. Goldman, *J. Am. Chem. Soc.* **2013**, *135*, 5127-5143.

(12) M. Gupta, C. Hagen, R. J. Flesher, W. C. Kaska, C. M. Jensen, *Chem. Commun.* **1996**, 2083-2084.

(13) F. Liu, A. S. Goldman, *Chem. Commun.* **1999**, 655-656.

(14) R. Ahuja, B. Punji, M. Findlater, C. Supplee, W. Schinski, M. Brookhart, A. S. Goldman, *Nature Chem.* **2011**, *3*, 167-171.

(15) Some olefin always remains in solution and can be identified by comparison of its retention time with authentic samples. Mixtures observed appear to be the equilibrium distribution of isomers due to facile isomerization by the catalyst, see: S. Biswas, Z. Huang, Y. Choliy, D. Y. Wang, M. Brookhart, K. Krogh-Jespersen, A. S. Goldman, *J. Am. Chem. Soc.* **2012**, *134*, 13276-13295.

(16) The formation of Fischer carbene complexes via the double C–H addition of linear alkyl ethers has been reported. See: a) M. T. Whited, R. H. Grubbs, *Acc. Chem. Res.* **2009**, *42*, 1607-1616; b) E. Carmona, M. Paneque, L. L. Santos, V. Salazar, *Coord. Chem. Rev.* **2005**, *249*, 1729-1735, and references therein. We cannot discount the relevance of this reaction to our catalytic processes at this time.

(17) a) D. L. Reger, E. C. Culbertson, *Inorg. Chem.* **1977**, *16*, 3104-3107; b) W. D. Jones, E. T. Hessell, *J. Am. Chem. Soc*. **1993**, 115, 554-562; c) J. L. Bennett, P. T. Wolczanski, *J. Am. Chem. Soc.* **1997**, 119, 10696-10719.

(18) This conclusion is extrapolated from the thermodynamics of branched vs. linear propyl methyl ether; heat of formation of the linear ether is 14.3 ± 2.0 kJ/mol higher: NIST Chemistry WebBook, NIST Standard Reference Database Number 69, Eds. P.J. Linstrom and W.G. Mallard, National Institute of Standards and Technology, Gaithersburg MD, 20899, http://webbook.nist.gov (retrieved 9 May, 2014)

(19) We also carried out the reaction in entry 11 in the presence of Hg. 74% conversion was observed after 1 hour. The measurable, but not major decrease in activity may reflect the reactive nature of free Hg atoms in solution ("dissolved vapor") generated at high temperature. This preliminary evidence against catalysis by Ir nanoparticles has been supported by a kinetic analysis not yet submitted for publication. We thank a reviewer for this suggestion.

(20) See the supporting information for details. The vinyl ether was prepared as previously described: Z. Wan, C. D. Jones, T. M. Koenig, J. Pu, D. Mitchell, *Tetrahedron Lett.* **2003**, *44*, 8257-8259.

Chapter 5.2 Experimental Section

General Information: All manipulations were carried out under argon using standard Schlenk or glovebox techniques. Anhydrous *p*-xylene was purchased from Sigma-Aldrich and purged with argon before use. Authentic samples of 3,5-dimethylphenol, 2-naphthol, 4-methoxyphenol, 4-methylphenol, 4-fluorophenol, and phenol were purchased from Sigma-Aldrich. 1-isopropoxy-3,5-dimethylbenzene[1], 1-ethoxy-3,5-dimethylbenzene[2], 1-(2-butoxy)-3,5-dimethylbenzene[3], isopropoxybenzene[4], 2-isopropoxynaphthalene[5], 4-isopropoxyanisole[6], 1-fluoro-4-isopropoxybenzene[7], 1-isopropoxy-4-methylbenzene[4], (^{tBu}PCP)IrH_2[8], (^{iPr}PCP)Ir(C_2H_4)[9], and (^{iPr}PCOP)Ir(C_2H_4)[9] were prepared according to the literature, degassed via freeze-pump-thaw cycles, and dried over 4Å.

^{1}H, ^{13}C, and ^{31}P NMR were recorded on 300, 400, and 500 MHz Varian spectrometers and chemical shifts are reported in ppm. ^{1}H and ^{13}C NMR are referenced to the residual solvent signals, and ^{31}P NMR is referenced to an external standard of 85% H_3PO_4. GC analyses (FID detection) were conducted on a Varian 430 instrument equipped with a Varian FactorFour capillary column (stationary phase = VF-1ms, dimensions = 15 m x 0.25 mm, film thickness = 0.25 μm). The following method parameters were used:

Starting temperature: 38 °C

Time at starting temperature: 1.4 min

Ramp 1: 20 °C per min up to 250 °C with hold time 15 min

Ramp 2: 30 °C per min up to 280 °C with hold time 36 min

Injector temperature: 300 °C

Detector temperature: 310 °C

General Procedure for catalytic ether cleavage using (^{iPr}PCOP)Ir

Inside an argon glovebox, a stock solution of 500 mM ether, 10 mM (^{iPr}PCOP)Ir(C_2H_4) and the C_6Me_6 standard is prepared in *p*-xylene. 100 µL of stock solution is added to a 5 mL sealable glass ampoule (Wheaton brand Vacules, Sigma-Aldrich), which is then connected to a Kontes high-vacuum adapter via a length of Tygon tubing. The adapter is attached to a vacuum line, the solution frozen in liquid N_2, and the headspace of the ampoule is evacuated down to 10 mTorr. With the bottom of the ampoule still immersed in liquid N_2, the neck of the ampoule is sealed using an oxygen torch. The sealed ampoule is allowed to reach room temperature, then heated inside a GC oven for the desired amount of time. Products were identified by comparison with authentic samples of the phenols and concentrations were calculated using the internal standard.

General Procedure for preparative scale examples

Inside an argon glovebox, a 25 mL sealable glass ampoule was charged with 46.6 mg 2-isopropoxynaphthalene (0.250 mmol), 2.7 mg (^{iPr}PCOP)Ir(C_2H_4) (0.0050 mmol), and 0.50 mL *p*-xylene. The ampoule was connected to a Kontes high-vacuum adapter via a length of Tygon tubing and the ampoule was flame sealed under 10 mTorr as described above. The sealed ampoule is heated in a GC oven for 48 hours at 150 °C, then frozen in liquid N_2 and carefully cracked open. The solution was diluted with 5 mL hexanes and 5 mL diethyl ether and extracted five times with 10 mL of 1 M KOH solution. The combined extracts were adjusted to pH 0-1 with conc. HCl, and then extracted five times with 10 mL diethyl ether. The combined extracts were washed with brine, dried over anhydrous Na_2SO_4, and concentrated to afford 26.0 mg (0.180 mmol, 72% yield) 2-naphthol as a white solid.

The same procedure was repeated with 2-(isopropoxy)-3,5-dimethylbenzene to afford 25.5 mg (0.207 mmol, 83% yield) of 3,5-dimethylphenol as a light pink solid. Similarly, 1-fluoro-4-isopropoxybenzene afforded 14.5 mg (0.129 mmol, 52% yield) as a yellow oil. 4-isopropoxyanisole afforded 17.1 mg 4-methoxyphenol (0.138 mmol, 55% yield) as a clear oil. Isopropoxybenzene afforded 14.8 mg phenol (0.157 mg, 63% yield) as a pink oil.

2-(3,5-dimethylphenoxy)propene (S1)

The new compound **S1** was prepared according to a general literature procedure[9] with minor modifications. 1.85 g 3,5-dimethylphenol (15.0 mmol), 0.89 mL 2-bromopropene (10.0 mmol), 6.52 g Cs_2CO_3, 247 mg CuCl (2.50 mmol), and 75 mL HPLC grade toluene (0.2 M) were stirred at reflux for 6 hours. The solution was filtered through a plug of Celite, washed three times with 25 mL 28% aq. NH_3, then concentrated and the residue was dissolved in 20 mL Et_2O. This solution was washed five times with 10 mL 1.0 M KOH, once with 20 mL brine, then dried over K_2CO_3. The dried solution was flushed through a plug of neutral Al_2O_3 and the plug was washed with 100 mL Et_2O. Concentration of the solution afforded 1.17 g of **S2** as a light yellow oil (7.17 mmol, 72% yield). ^{1}H NMR (400 MHz, $CDCl_3$): δ 6.79 (s, 1H), 6.71 (s, 2H), 4.19 (s, 1H), 4.03 (s, 1H), 2.33 (s, 6H), 2.01 (s, 3H). ^{13}C NMR (101 MHz, $CDCl_3$): δ 159.53, 155.29, 139.20, 125.49, 118.17, 89.54, 21.20, 20.00. **S2** was degassed by freeze-pump-thawing.

Determination of Catalyst Stability

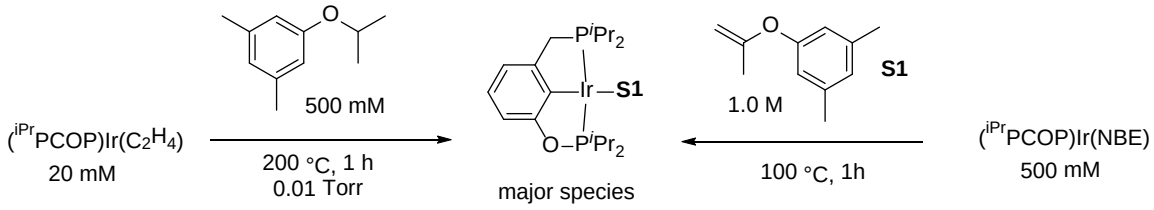

(^iPrPCOP)Ir(η2-S1)

5.6 mg norbornene (0.06 mmol) was added to a solution of 0.02 mmol (^{iPr}PCOP)IrH_4 in 0.4 mL *p*-xylene-d_{10}. The solution was heated in a J-Young NMR tube at 100 ºC for 1 hour, then the ^{31}P NMR spectrum of the resulting (^{iPr}PCOP)Ir(NBE) was recorded at room temperature (161 MHz, *p*-xylene-d_{10}): δ 180.7 (d, J = 245 Hz), 59.9 (d, J = 245 Hz). To this solution was added an excess (ca. 50 μL) of **S2**, and the solution was heated at 100 ºC for 1 hour, then the ^{31}P NMR spectrum was recorded at room temperature. A new species was observed at δ 191.7 (d, J = 295 Hz), 73.2 (d, J = 295 Hz) for **(^iPrPCOP)Ir(η2-S1)**. These signals match those of the major organometallic species present after the reaction of 3,5-dimethyl-2-isopropoxybenzene with (^{iPr}PCOP)Ir(C_2H_4).

Chapter 5.3 Experimental Section References

(1) M. Wolter, G. Nordmann, G. E. Job, S. L. Buchwald, *Org. Let.* **2002**, *4*, 973-976.
(2) A. B. Naidu, E. A. Jaseer, G. Sekar, *J. Org. Chem.* **2009**, *74*, 3675-3679.
(3) J.-i. Tateiwa, T. Nishimura, H. Horiuchi, S. Uemura, *J. Chem. Soc., Perkin Trans. 1* **1994**, 3367-3371.
(4) W. T. Olson, H. F. Hipsher, C. M. Buess, I. A. Goodman, I. Hart, J. H. Lamneck, L. C. Gibbons, *J. Am. Chem. Soc.* **1947**, *69*, 2451-2454.
(5) M. Barbasiewicz, A. Szadkowska, A. Makal, K. Jarzembska, K. Woźniak, K. Grela, *Chem–Eur. J.* **2008**, *14*, 9330-9337.
(6) J. R. Siegman, J. J. Houser, *J. Org. Chem.* **1982**, *47*, 2773-2779.
(7) B. Jones, *J. Chem. Soc.* **1938**, 1414-1417.
(8) A. S. Goldman, R. Ghosh, in *Handbook of C-H Transformations - Applications in Organic Synthesis* (Ed.: G. Dyker), Wiley-VCH, New York, **2005**, pp. 616-622, 649-651.
(9) R. Ahuja, B. Punji, M. Findlater, C. Supplee, W. Schinski, M. Brookhart, A. S. Goldman, *Nature Chem.* **2011**, *3*, 167-171.
(10) Z. Wan, C. D. Jones, T. M. Koenig, J. Pu, D. Mitchell, *Tetrahedron Lett.* **2003**, *44*, 8257-8259.